AquaFlow Technologies

ENGINEERING REFERENCE EDITION

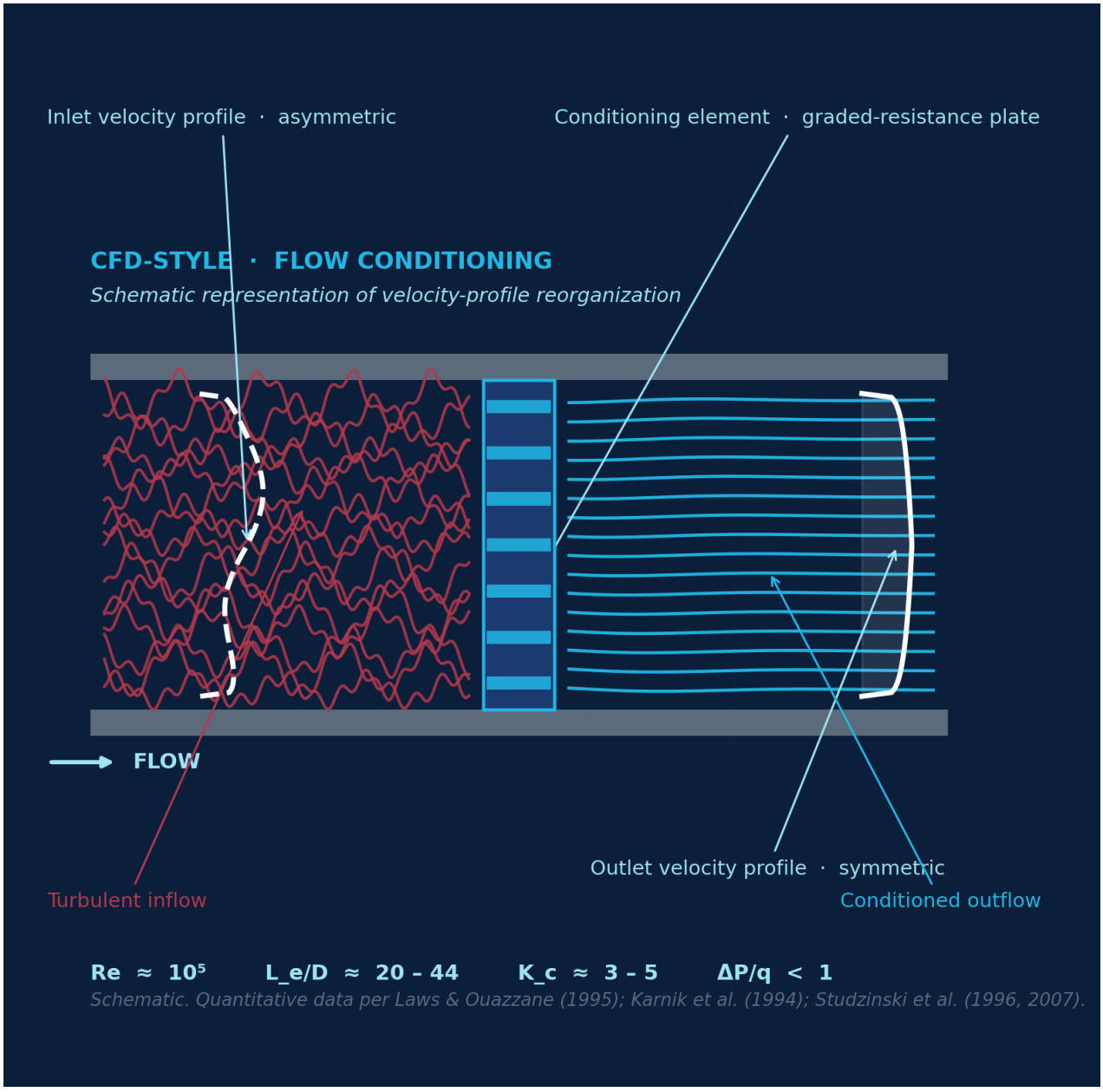

Velocity-profile development across a facility distribution. Each fitting restarts the development clock; in typical commercial pipework the fully-developed reference is rarely reached because the spacing between fittings is shorter than the entrance length.

AQUAFLOW TECHNOLOGIES, INC.

Engineering Reference Series · AF-ERE-2026-001 · Rev 2.0 · 2026

Prepared for technical review by municipal, mechanical, and fluid-dynamics engineers.

PUBLICATION NOTE

This volume is prepared for critical technical review by municipal water engineers, mechanical and fluid-dynamics academics, pump-manufacturer engineering directors, facility directors, ASME / AWWA / Hydraulic Institute reviewers, and independent consulting engineers.

HOW TO READ THIS DOCUMENT

Parts I and II establish the underlying physics from the published engineering literature, independent of any product. Part III introduces the AquaFlow Valve as one device within the conditioning lineage.

Every quantitative claim is grounded in published literature, recognized standards, or peer-reviewed studies. Where evidence is partial, anecdotal, or based on field observation, the limitation is stated explicitly.

This is an engineering reference. It does not address billing, consumption, water-bill savings, return on investment, or payback.

DOCUMENT CONTROL	VALUE
Document number	AF-ERE-2026-001
Revision	Rev 2.0 (redesigned engineering edition)
Effective year	2026
Series	AquaFlow Engineering Reference Series
Editorial standard	ASME technical publication / AWWA engineering reference manual
Sponsor	AquaFlow Technologies, Inc.

Editorial Foreword

This document is published as an engineering reference on the mechanisms by which unconditioned flow degrades commercial water systems, and on the engineering discipline of upstream hydraulic conditioning. The treatment is organized in three parts. Parts I and II establish the underlying physics from the published literature. AquaFlow Technologies is the sponsor of this publication and the manufacturer of one device within the conditioning lineage; that device is introduced in Part III after the engineering background has been set out on its own terms.

Every quantitative claim in this document is grounded in published engineering literature, recognized industry standards, or peer-reviewed studies. Where evidence is partial, anecdotal, or based on field observation, the limitation is stated explicitly. Where a claim cannot be substantiated from the literature, it has been removed. The objective is a document that can be evaluated by skeptical reviewers on its technical content.

INTENDED REVIEWERS

This document is written to be read critically by municipal water engineers, mechanical engineering professors specializing in fluid dynamics, pump-manufacturer engineering directors, Fortune 500 facility directors, ASME and AWWA reviewers, and independent consulting engineers. It is intended to be evaluated as a technical publication.

Part I (Sections 1–11) covers the fluid-mechanics of commercial service: Reynolds-number regimes, the velocity profile, Dean vortices and secondary flow at fittings, pressure pulsation and its frequency content, entrained-air thermodynamics, cavitation theory, water hammer and column separation, flow-induced vibration, and the documented failure mechanisms of rotating equipment, valves, heat-transfer equipment, infrastructure, and instrumentation. Part II (Sections 12–15) introduces hydraulic conditioning as an engineering discipline and reviews the published performance of conditioning plates including the Zanker, the Canadian Pipeline Accessories CPA 50E (Laws plate), the étoile, and the tube bundle. Part III (Sections 16–19) introduces the AquaFlow Valve as one device within that lineage, applied immediately downstream of the master meter on the customer-owned side of the property.

GOVERNING REFERENCES

Water industry	AWWA M6 · M11 · M14 · M51 · C512 · C700–C712 · AWWA WITAF #4660 · NSF/ANSI 61 · IAPMO UPC · USC FCCCHR · ASSE 1013
Mechanical / rotating	ANSI/HI 9.6.1 · ANSI/HI 9.8 · ANSI/API 682 · API 610 · ASME B73.1 · ASME Section VIII Div. 2 · ASME Section III NG-3133 · ASTM G32-16
Metering / flow	ISO 4064 · ISO 5167 · ISO 17089 · OIML R 49 · API MPMS Ch. 5 / Ch. 22 · AGA Report No. 9 · NIST Handbook 44
Building / process	ASHRAE Handbook—HVAC Systems & Equipment · CTI STD-202 · TEMA RGP-RCB-4 · Crane TP-410 · USP <645> · FDA 21 CFR 110

Contents

ENGINEERING REFERENCE EDITION · AF-ERE-2026-001

Scope and Limitations

This document is published as an engineering reference on the mechanisms by which unconditioned flow degrades commercial water systems and on the published performance of upstream hydraulic-conditioning devices. To support technically rigorous review, this section explicitly defines what the device described in Part III is, and equally explicitly defines what it is not.

DEFINITION — AQUAFLOW IS A HYDRAULIC CONDITIONING DEVICE

A passive, sealed, inline mechanical device installed immediately downstream of the master meter on the customer-owned side of the property. It combines three published conditioning functions — pressure stabilization, entrained-air management, and flow conditioning — in a single body, applying engineering principles codified across API, ISO, AGA, OIML, AWWA, and ASHRAE standards.

What AquaFlow is not

To prevent any confusion with adjacent device classes and to make the engineering scope unambiguous, the following list identifies functional categories that the device does not occupy.

CATEGORY	STATEMENT OF NON-EQUIVALENCE
Pressure-reducing valve (PRV)	Not a PRV. The device does not set or regulate a downstream pressure target. PRV functionality remains a separate engineered device.
Water softener / treatment	Not a water-treatment device. The device does not alter the chemical, mineral, or microbiological composition of the water.
Leak-repair / pipe-condition device	Not a leak-repair or pipe-rehabilitation device. The device does not alter pipe-wall roughness, integrity, or condition.
Flow-meter / measurement device	Not a flow meter. The device performs no metering function; it may improve inlet conditions for a downstream meter installed per AWWA M6.
Surge suppression / air chamber	Not a substitute for engineered surge protection. Surge tanks, air chambers, and programmed valve-closure remain required where surge analysis indicates them.
Air-release / air-vacuum valve	Not a substitute for engineered air valves per AWWA M51 / C512. The device manages micro-bubble entrainment, not free-air pocket release at high points.
Laminar-flow generator	Does not produce laminar flow. Laminar flow at commercial service Reynolds numbers (Re > 4,000) is not physically achievable; the device organizes turbulent flow.
Roughness modifier	Does not alter the roughness of any pipe in the system. Friction-factor behavior at downstream pipes is unchanged.

REVIEWER NOTE · SCOPE DISCIPLINE

- Engineering claims throughout this document are restricted to the conditioning functions defined above.
- Adjacent claims that fall outside the conditioning discipline are explicitly excluded.
- Quantitative outcomes at any specific facility are application-specific and require before-and-after instrumentation and maintenance-record analysis.
- This document is suitable for technical review by engineering committees; it is not a sales document.

EDITORIAL METHOD & EVIDENCE BASIS

50+ refs	**30+ standards**	**3 parts**
peer-reviewed papers and engineering texts cited (Appendix C)	governing standards across API, ISO, AGA, AWWA, ASME, ASHRAE	physics from the literature, the conditioning discipline, then the device

HOW CLAIMS IN THIS DOCUMENT ARE SUBSTANTIATED

Every quantitative claim is traced to a published source, a recognized standard, or peer-reviewed research. Where evidence is partial, anecdotal, or based on field observation, the limitation is stated at the point of use. Conceptual and directional statements are labeled as such and are not presented as measured field data. Reviewers are encouraged to verify each reference independently.

PART I

Fluid-Mechanics Mechanisms.

How turbulent flow, pressure instability, entrained air, cavitation inception, water hammer, flow-induced vibration, and velocity-profile asymmetry actually affect commercial water systems — established from the published engineering literature.

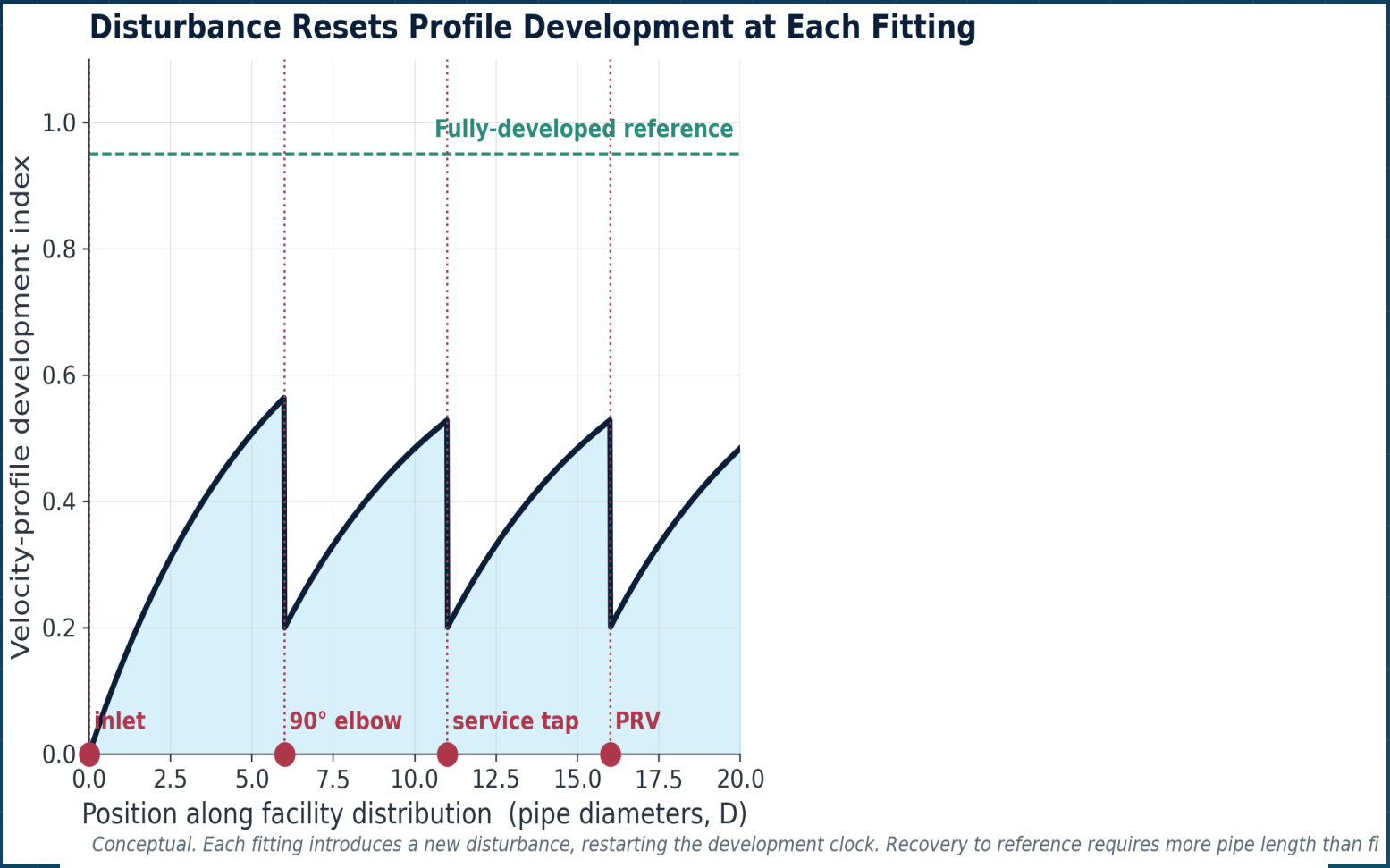

Figure I.1 — Each fitting in a facility distribution restarts the velocity-profile development clock. In typical commercial pipework the fully-developed reference is rarely reached because the spacing between fittings is shorter than the entrance length.

Reynolds Number, Flow Regimes, and the Velocity Profile

Fluid flow in a closed conduit organizes itself into one of three regimes characterized by the Reynolds number, Re = ρvD/μ, the dimensionless ratio of inertial to viscous forces. Below Re ≈ 2,300 the flow is laminar — parallel streamlines and a parabolic velocity profile (the Hagen–Poiseuille solution). Above Re ≈ 4,000 the flow is turbulent — three-dimensional, time-dependent, irregular motion characterized by a mean velocity profile well approximated by a 1/n power law (Nikuradse, 1932) with n ≈ 7 at Re ≈ 10⁵ and increasing weakly with Re. Between the two lies a transitional regime in which intermittent turbulent bursts grow and coalesce (Reynolds, 1883; Rotta, 1956; Wygnanski & Champagne, 1973).

$$Re = \rho \, v \, D / \mu \approx v \, D / \nu$$

Reynolds number; v is the mean cross-sectional velocity, D the pipe inside diameter, ρ the liquid density, μ the dynamic viscosity, ν = μ/ρ the kinematic viscosity.

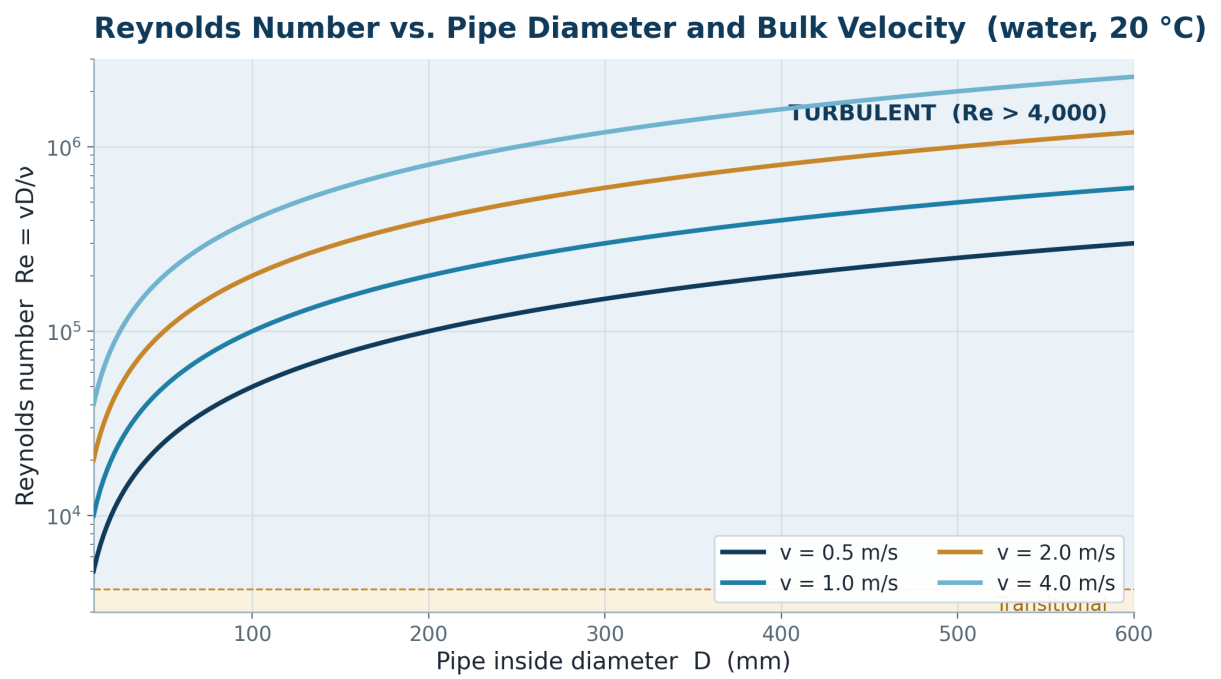

FIGURE 1.1 Reynolds number as a function of pipe diameter and bulk velocity at 20 °C (ν = 1.0 × 10⁻⁶ m²/s). Across the practical commercial-service envelope, Re is firmly turbulent.

ENGINEERING INTERPRETATION	The figure demonstrates that commercial water service, across every realistic combination of pipe diameter and bulk velocity, operates at Reynolds numbers between approximately 10^4 and 4×10^5 — firmly within the turbulent regime.
DESIGN IMPLICATION	Equipment installation, sizing, and accuracy calculations should assume turbulent flow conditions. The engineering question is not whether turbulence exists, but how organized it is at the inflow to each downstream component.

1.1 Commercial service Reynolds numbers

In a 2-inch (50 mm) service line carrying water at 5 ft/s (1.5 m/s) at 20 °C, Re ≈ 7.5×10^4. A 6-inch (150 mm) main at 8 ft/s reaches Re ≈ 3.7×10^5. These flows are firmly turbulent. The implication for the rest of this document is that the laminar-flow assumption sometimes embedded in casual discussion of plumbing hydraulics does not apply; commercial service flow is always turbulent, and the relevant engineering question is how organized the turbulence is, not whether it exists. Conditioning improves flow organization, profile symmetry, and swirl reduction within a turbulent regime; it does not produce laminar flow at service-line Reynolds numbers.

1.2 Laminar versus turbulent velocity profile

The laminar velocity profile in a circular pipe is exactly parabolic (Hagen, 1839; Poiseuille, 1840). The turbulent profile is much flatter and is well approximated by a power law u/u_max = (1 − |y|/R)^(1/n) with n ≈ 7 at Re ≈ 10^5 and n increasing slowly with Re (Nikuradse, 1932; Schlichting & Gersten, 2017). The flatness has engineering consequences: the ratio of mean to centerline velocity is approximately 0.82 for turbulent flow at typical service Re, compared with 0.50 for laminar flow.

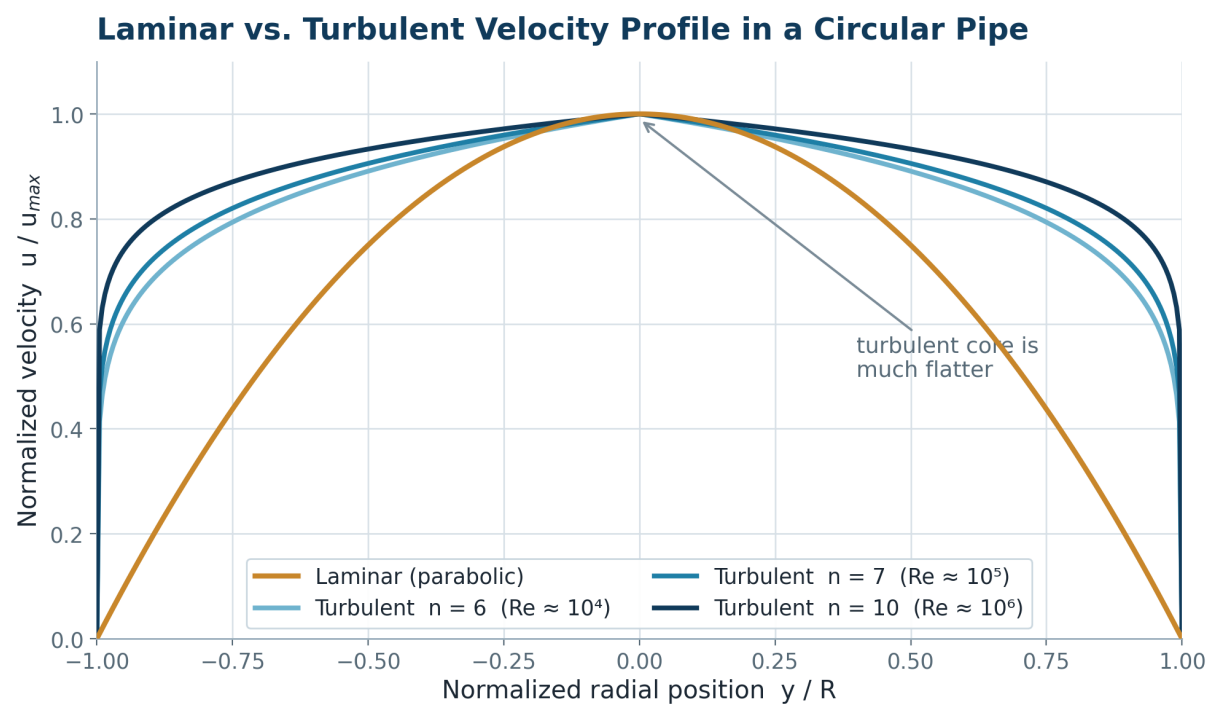

FIGURE 1.2 Laminar parabolic profile compared with turbulent 1/n power-law profiles at three Reynolds numbers. The turbulent profile flattens with increasing Re.

0.82	**0.50**	**n ≈ 7**
mean-to-centerline velocity ratio (turbulent, typical service Re)	mean-to-centerline velocity ratio (laminar, parabolic)	power-law exponent at Re ≈ 10⁵ (Nikuradse 1932)

PROFILE INTERPRETATION

The flat turbulent core concentrates the velocity gradient near the wall. A meter or pump inlet sampling the core sees a far more uniform profile than the laminar parabola — provided the upstream flow is organized.

DESIGN IMPLICATION

Component calibrations assume the fully-developed turbulent profile. Partially-developed flow from a nearby fitting biases every velocity-sampling device.

1.3 The Moody diagram

Pressure drop through a circular pipe is governed by the Darcy–Weisbach equation, $\Delta P = f\,(L/D)(\rho v^2/2)$. In the laminar regime $f = 64/Re$; in the turbulent regime f depends on both Re and relative roughness ε/D, as captured in the Moody diagram (Moody, 1944) and the Colebrook–White correlation. Commercial pipe absolute roughness ranges from approximately 0.0015 mm (drawn copper, smooth PVC) to 0.045 mm (commercial steel) to 0.15 mm (galvanized iron); cement-lined ductile iron is typically 0.12 mm (Crane TP-410, 2018). At high Re the friction factor approaches a Re-independent asymptote that depends only on roughness — the regime where most commercial service operates.

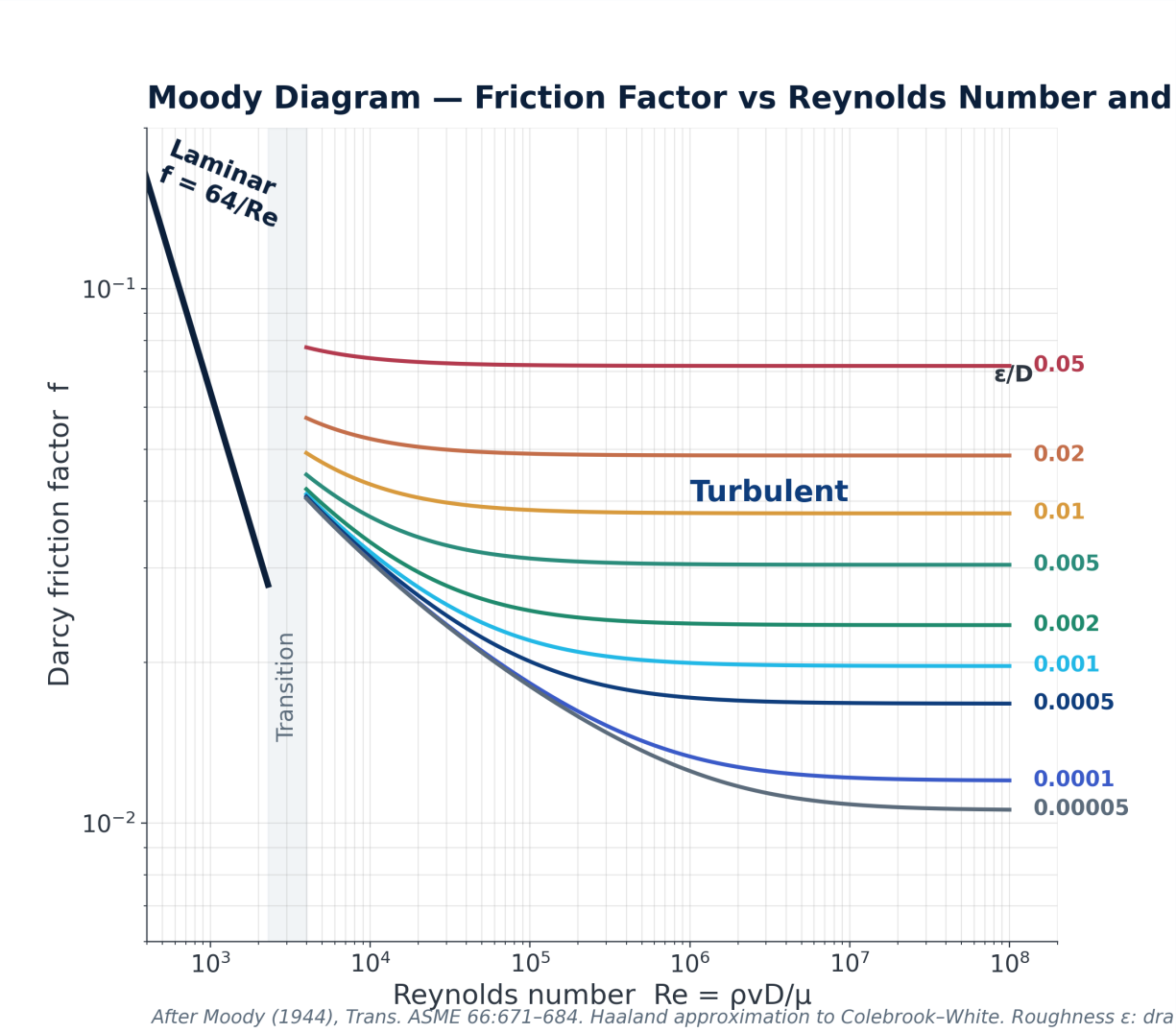

FIGURE 1.3 Moody diagram. Darcy friction factor f vs. Re and relative roughness ε/D. Plot uses the explicit Haaland approximation to Colebrook–White.

ENGINEERING INTERPRETATION	In the fully-rough turbulent regime — where commercial service routinely operates — friction factor depends only on relative roughness, not Re. Pipe-wall condition therefore dominates pressure-drop behavior at high flow rates.
DESIGN IMPLICATION	Aging pipe surfaces (corrosion, tuberculation, scale) increase ε/D and may shift the system operating point substantially. Hydraulic conditioning addresses inflow organization; it does not modify the roughness of downstream piping.

1.4 Hydrodynamic entrance length

The velocity profile in a circular pipe approaches its asymptotic, fully-developed shape only after a hydrodynamic entrance length. For turbulent flow the conventional engineering estimate is L_e/D ≈ 4.4 · Re^(1/6), placing L_e at approximately 20 D for Re ≈ 10⁴, 30 D for Re ≈ 10⁵, and 44 D for Re ≈ 10⁶ (Bhatti & Shah, 1987; White, 2015). This estimate assumes a clean,

low-disturbance inlet. In service, every elbow, tee, expansion, valve, or fitting resets the development clock. The practical consequence is that commercial water pipework rarely presents fully-developed flow to any downstream component — a fact codified in the upstream and downstream straight-pipe requirements of every meter installation standard (AWWA M6, ISO 4064, ISO 5167, OIML R 49). Recovery has been measured experimentally by Mattingly & Yeh (1991), Laws & Ouazzane (1995), and Studzinski et al. (1996); velocity-profile recovery to within engineering tolerance requires 25–50+ D after a single elbow.

ENGINEERING SIGNIFICANCE · SECTION 1

- Commercial water service operates at Re ≈ 7,500 to 4 × 10^5, firmly within the turbulent regime.
- The fully-developed reference profile requires 20 D at Re ≈ 10^4 and 44 D at Re ≈ 10^6; commercial fittings are typically spaced closer than this.
- Conditioning improves flow organization, profile symmetry, and swirl reduction within a turbulent regime; it does not produce laminar flow at service Re.
- The downstream component sees a turbulent inflow whose organization depends on the cumulative upstream disturbance history.

This is the engineering baseline for the remainder of the document. The turbulence cannot be removed; the engineering objective is to organize it. The mechanisms by which disorganized turbulence interacts with downstream equipment are covered in the following sections.

Velocity Profile Distortion, Dean Vortices, and Secondary Flow

Beyond Reynolds-number regime and entrance length, the engineering content of “disorganized turbulence” in commercial pipework is dominated by three structural disturbances: (i) Dean vortices produced by curved-pipe flow; (ii) secondary flow superimposed on the bulk axial component; and (iii) swirl, the coherent tangential velocity component that persists for tens of pipe diameters downstream of fittings. Each is well characterized in the open literature.

① Dean vortices	② Secondary flow	③ Swirl
counter-rotating pair from curved-pipe flow — persist 15–30+ D	cross-sectional circulation superimposed on the bulk axial flow	coherent tangential motion — persists 40–50+ D after coupled elbows

2.1 Dean vortices in curved pipe

When fluid flows around a bend, the centrifugal acceleration sets up a pressure gradient across the pipe cross section. The result is a pair of counter-rotating vortices, first analyzed by Dean (1928) for fully-developed laminar flow in curved pipes and subsequently extended to turbulent flow by Berger et al. (1983). The Dean number, De = Re · (D / 2R_c)^(1/2), with R_c the centerline radius of curvature, is the dimensionless parameter governing vortex strength. For a typical 6-inch service-line elbow of 9-inch centerline radius, De at service velocity is in the range 10^4–10^5; the resulting vortex pair persists for 15–30+ D downstream before viscous decay dominates.

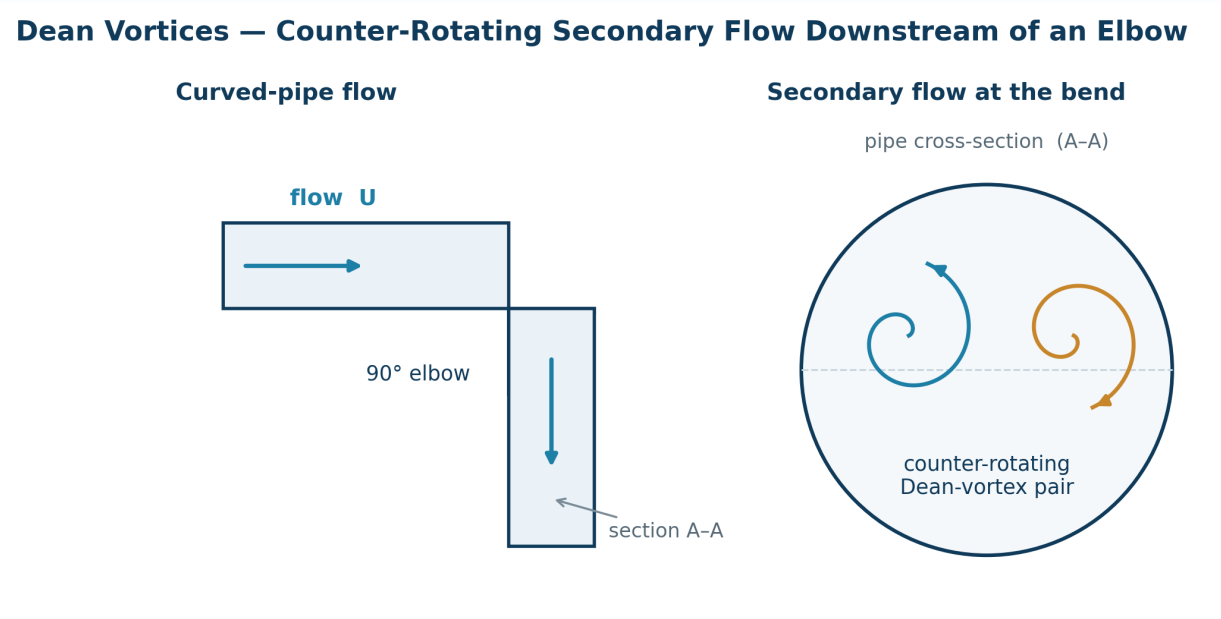

FIGURE 2.1 Counter-rotating Dean-vortex pair downstream of a 90° elbow. The vortex strength scales with Dean number; persistence is set by viscous decay against pipe-wall shear.

10^4–10^5 De	**15–30+ D**	**2 vortices**
Dean number at service velocity, 6-inch elbow	downstream persistence of the vortex pair	counter-rotating cells set up by the bend

FIELD OBSERVATION

Every elbow in a facility distribution launches a Dean-vortex pair into the downstream run. Because fittings are usually spaced closer than the decay length, the vortices rarely dissipate before reaching the next component.

2.2 Secondary-flow patterns at fittings

Different fitting geometries produce different secondary-flow signatures. A single 90° elbow produces a clean Dean-vortex pair. Coupled in-plane elbows produce either constructive (intensified) or destructive (partially canceling) secondary-flow patterns depending on the relative orientation. Coupled out-of-plane elbows are the most disruptive: they generate strong swirl with persistence measured at 40–50+ D in the open literature (Murakami et al., 1969; Studzinski et al., 1996, 2007). Tees, reducers, and partially-open valves each contribute their own characteristic disturbance. The cumulative effect through a facility distribution is a persistent, three-dimensional velocity field that is far from the axisymmetric ideal assumed in component design.

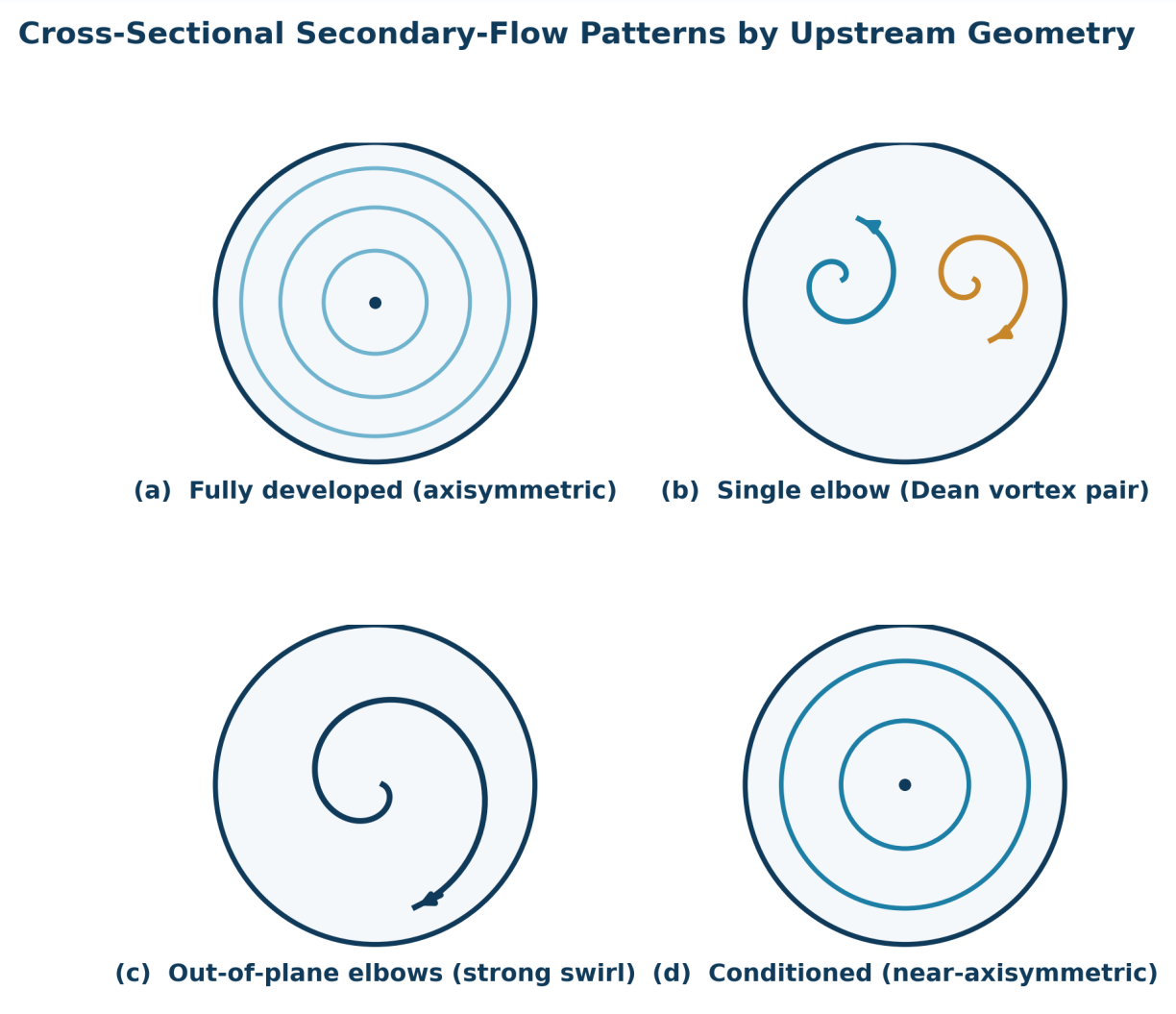

FIGURE 2.2 Cross-sectional secondary-flow patterns. Fully-developed flow is axisymmetric; elbows generate Dean vortices; coupled out-of-plane elbows generate strong swirl; a graded-resistance conditioner re-imposes near-axisymmetric structure.

PATTERN INTERPRETATION	The cross-sectional signature encodes the upstream disturbance history. Axisymmetric flow is the design ideal; the Dean-pair and swirl states are what downstream equipment actually receives in unconditioned service.
CONDITIONING TARGET	A graded-resistance plate remaps any of these distorted states back toward the axisymmetric reference — the engineering objective of upstream conditioning.

2.3 Fitting minor-loss coefficients

Each fitting contributes a minor pressure loss characterized by a dimensionless loss coefficient K. The minor loss adds to the major Darcy–Weisbach loss to give the total system pressure drop. K values are tabulated in Crane TP-410 (2018), “Flow of Fluids through Valves, Fittings and Pipe,” for every commercial fitting class. More important than the loss itself for downstream equipment is the secondary-flow disturbance the fitting introduces; the recovery distance is typically 10–50 D,

depending on the fitting class and the proximity of upstream disturbances. The recovery length is what determines whether downstream components see organized or disorganized inflow.

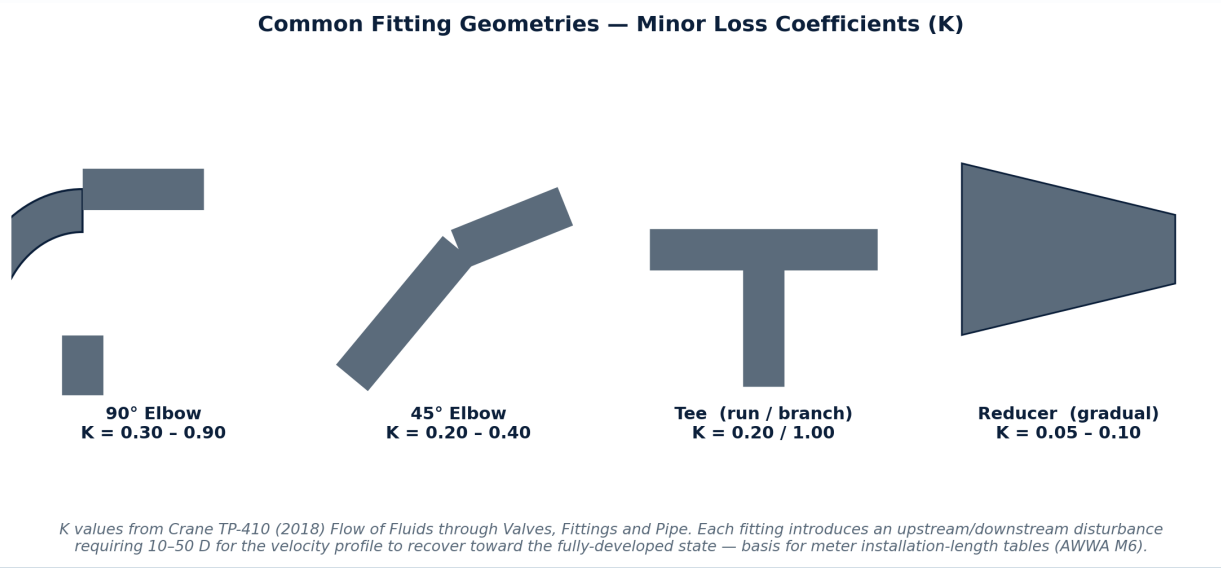

FIGURE 2.3 Common fitting geometries and their minor-loss coefficients. K values per Crane TP-410 (2018). Each fitting introduces a velocity-profile disturbance that requires 10–50 D for recovery.

ENGINEERING INTERPRETATION	Minor-loss coefficients quantify the localized pressure drop at each fitting. The associated velocity-profile disturbance — Dean vortices at elbows, asymmetric shear at tees, expansion-zone separation at reducers — persists for 10–50 D downstream.
DESIGN IMPLICATION	AWWA M6 upstream / downstream straight-pipe requirements at meter installations exist precisely because of this recovery distance. In practice, fittings spaced closer than the recovery length present partially-developed flow to every downstream component.

STANDARDS PERSPECTIVE · CRANE TP-410 AND AWWA M6

- Crane TP-410 (2018) catalogs K values for every commercial fitting class; values shown are representative ranges for water service.
- AWWA M6 specifies meter-installation straight-pipe requirements derived from these recovery-length data.
- ISO 5167 codifies analogous requirements for differential-pressure flow measurement.
- Recovery-length data underpin the entire engineering case for upstream conditioning at the service entrance.

Pressure Pulsation and Dynamic Pressure Behavior

Static pressure at a fixed point in a commercial water system is not a steady value. It is a time-varying signal composed of: (i) slow secular drift driven by municipal distribution dynamics on a minute time scale; (ii) intermediate oscillation from district pressure-zone management, pump-station operation, and consumption swings on a seconds time scale; (iii) higher-frequency pulsation from turbulent wall-pressure fluctuations and from local valve and pump dynamics on time scales of tenths of a second to milliseconds; and (iv) discrete sub-second transient events from valve closures and consumption-point operations. Modern transient loggers (Badger PIPEMINDER, HWM, Mobiltex; AWWA WITAF #4660, 2017) sample at 100–1,000 Hz to resolve all components.

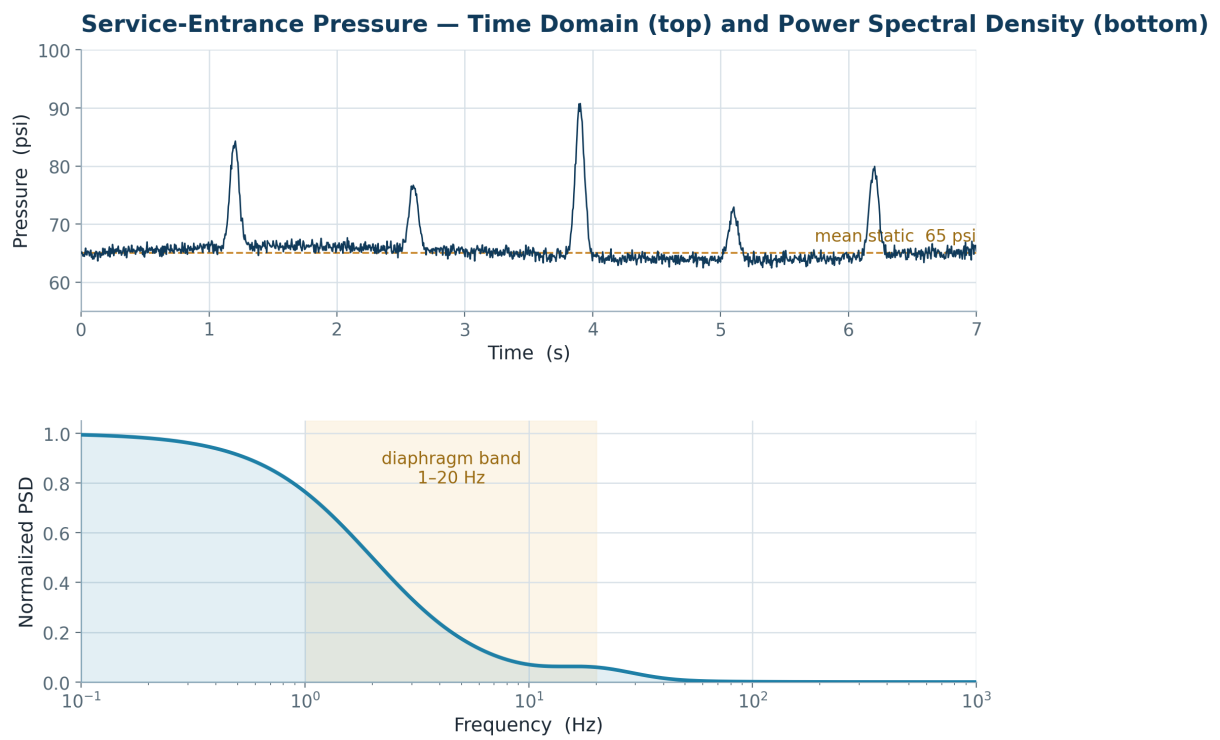

FIGURE 3.1 Time-domain pressure log (top) and power spectral density (bottom). The PSD identifies the frequency band most coupled to downstream equipment. Transient loggers per AWWA WITAF #4660 (2017).

ENGINEERING INTERPRETATION	High-frequency pressure logging at the service entrance resolves the broadband signal that downstream components actually receive — including transient events that would be invisible to a Bourdon gauge.
DESIGN IMPLICATION	Baseline transient profiling at the service entrance is a prerequisite to any quantitative before/after evaluation of an upstream conditioning intervention.

3.1 Turbulent wall-pressure spectrum

In a fully-developed turbulent pipe flow the wall-pressure spectrum is broadband, with characteristic frequencies set by the bulk velocity divided by the pipe diameter. For a 6-inch pipe at 8 ft/s, dominant turbulent-eddy frequencies lie in the 1–100 Hz band, with energy distributed across roughly two decades. The pressure-spectrum amplitude scales with ρv² and is typically 0.5–3% of the mean static pressure (Bull, 1996; Goody, 2004). For a 65 psi system, that is 0.3–2.0 psi of broadband fluctuation around the mean. Modal analysis of buried pipework (Liu et al., 2014, J. Sound Vibration) confirms that this pressure spectrum couples efficiently into bending- and shell-mode pipe vibration. The wall-pressure spectrum is present at every wetted surface in the network and contributes to the cumulative fatigue duty on every dynamic component.

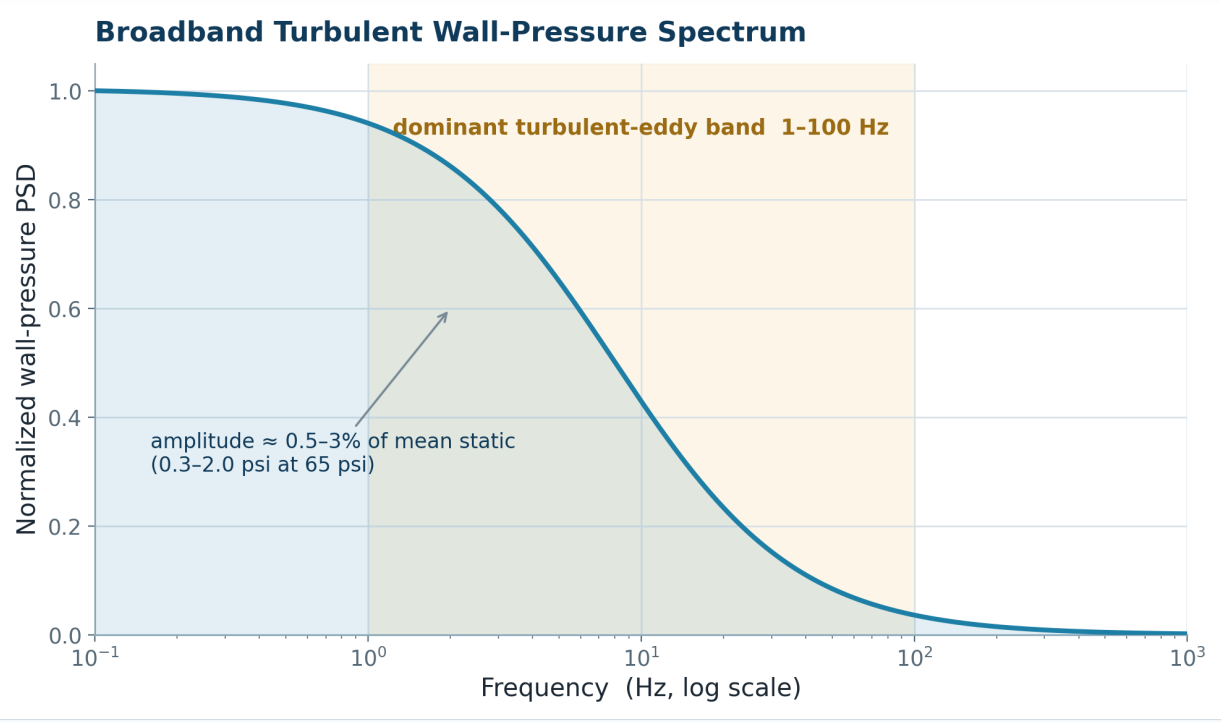

FIGURE 3.1A Broadband turbulent wall-pressure spectrum. Energy is distributed across the 1–100 Hz band at an amplitude of roughly 0.5–3% of mean static pressure. After Bull (1996); Goody (2004).

3.2 Discrete transient events and their distribution

Sub-second pressure events dominate the upper tail of the pressure distribution. A typical commercial building experiences hundreds of valve-closure events per day across solenoids, mixing valves, fixtures, and irrigation controllers. Each closure produces a small pressure transient; collectively, they generate hundreds of measurable pressure excursions of 5–30 psi above static per day. Stephens et al. (2008) reported that 95% of distribution-system pressure transients in a U.S. municipal network were below 30 psi peak, but the upper 1% exceeded 60 psi above static — and the upper 0.01% exceeded the pipe rating. AWWA WITAF #4660 (2017) found similar distributions in fourteen utility systems. Long-term pipe and component fatigue is driven by the cumulative count of these events, not by the rare extreme transient.

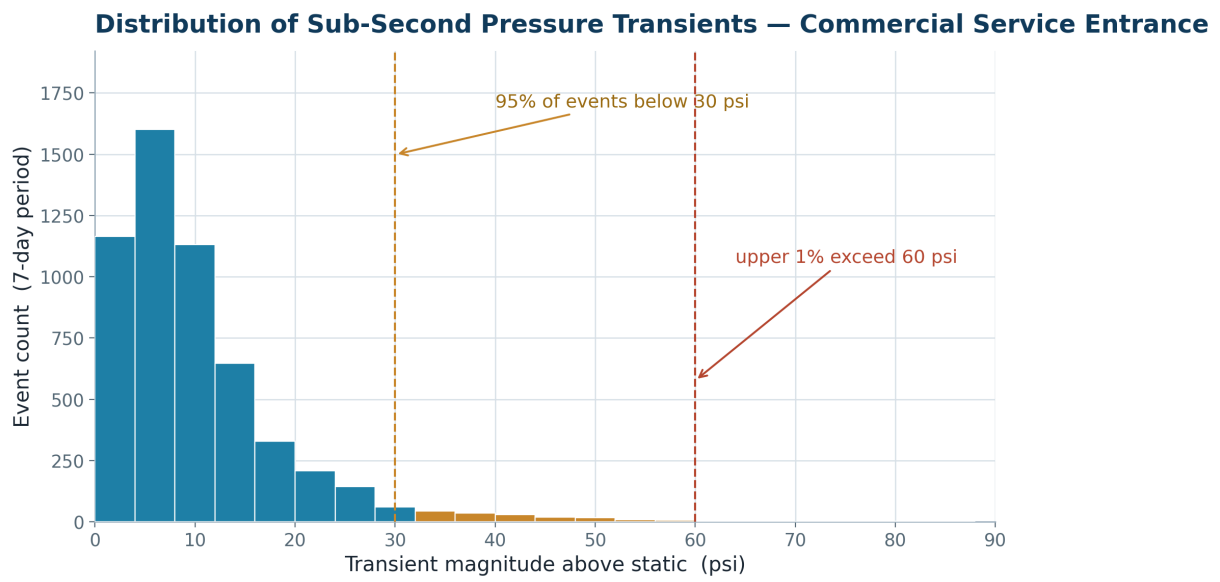

FIGURE 3.2 Representative distribution of sub-second pressure transients over a 7-day period at a commercial service entrance. Most events are small; the upper tail dominates fatigue accumulation. After Stephens et al. (2008); AWWA WITAF #4660 (2017).

PRACTICAL IMPLICATION · SECTION 3

- Service-entrance pressure is a broadband time-varying signal, not a steady value.
- Pressure-spectrum amplitude is typically 0.5–3% of mean static, equivalent to 0.3–2.0 psi at 65 psi static.
- Sub-second transients of 5–30 psi above static occur hundreds of times per day in typical commercial service.
- Cumulative cycle count drives long-term fatigue duty; the upper-tail transient distribution defines acute exposure.

3.3 Time domain versus frequency domain interpretation

The time-domain record provides the peak and envelope of every transient event. The frequency-domain representation (power spectral density, PSD) identifies the frequency bands that contain the most pressure-signal energy. The two views are complementary: peak transients drive single-event failure modes, while the broadband spectrum drives cumulative fatigue. Equipment classes are sensitive to different bands. Solenoid valve diaphragms respond to the 1–20 Hz pulsation band; mechanical-seal face films respond to the 50–500 Hz band; pipe-system structural fatigue responds to the 0.5–5 Hz band that includes typical building structural resonances. The PSD is the engineering tool that maps the signal to the affected component class.

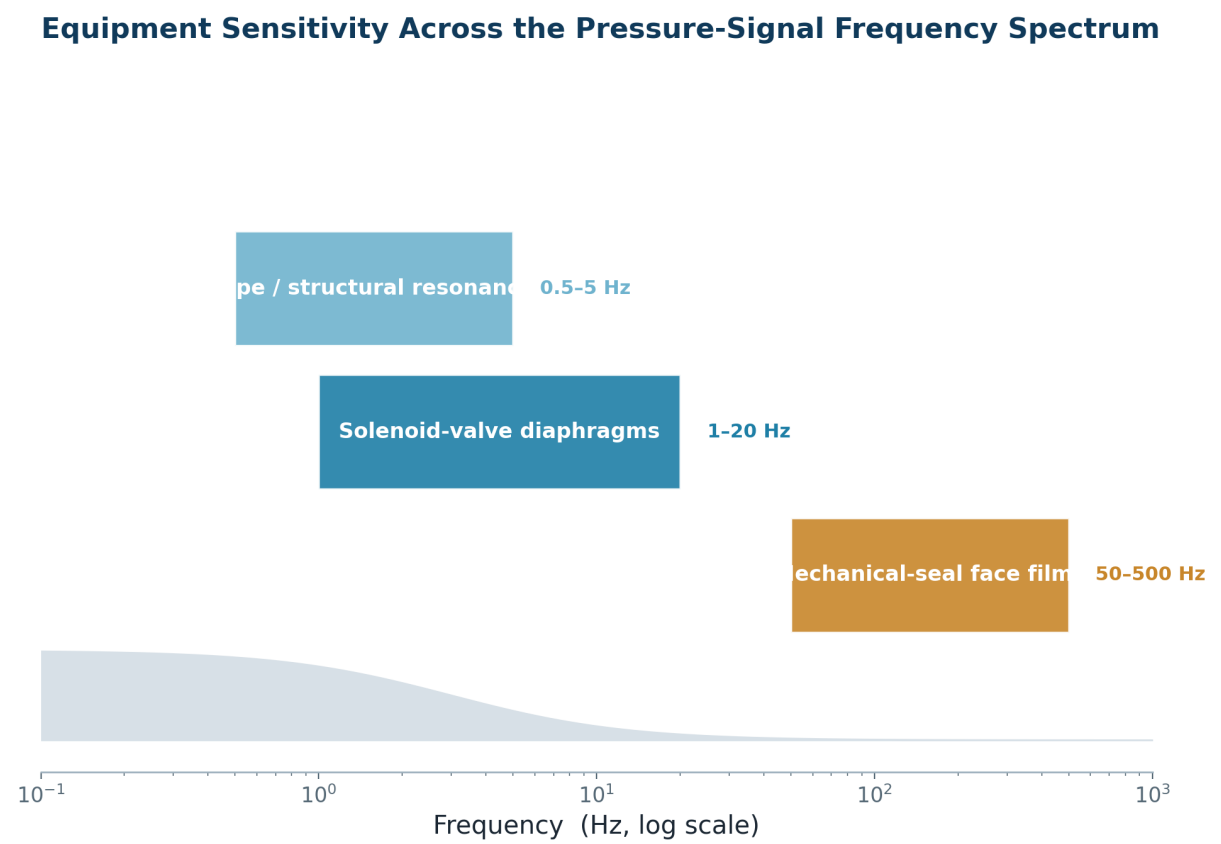

FIGURE 3.3 Equipment sensitivity mapped across the pressure-signal frequency spectrum. Each component class couples to a distinct band of the broadband signal; the PSD identifies which band dominates a given failure mode.

METERING PERSPECTIVE	The frequency-band map is the diagnostic bridge between a measured PSD and the affected hardware: a dominant 1–20 Hz peak implicates solenoid diaphragms; a 50–500 Hz peak implicates mechanical-seal films.
DESIGN IMPLICATION	Targeting an intervention to the dominant band — rather than the peak transient alone — is what reduces the failure mode that actually governs a given component class.

Entrained Air — Three States and Two-Phase Flow

Water in commercial service rarely contains zero gas. At municipal treatment plants water leaves typically saturated or near-saturated in atmospheric oxygen (7–12 ppm at typical service temperatures), nitrogen (12–18 ppm), and carbon dioxide (0.5–5 ppm depending on pH and alkalinity). Gas exists in three physically distinct states that interconvert continuously as pressure, temperature, and flow conditions change.

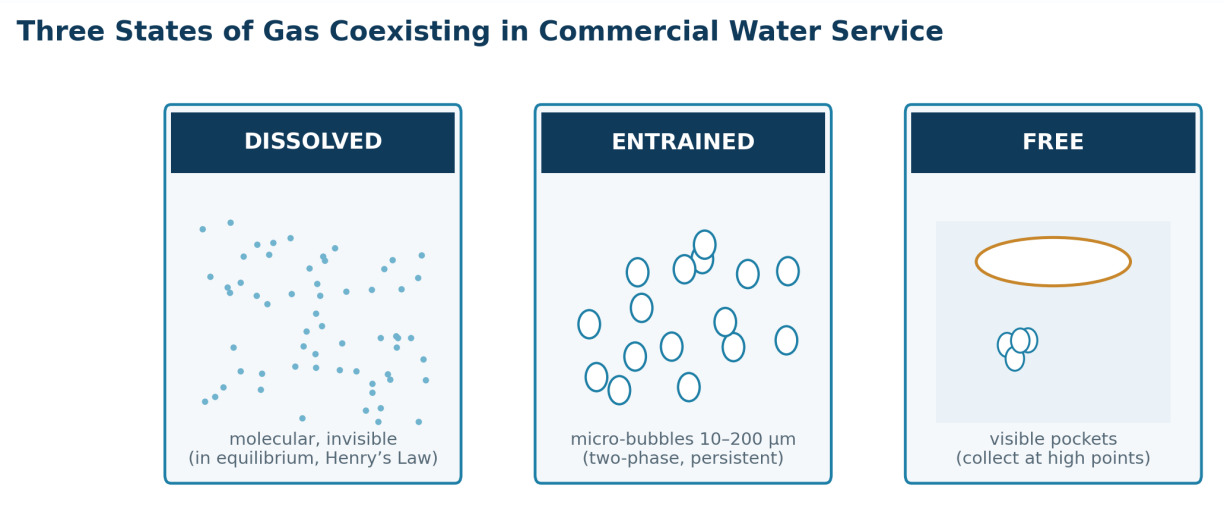

FIGURE 4.1 Three states of gas in commercial water: dissolved (molecular, invisible), entrained (micro-bubbles 10–200 µm), and free (visible pockets, typically at high points). After Wallis (1969); Whalley (1996); ASHRAE 2020.

4.1 Henry's Law and gas breakout

Henry's Law states that the equilibrium concentration of a dissolved gas in a liquid is proportional to the partial pressure of the gas in equilibrium with the liquid: $C = k \cdot P$, with k a temperature-dependent constant unique to each gas–liquid pair (Sander, 2015, Atmos. Chem. Phys. 15). The engineering consequence is precise: any local pressure reduction below saturation forces excess dissolved gas out of solution. The reduction can be modest — a PRV drop of 30–80 psi at a district boundary is sufficient to release a substantial dissolved-gas fraction as entrained micro-bubbles. Once released, the micro-bubbles persist as a two-phase flow for distances measured in hundreds of pipe diameters; re-dissolution requires recovery of equivalent partial pressure, a condition rarely met before the bubbles reach downstream equipment.

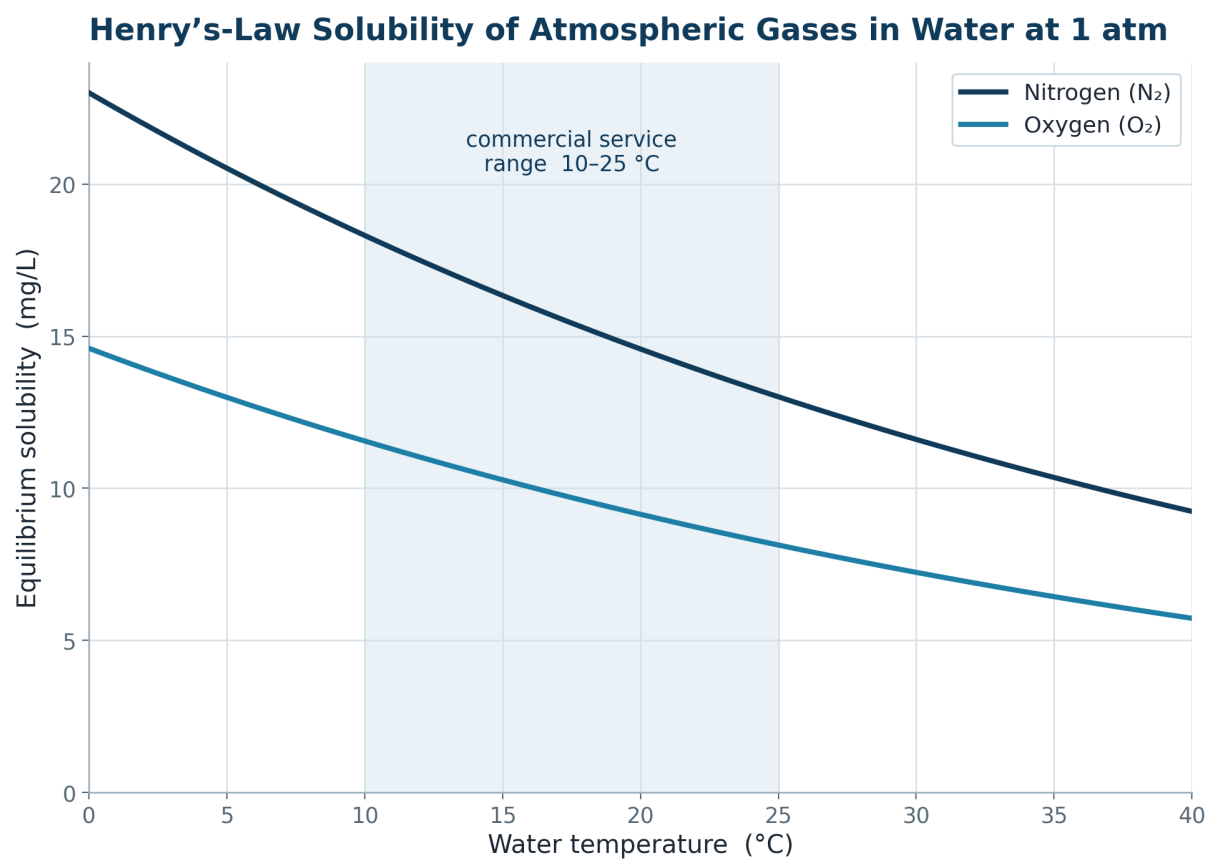

FIGURE 4.2 Henry’s Law solubility curves for atmospheric gases in water at 1 atm. Solubility falls with temperature; commercial service range 10–25 °C shaded. Constants from NIST; Sander (2015).

SOLUBILITY INTERPRETATION	Atmospheric gases dissolve into water in equilibrium with the partial pressure above the surface. In the typical commercial service range (10–25 °C) dissolved O_2 ≈ 8–11 mg/L and N_2 ≈ 14–18 mg/L.
DESIGN IMPLICATION	Any pressure-reduction event below saturation — a PRV drop, a hill-crest pressure minimum, a fitting recovery zone — forces the excess dissolved gas out of solution as entrained micro-bubbles that persist for hundreds of pipe diameters.

HISTORICAL ENGINEERING CONTEXT · HENRY’S LAW

Henry’s Law was formulated in 1803 and remains the modern reference for gas solubility — Sander (2015) catalogs constants for over 18,000 gas-liquid pairs. The same physics underlies API MPMS Ch. 5 crude-oil custody-transfer metering (the reason LACT skids exist) and the AWWA M51 air-valve sizing methodology.

4.2 Wood’s equation and mixture sound speed

A small free-gas content has a remarkable effect on the speed of sound in the mixture. Wood’s equation (Wood, 1930) gives the mixture sound speed a_mix as a function of void fraction α and the component properties. The function is non-monotonic

and is dominated by the compressibility of the gas phase even at very small α. At α = 0.3% the mixture sound speed collapses from approximately 1,480 m/s in pure water to roughly 200 m/s — a factor of 7× reduction (Karplus, 1958, Argonne ANL-4996; Crighton, 1985). At α = 5% the mixture sound speed is approximately 70 m/s. The dependence is independent of bubble size for bubbles smaller than the acoustic wavelength.

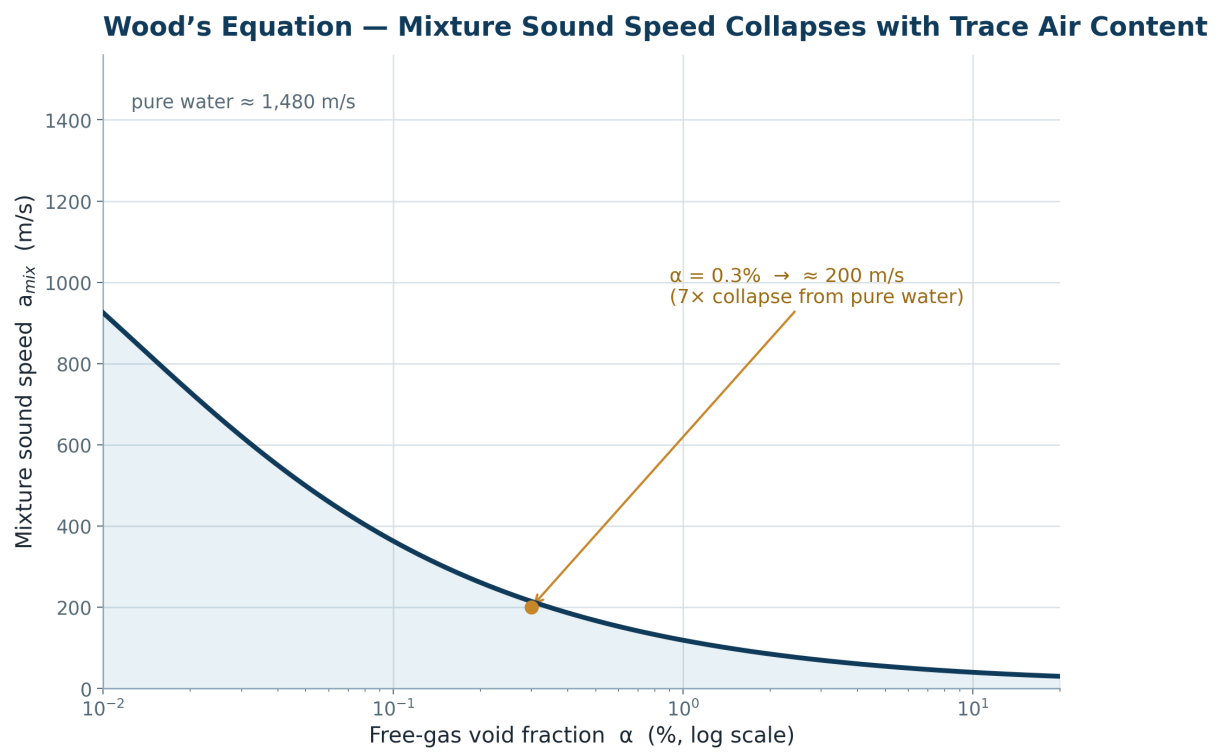

FIGURE 4.3 Wood's equation — mixture sound speed collapses with vanishingly small air content. The dependence is central to water-hammer surge calculation; ΔP = ρ·a·Δv scales linearly with a.

ENGINEERING INTERPRETATION	A void fraction of just 0.3% reduces the mixture sound speed by a factor of seven. Because the Joukowsky surge magnitude scales linearly with wave speed, even very small entrained-gas content materially alters transient behavior.
DESIGN IMPLICATION	Air management is a first-order parameter in surge analysis, not a secondary effect. AWWA M51 codifies this engineering position.

A NECESSARY CAUTION

Entrained air has a complex, direction-dependent effect on system dynamics. Modest air content lowers mixture wave speed and may reduce the Joukowsky surge peak, but it increases the susceptibility to column-separation collapse events. AWWA M51 codifies the engineering position: manage air rather than rely on it. Removing all air is neither realistic nor universally desirable; the engineering objective is to keep the system in a predictable, well-organized state.

4.3 Two-phase flow regimes

When gas and liquid share a pipe, the resulting flow organizes into one of several distinct regimes — bubbly, plug, slug, churn, annular, or mist — depending on the superficial velocities of each phase. The Taitel–Dukler (1976) and Mandhane et al. (1974) flow-regime maps are the canonical references for horizontal pipe. Each regime has a distinct velocity profile, a distinct pressure-drop signature, and a distinct effect on every class of flowmeter. Commercial water service operates in the low-α bubbly and plug regimes — the engineering domain in which entrained-air effects on meters, pumps, and valves are most consequential, and in which the two-phase mixture is essentially invisible to the naked eye.

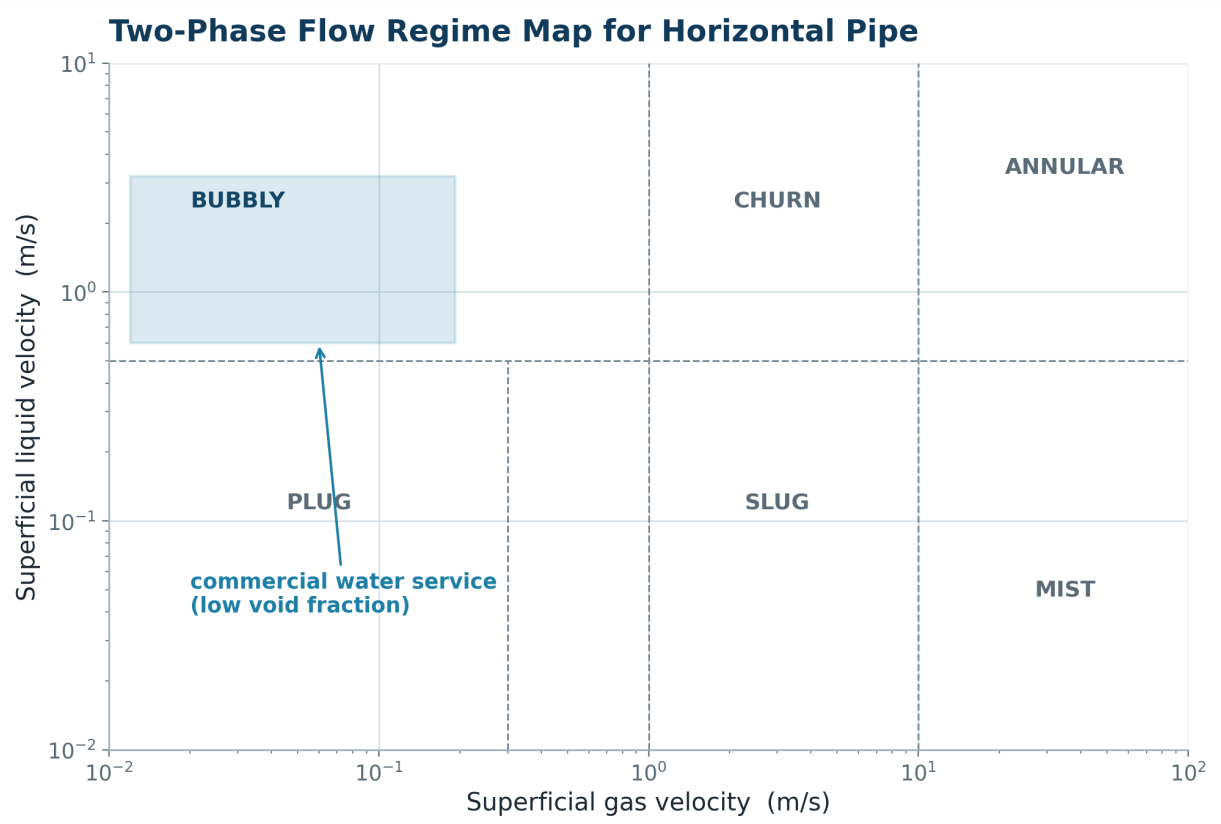

FIGURE 4.4 Two-phase flow regime map for horizontal pipe (Taitel–Dukler 1976; Mandhane et al. 1974). Commercial water service operates in the bubbly and plug regimes at low void fraction.

METERING PERSPECTIVE	Commercial water service sits in the low-α bubbly/plug corner — the regime where entrained-air effects on meters, pumps, and valves are most consequential and the two-phase mixture is invisible to the naked eye.
DESIGN IMPLICATION	Because the mixture is invisible at these void fractions, the only reliable indication is instrumentation — meter error, pump-suction pressure, or a dissolved-gas measurement — not visual inspection.

The engineering position embedded in API MPMS Chapter 5 (Liquid Metering) is that single-phase, fully-developed flow at the meter inlet is a prerequisite for the published meter-class accuracy. Once even a small void fraction is present, every meter type — positive displacement, turbine, ultrasonic, electromagnetic, or Coriolis — reports a value that differs from the

actual liquid mass passing through. The same engineering judgment carries to other downstream components: pumps, heat exchangers, control valves, and instrumentation all respond differently to a two-phase inlet than to the single-phase calibration condition.

Cavitation Theory and Erosion Mechanisms

Cavitation is the formation and subsequent collapse of vapor cavities in a flowing liquid when local static pressure drops below the liquid vapor pressure (Brennen, 1995, “Cavitation and Bubble Dynamics,” Oxford). The phenomenon is fundamentally different from gas entrainment: cavitation involves a liquid-to-vapor phase change of the working fluid itself, with the resulting cavity containing essentially pure vapor at saturation pressure. When the cavity is convected to a region of higher static pressure, the vapor condenses and the cavity collapses. The collapse is asymmetric in the presence of a nearby solid surface — the side facing the surface accelerates more slowly than the opposite side, producing a high-velocity liquid micro-jet that impinges the surface (Plesset & Chapman, 1971; Tomita & Shima, 1986). Reported micro-jet velocities at collapse are typically in the range 100–500 m/s under reasonable assumptions about the local pressure history.

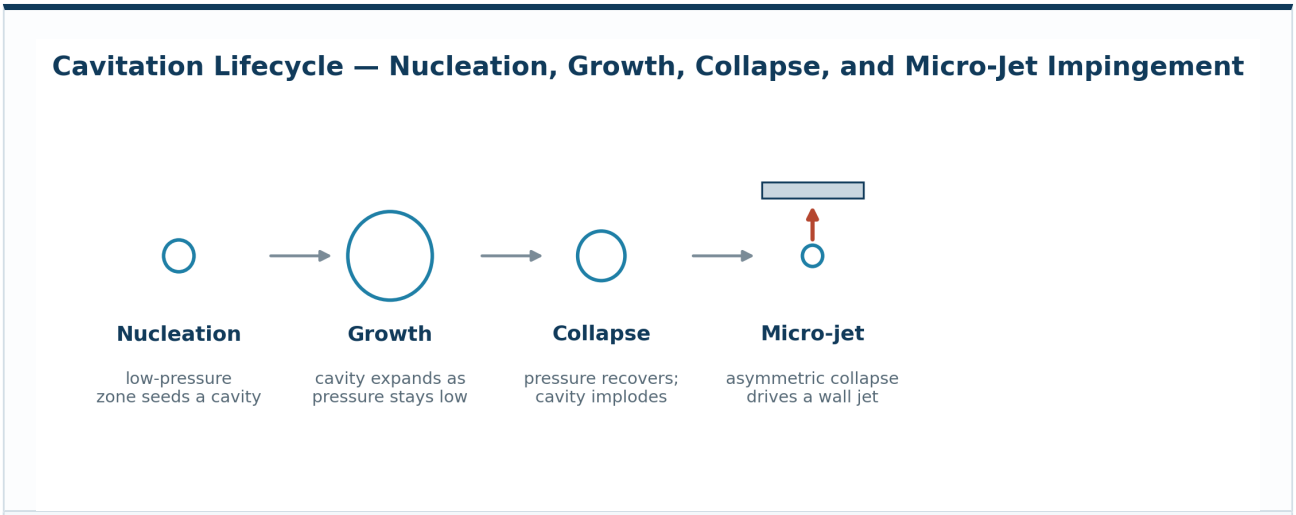

FIGURE 5.1 Cavitation lifecycle — nucleation, growth, asymmetric collapse, micro-jet impingement. The mechanism is distinct from gas entrainment, although the two coexist in commercial water systems.

5.1 The cavitation number

The dimensionless cavitation number σ = (P − P_v) / (½ρU²) characterizes the propensity for cavitation in a flowing system. Cavitation inception (the first appearance of vapor) occurs at a critical value σ_i; cavitation that produces a 3% head drop in a pump (the industry definition of operating cavitation) occurs at σ_3, typically a factor of 2–4× lower than σ_i (Brennen, 1994, “Hydrodynamics of Pumps”). Erosive cavitation — the regime producing measurable mass loss on the surface — corresponds to σ values lower still, with the relationship between σ and erosion rate non-linear and material-dependent. ANSI/HI 9.6.1 (2024) codifies the NPSH-margin requirement that establishes acceptable σ for pump service: minimum margin of 0.6 m or 10%, whichever is greater, with full cavitation suppression requiring NPSH-margin ratios of 1.5–4.0 across application classes.

Cavitation Bubble Dynamics — Rayleigh–Plesset Response and Micro-Jet Impingement

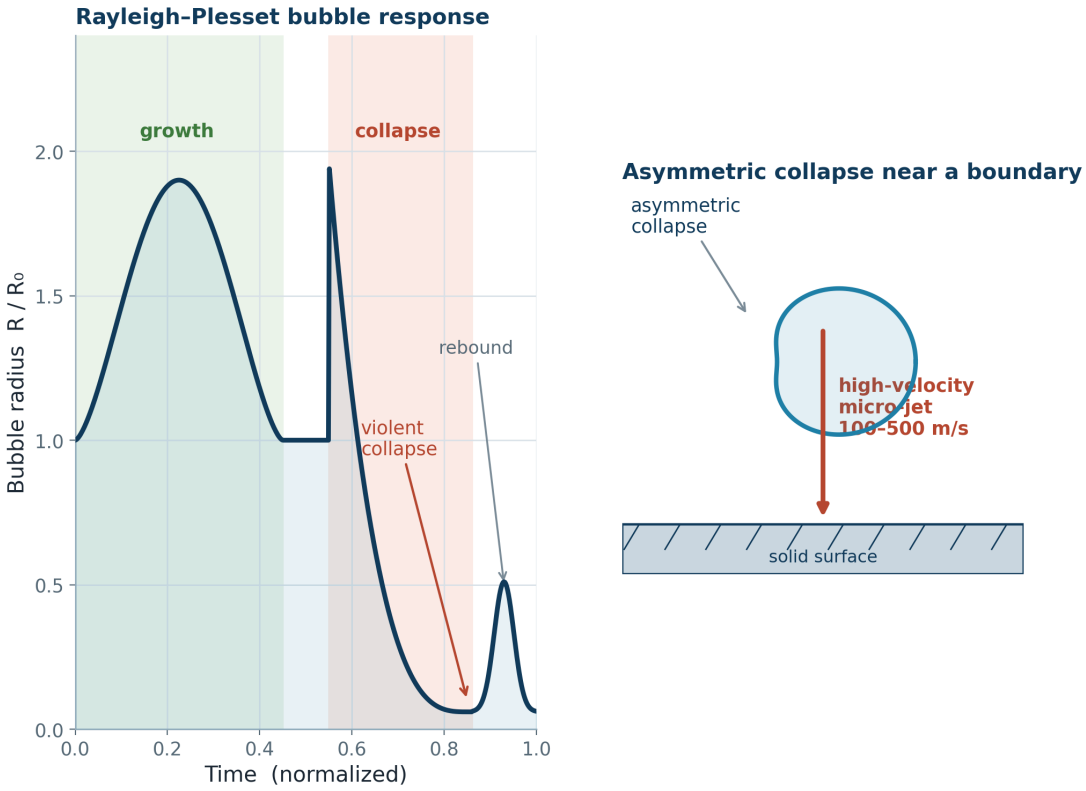

FIGURE 5.1A Cavitation bubble dynamics — Rayleigh–Plesset radius response (left) and asymmetric collapse near a solid boundary producing a high-velocity micro-jet (right). After Rayleigh (1917); Plesset (1949); Brennen (1995).

100–500 m/s	**µs scale**	**GPa local**
reported micro-jet velocity at collapse	collapse occurs on a microsecond timescale	transient impact pressures at the surface

MECHANISM INTERPRETATION	The collapse is violent and asymmetric whenever a solid surface is nearby: the far side accelerates faster, driving a liquid micro-jet straight into the wall. Repeated impingement is what removes material.
EQUIPMENT IMPACT	Impeller vanes, valve seats, and pump casings are the surfaces this jet strikes. Erosion resistance (Figure 5.3) and inflow conditioning together set the service life.

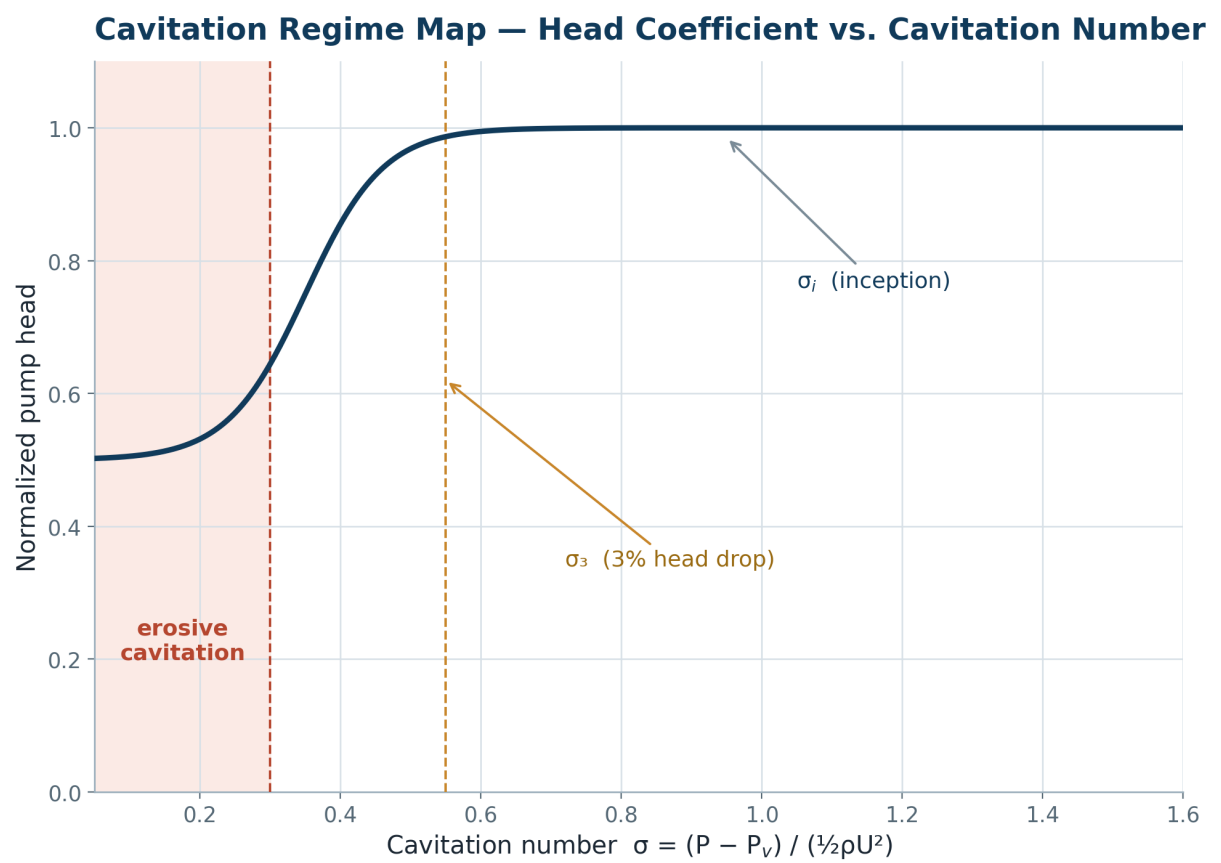

FIGURE 5.2 Cavitation regime map — head coefficient vs. cavitation number. Cavitation inception (σ_i), 3% head-drop (σ_3), and erosive-cavitation regions identified. After Brennen (1994).

ENGINEERING INTERPRETATION	Pump head remains essentially flat at σ above σ_i, then degrades through the 3% head-drop point at σ_3 and into the erosive regime at lower σ. The cavitation-number gap between inception and 3% head drop is typically a factor of 2–4.
DESIGN IMPLICATION	Operating on the steep portion of the curve — even at acceptable nameplate margin — exposes the impeller to cavitation damage that does not appear in the pump performance test.

5.2 Erosion rates by material

Cavitation erosion rates have been measured systematically for engineering materials using the ASTM G32-16 vibratory cavitation test, which specifies a 19.5 kHz, 50 µm amplitude horn submerged in a controlled liquid. Hammitt (1980), Heymann (1992), and subsequent literature established that 316L stainless steel exhibits erosion rates approximately 200% lower than mild carbon steel; duplex 2205 and Stellite 6 represent practical industry references for severe service. Aluminum alloys, despite high yield strength in some grades, are particularly susceptible to cavitation erosion because the protective oxide film is repeatedly removed by micro-jet impingement (Chiu et al., 2005, Wear).

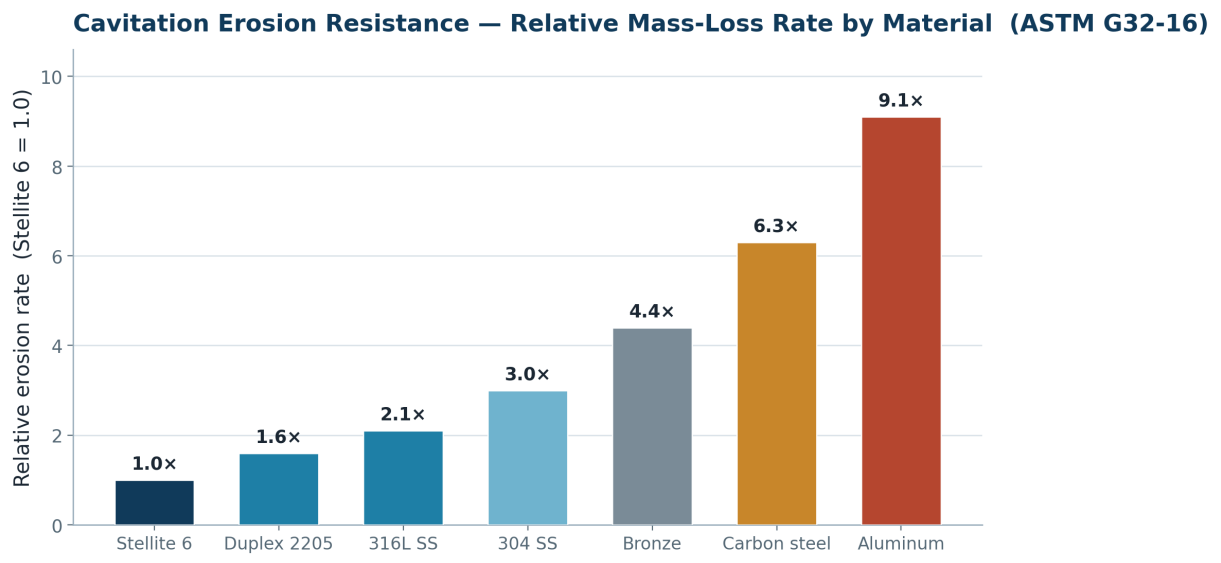

FIGURE 5.3 Relative cavitation erosion rates by material (Stellite-6 reference = 1.0). ASTM G32-16 vibratory test. Data compiled from Hammitt (1980), Heymann (1992).

MATERIAL SELECTION	316L stainless resists cavitation erosion roughly 3× better than carbon steel; duplex 2205 and Stellite 6 are the severe-service references. Aluminum is the worst performer despite high yield strength — its oxide film is stripped on each collapse.
EQUIPMENT-LIFE IMPLICATION	Where cavitation cannot be fully suppressed, wetted-surface alloy selection sets the erosion-limited service interval; 316L — the AquaFlow body material — is chosen for this erosion-resistance margin (ASTM G32-16).

5.3 Cavitation locations in centrifugal pumps

In a centrifugal pump, cavitation initiates predictably at locations where local static pressure is lowest: the impeller-eye recirculation zone at off-BEP operation, the leading edge of the suction-side blade, and the volute cutwater tongue. The locations are well characterized in the pump-engineering literature (Karassik et al., 2008, “Pump Handbook,” 4th ed., McGraw-Hill). Incipient cavitation depends on the upstream pressure signal, the entrained-gas content (which lowers the effective nucleation threshold), and the velocity-profile asymmetry at the impeller eye (which produces local low-pressure zones not present in the design analysis).

Asymmetric inflow from a single 90° elbow has been measured at the pump suction by Wang et al. (2020, Springer Applied Water Science) to reduce pump head by 4% and efficiency by 5.2% at the BEP. Liu et al. (2023, Physics of Fluids) reported efficiency reductions of approximately 8% under coupled-elbow inflow distortion. The same asymmetry that degrades efficiency increases the local low-pressure zone where cavitation initiates.

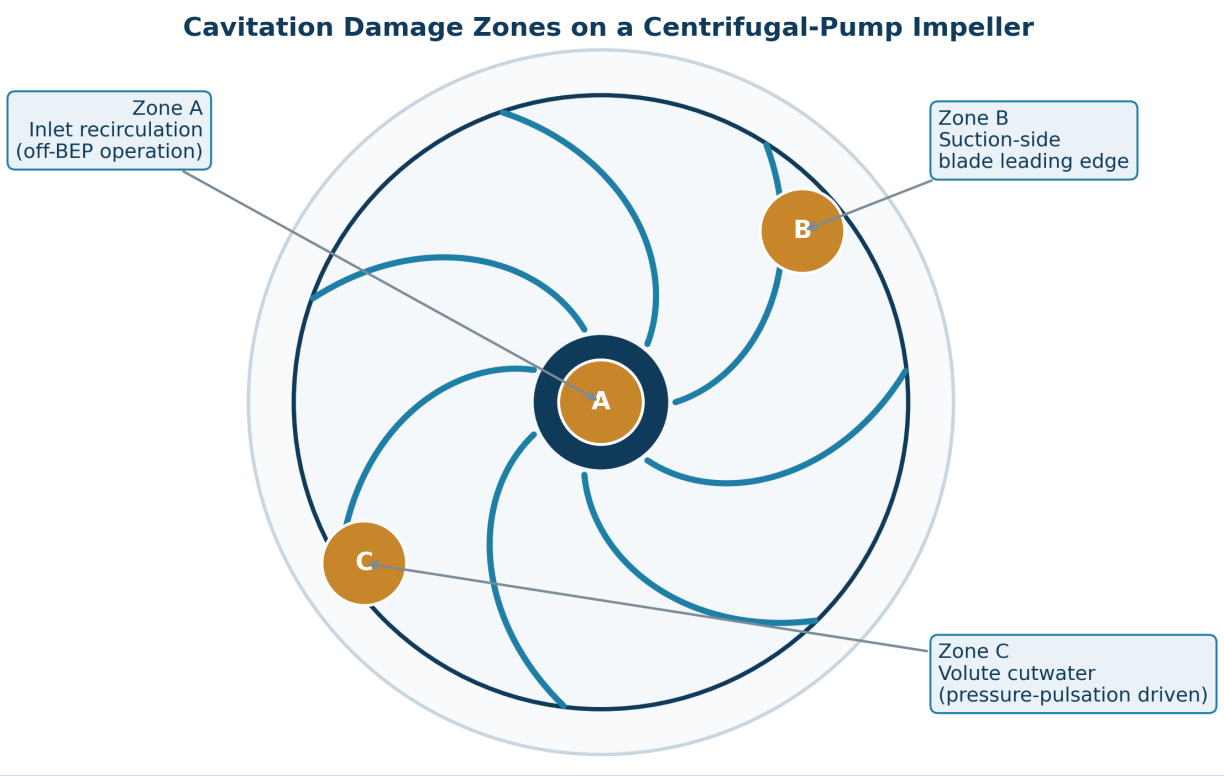

FIGURE 5.4 Cavitation damage zones on a centrifugal pump impeller. Zone A: inlet recirculation (off-BEP). Zone B: suction-side blade LE. Zone C: volute cutwater (pressure-pulsation driven). After Karassik et al. (2008); Brennen (1994); Hydraulic Institute (2017).

PUMP PERSPECTIVE	All three damage zones are seeded by the same upstream conditions — low inlet pressure, entrained gas, and profile asymmetry at the eye. They are the physical locations where the Section 5.1 cavitation number falls below σ_i first.
DESIGN IMPLICATION	Because the initiating conditions are set upstream of the pump, inflow organization influences damage at every zone simultaneously — it is not a single-point fix.

Water Hammer — Joukowsky Surge and Column Separation

Water hammer is the family of pressure transients produced when fluid velocity in a closed conduit changes rapidly. The classical analysis is due to Joukowsky (1898), who showed that for a sudden velocity change Δv, the resulting pressure surge ΔP is given by ΔP = ρ·a·Δv, where ρ is fluid density and a is the wave speed in the pipe-fluid system. Wave speed in a real piping system is less than the acoustic velocity in an unbounded fluid because the elastic compliance of the pipe wall increases the system's compliance; for typical commercial steel and ductile-iron piping, a is in the range 1,000–1,400 m/s; for PVC and HDPE, a falls typically to 300–600 m/s because the higher pipe-wall compliance lowers the system bulk modulus (Wylie & Streeter, 1993, "Fluid Transients in Systems," Prentice Hall). Even at modest velocity changes the resulting transient can be substantial.

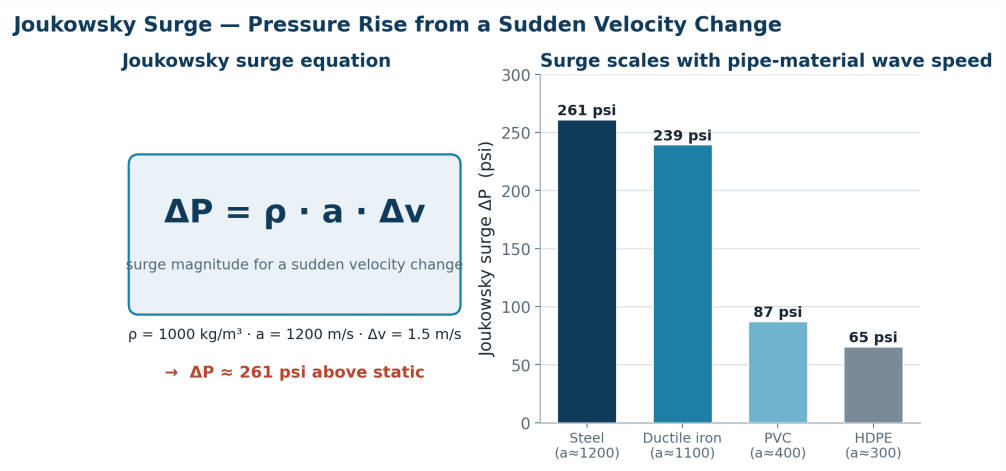

FIGURE 6.1 Joukowsky equation and its derivation. For ρ = 1000 kg/m³, a = 1,200 m/s, and Δv = 1.5 m/s, ΔP ≈ 261 psi above static. After Joukowsky (1898); Wylie & Streeter (1993).

ENGINEERING INTERPRETATION	The Joukowsky equation gives the upper-bound pressure surge for a rapid velocity change. The wave speed a is set jointly by the fluid bulk modulus, the pipe-wall elasticity, and the entrained-gas content of the fluid.
DESIGN IMPLICATION	Surge analysis on real systems requires the actual pipe-material wave speed (steel ~1,200 m/s, PVC ~400 m/s) and the actual fluid air content — published nameplate values may not match field conditions.

6.1 Method of characteristics and wave propagation

Surge propagation in a pipe network is governed by the one-dimensional unsteady momentum and continuity equations, which reduce to ordinary differential equations along characteristic lines dx/dt = ±a. The method-of-characteristics (MOC) is the canonical numerical scheme and is implemented in essentially every commercial surge-analysis package (AFT Impulse, KYPipe Surge, Bentley HAMMER, Hytran). MOC analysis reveals the structure of pressure-wave reflection and re-reflection

following a valve closure: the initial surge travels upstream at +a, reflects at the boundary, returns downstream at −a, and produces secondary minima and maxima at wave-period intervals 2L/a until energy dissipates. For a 500 m main, the wave period is approximately 0.7 s; for a 3 km transmission main, 4 s. The repeated cycling is a principal source of fatigue damage to downstream equipment.

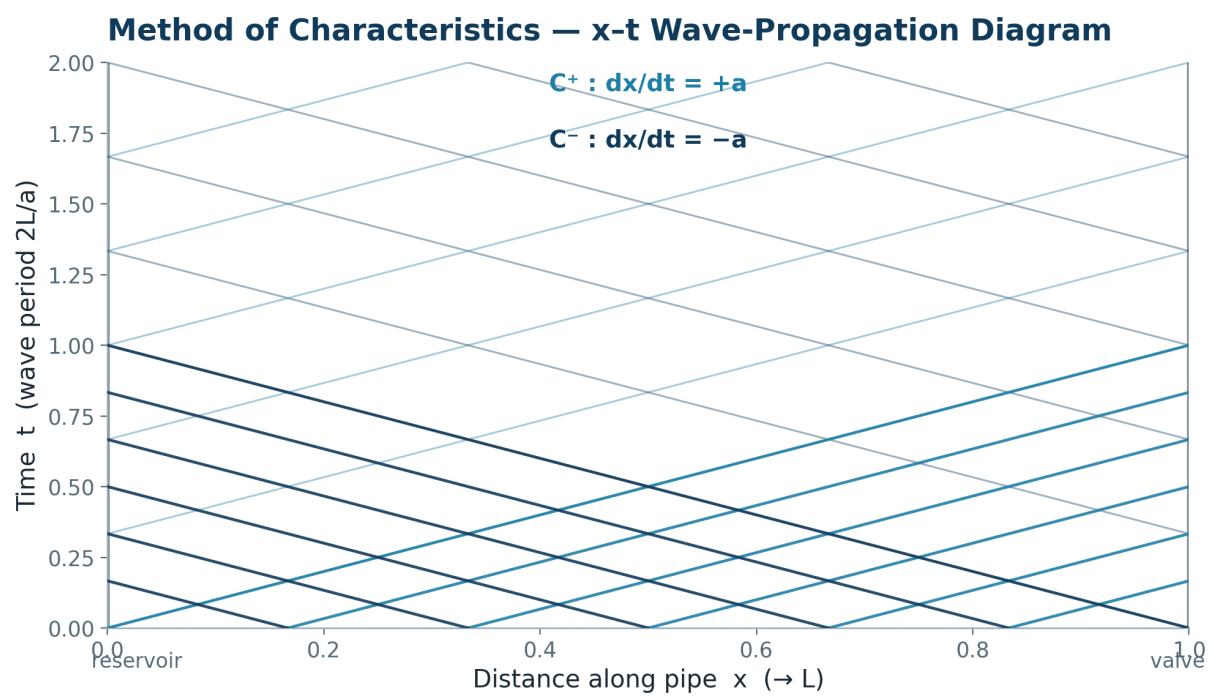

FIGURE 6.2 Method-of-characteristics x–t diagram. C+ and C− characteristic lines along which the unsteady PDEs reduce to ODEs. After Wylie & Streeter (1993).

ENGINEERING INTERPRETATION	The method of characteristics resolves the unsteady continuity and momentum PDEs along propagation lines at ±a, the local wave speed. Surge events propagate through a network as a sequence of reflections at boundaries (closed ends, open ends, pump stations, joints).
DESIGN IMPLICATION	The wave period 2L/a sets the time scale over which a transient repeats and dissipates. For a 500 m main at a = 1,200 m/s, the period is ≈ 0.83 s; for a 3 km main, ≈ 5 s. Every system has a characteristic surge timescale that drives the cyclic-fatigue duty on downstream components.

INDUSTRY RELEVANCE · SURGE ANALYSIS CODES

- Commercial MOC implementations include AFT Impulse, KYPipe Surge, Bentley HAMMER, and Hytran.
- Surge studies are standard practice for transmission mains, pump stations, and high-value distribution networks.
- AWWA M51 specifies the analytical framework; ASME B31.4/B31.8 for petroleum and gas analogs.
- Computational surge analysis is mature, but model fidelity depends on accurate wave-speed and air-content input.

6.2 Column separation and cavity collapse

When the low-pressure phase of a surge cycle drops local pressure below the vapor pressure of the liquid, a vapor cavity forms in the pipe. As the pressure recovers, the cavity collapses, and the two liquid columns re-join with an instantaneous velocity difference that produces a secondary Joukowsky surge often greater in magnitude than the original event. This is the column-separation phenomenon — historically the dominant failure mechanism in long pipelines subject to pump-station trip and rapid valve closure. Bergant et al. (2006, J. Fluids and Structures) documented over one hundred cases; the most cited is the 1950 Oigawa Power Station incident in Japan, in which a fast valve closure during draining produced a column-separation event that burst a 9-ft penstock, killed three workmen, and caused substantial damage. Tullis (1989) documented a 7,010-m, 500-mm pump-discharge pipeline destroyed by column separation following an electrical-power failure.

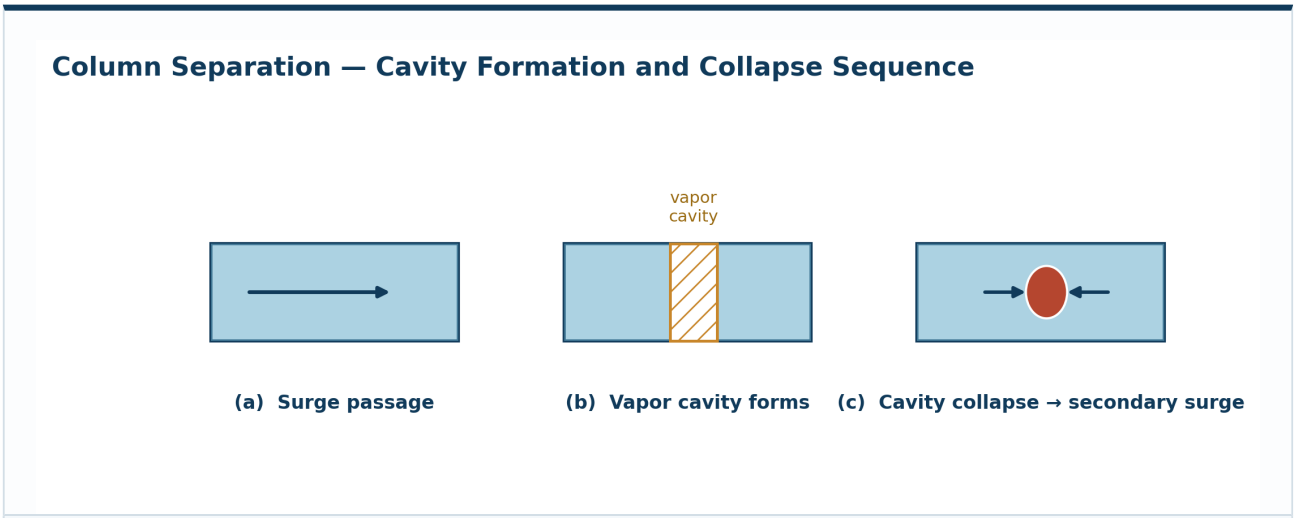

FIGURE 6.3 Column-separation sequence — surge passage, vapor cavity formation, cavity collapse. The secondary collapse transient may exceed the original surge. After Bergant et al. (2006).

PRACTICAL IMPLICATION · SECTION 6

- ΔP = ρ·a·Δv: for ρ = 1000 kg/m³, a = 1,200 m/s, Δv = 1.5 m/s, the Joukowsky surge is ~261 psi above static.
- Wave speed depends strongly on pipe material — steel 1,000–1,400 m/s; PVC/HDPE 300–600 m/s.
- Column-separation events may produce secondary surges exceeding the initial transient (Bergant et al., 2006).
- Upstream conditioning may reduce initiating velocity step and air content; it does not replace engineered surge protection.

Flow-Induced Vibration and Vortex Shedding

A flowing liquid drives the structure that contains it through several mechanisms. The first is broadband turbulent buffeting: the wall-pressure fluctuations of turbulent flow couple into bending- and shell-mode vibration of the pipe at all frequencies present in the wall-pressure spectrum (Bull, 1996). The second is periodic vortex shedding past a bluff body — a sensor probe, a thermowell, a heat-exchanger tube, or any irregularity in the flow path. The vortex-shedding frequency f is given by the Strouhal relation f = St·U/D, with St ≈ 0.21 over a broad range of Reynolds numbers from 10^3 to 10^5 (Schlichting & Gersten, 2017). When the shedding frequency coincides with a structural natural frequency, the resulting lock-in produces large-amplitude oscillation and rapid fatigue failure.

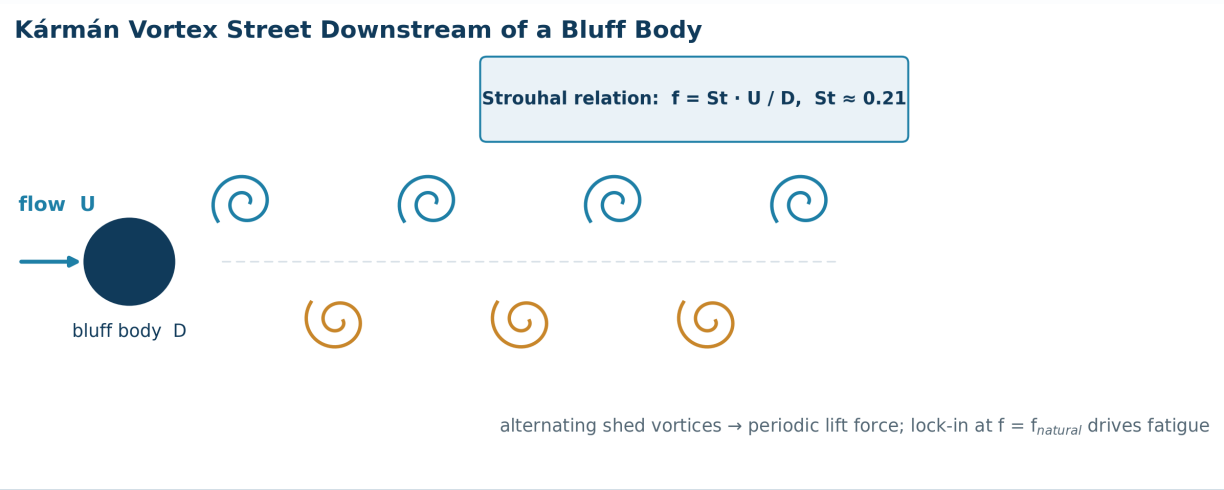

FIGURE 7.1 Kármán vortex street downstream of a bluff body and the Strouhal relation. Lock-in at f = f_natural produces fatigue failure. After Schlichting & Gersten (2017); ASME PVP proceedings.

7.1 Heat-exchanger tube vibration

The most consequential flow-induced-vibration mechanism in commercial-building equipment is cross-flow excitation of shell-and-tube heat-exchanger tubes. Three concurrent mechanisms operate: vortex shedding at St ≈ 0.21 (Païdoussis, 2014), turbulent buffeting (broadband), and fluidelastic instability above a critical gap velocity (Connors, 1970; Pettigrew & Taylor, 2003). The damage modes are fretting wear at the tube-support baffle holes (the location of highest contact stress) and ultimately tube fracture by fatigue. ASME Section III subsection NG-3133 and TEMA RGP-RCB-4 codify design criteria; failures remain common in service when the critical gap velocity is exceeded.

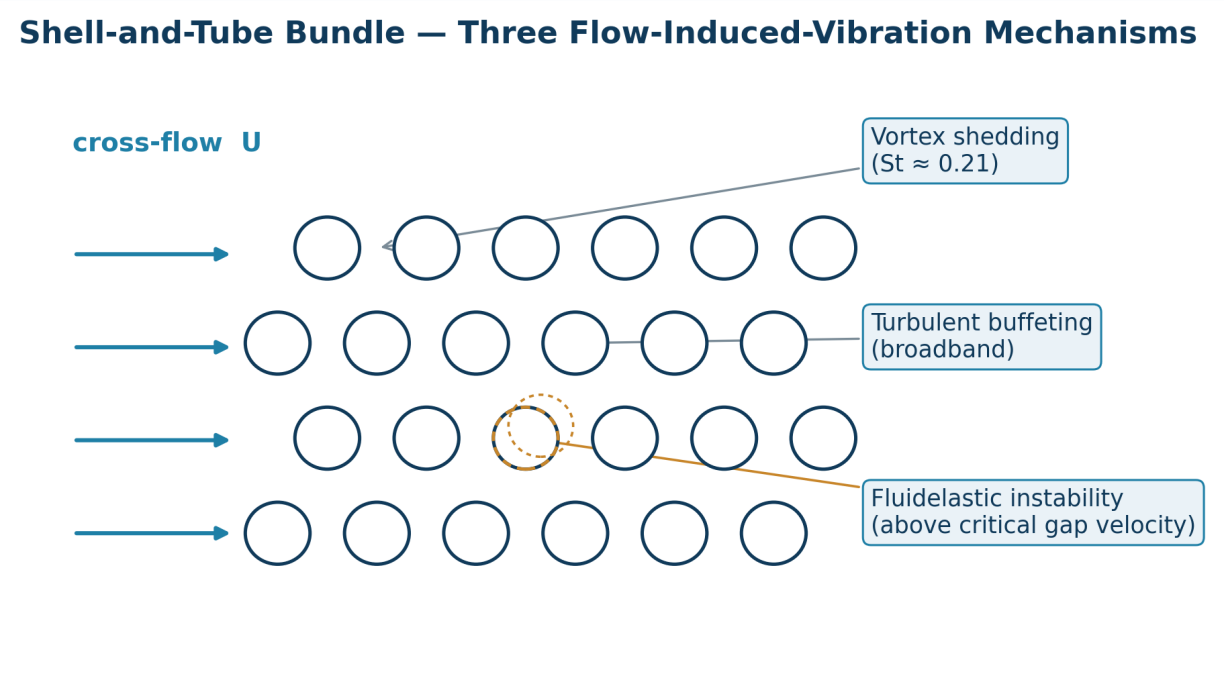

FIGURE 7.2 Heat-exchanger tube bundle geometry and three FIV mechanisms. Dashed displaced outlines indicate vibratory amplitude. After Païdoussis (2014); ASME PVP; Connors (1970); Pettigrew & Taylor (2003).

ENGINEERING INTERPRETATION	Cross-flow over a tube bundle excites three concurrent vibration mechanisms: periodic vortex shedding (St ≈ 0.21), broadband turbulent buffeting, and fluidelastic instability above a critical gap velocity. The damage signature is fretting at tube-support baffle holes and ultimately tube fracture by fatigue.
DESIGN IMPLICATION	TEMA RGP-RCB-4 and ASME Section III subsection NG-3133 set the engineering criteria. Field failures continue to occur when operating gap velocity exceeds the Connors threshold — particularly under pressure-pulsation amplification at the shell-side inlet.

REVIEWER NOTE · HX FIV FAILURE FREQUENCY

- Connors (1970) established the gap-velocity criterion for fluidelastic instability.
- Pettigrew & Taylor (2003) reviewed industrial failure statistics and confirmed FIV as a leading shell-and-tube failure mode.
- Vibration damage is not visible without disassembly; UT thickness measurement at baffle-hole contact is the standard NDT method.
- Upstream pressure-pulsation reduction at the heat-exchanger inlet may extend service interval between mandated tube-bundle inspections.

7.2 Pipe pressure-cycle fatigue

Long-term pipe and component fatigue is driven by the cumulative count of pressure-cycle events. The S–N curve for carbon-steel piping, codified in ASME Section VIII Div. 2 Annex 3.F, shows that at typical service-stress amplitudes (40–80

ksi) cycles-to-failure range from 10^5 to 10^7. At a system experiencing 100 pressure cycles per day, the cumulative cycle count over a 20-year service life reaches 7.3×10^5 — within the fatigue-damage region of the curve. Antaki (2003, “Piping and Pipeline Engineering”) documents a chemical-plant recirculation line that failed by pressure-cycle fatigue in 4.2 years from a 1.3-Hz pulsation source. The damage is not visible by external inspection and is detected only by ultrasonic thickness measurement at the location of crack initiation — typically a high-stress concentration point such as a weld toe or threaded joint.

7.3×10^5 cycles	**40–80 ksi**	**4.2 years**
cumulative count over a 20-yr life at 100 cycles/day	typical service-stress amplitude band on the S–N curve	documented pressure-cycle fatigue failure, 1.3-Hz source (Antaki 2003)

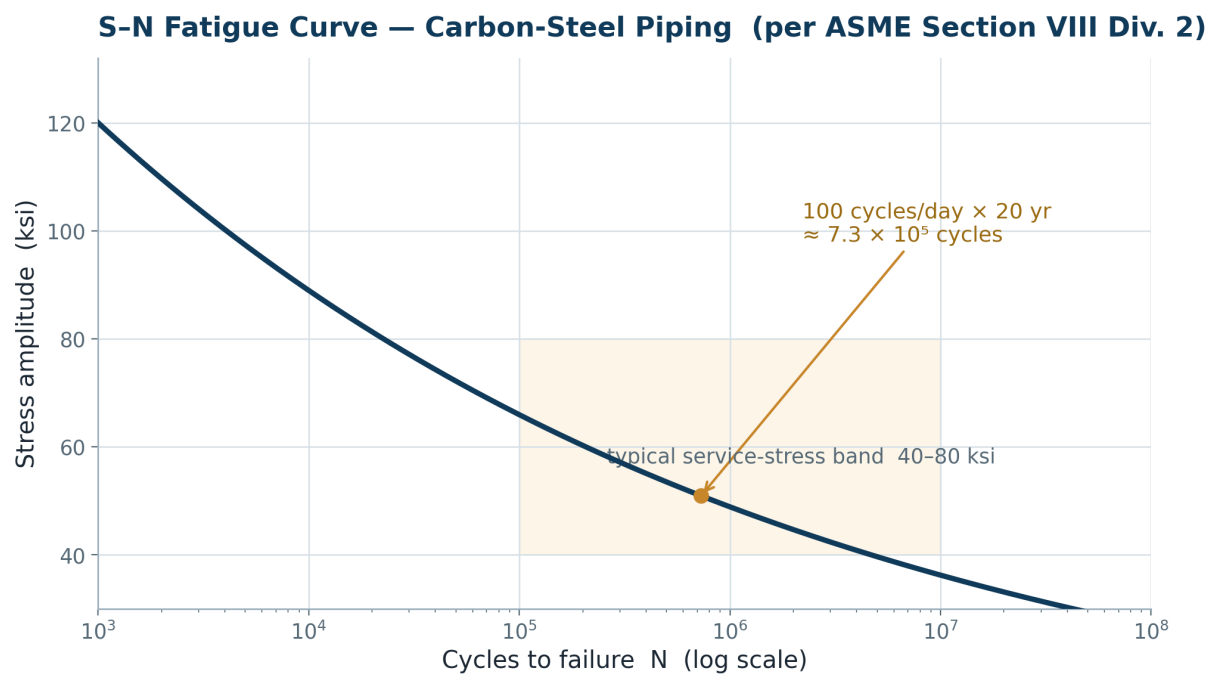

FIGURE 7.3 S–N fatigue curve for carbon-steel piping. Annotation marks cumulative cycle counts at representative event rates. The curve illustrates fatigue principles; commercial-system life depends on alloy, weld quality, stress concentration, and corrosion environment and is not predicted by a single curve. Per ASME Section VIII Div. 2.

ENGINEERING INTERPRETATION	Cumulative cycle counts in unconditioned commercial service reach the fatigue-damage region of the carbon-steel S-N curve within typical service-life time scales. Damage is invisible to external inspection.
DESIGN IMPLICATION	Pressure-cycle reduction at the service entrance is a fatigue-life intervention with effect proportional to cycle-count reduction, not transient peak reduction.

DESIGN CONSEQUENCE · SECTION 7

- Vortex shedding at St ≈ 0.21 produces lock-in when shedding frequency coincides with structural natural frequency.
- Three FIV mechanisms in HX tubes: vortex shedding, turbulent buffeting, fluidelastic instability (Connors criterion).
- Cumulative pressure-cycle counts of 10^5/year place commercial systems within the fatigue-damage region of the carbon-steel S-N curve.
- Fatigue damage is not visible by external inspection; detected only by UT at crack-initiation points (weld toes, threaded joints).

Effects on Centrifugal and Positive-Displacement Pumps

Centrifugal pumps are the highest-population, highest-cost dynamic component in most commercial water systems. Their service life is governed by a small set of failure modes, each of which is influenced by the upstream hydraulic environment.

8.1 Mechanical-seal failure modes

Mechanical-seal failure accounts for a substantial fraction of pump failures in process service. Of those, a substantial fraction fail before reaching design wear-out — they fail by mechanism rather than by wear (Flitney & Nau, 1990/1992, Univ. Southampton EPSRC; Bloch & Geitner, 1994, Machinery Failure Analysis). The representative root-cause distribution places dry-running, shaft vibration and deflection, pressure pulsation, shaft misalignment, and particulate contamination as the dominant categories. Three of the top four categories — vibration, pressure pulsation, and misalignment — are amplified by unconditioned upstream flow.

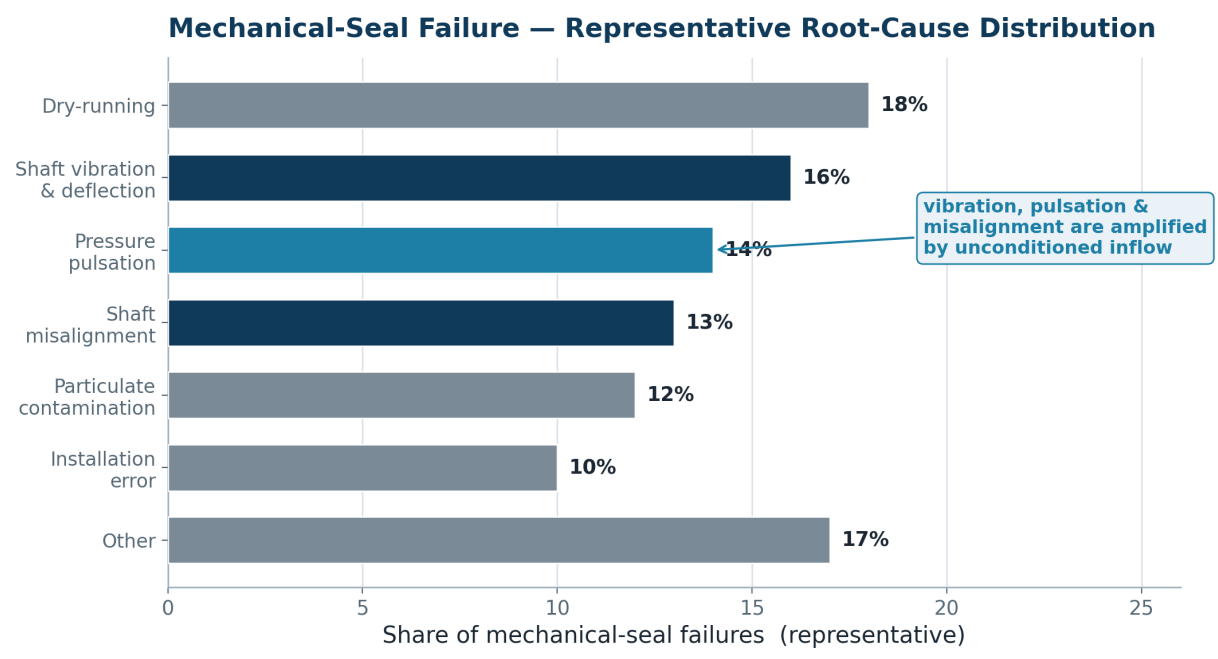

FIGURE 8.1 Mechanical-seal failure — representative root-cause categories. Exact percentages vary by industry, service, and installation; values are representative engineering estimates from Flitney & Nau (1990, 1992); Bloch & Geitner (1994).

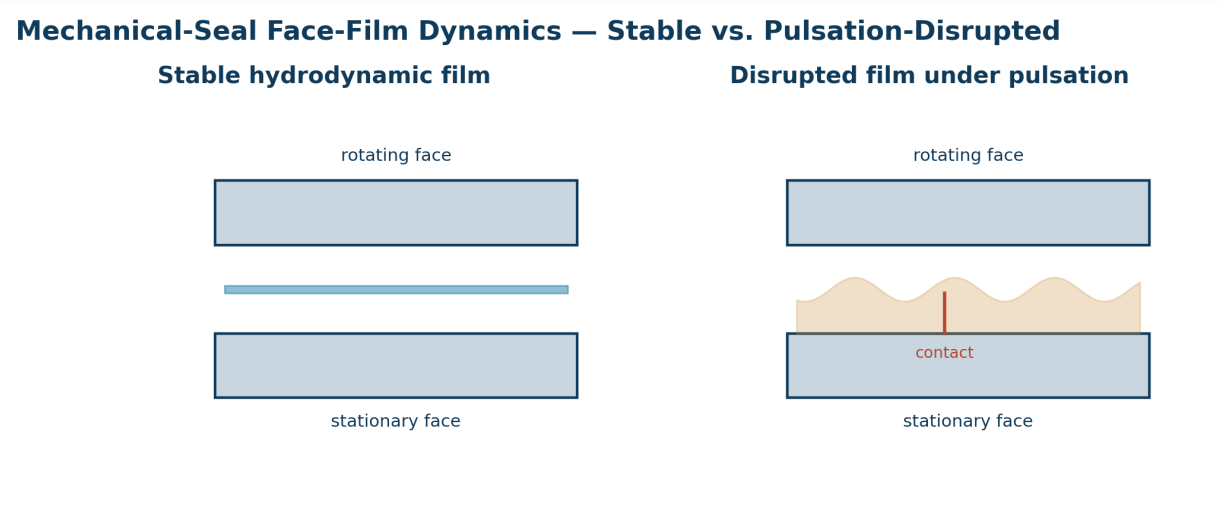

FIGURE 8.2A Mechanical seal face-film dynamics — stable hydrodynamic regime (left) vs disrupted film under pressure pulsation (right). After ANSI/API 682; Flitney & Nau (1990, 1992).

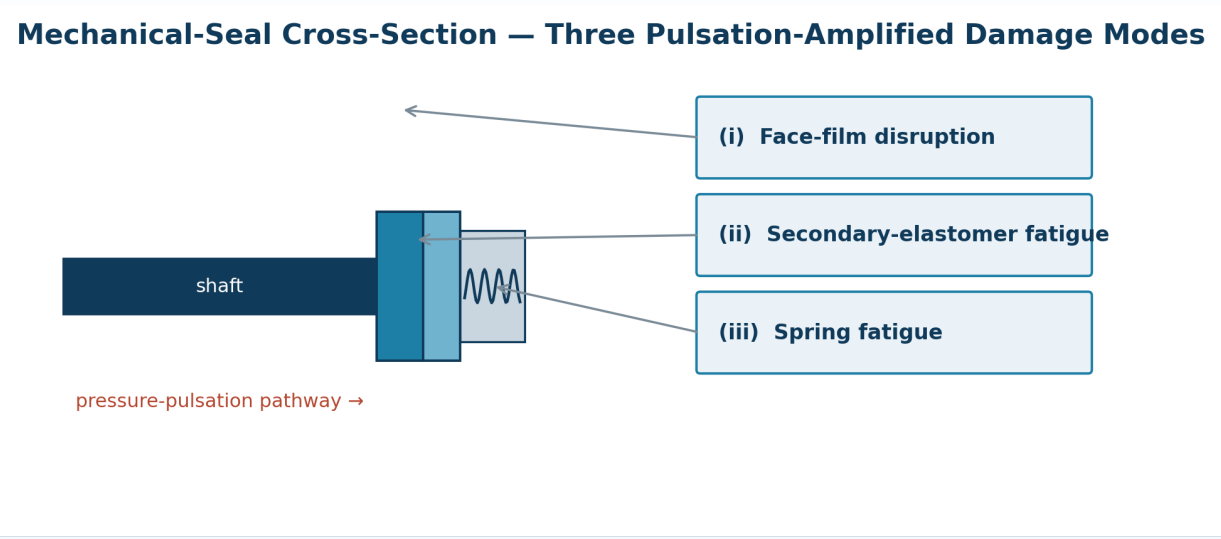

FIGURE 8.2B Mechanical-seal cross-section and pressure-pulsation pathway. Three damage modes amplified by upstream pulsation: (i) face-film disruption, (ii) secondary-elastomer fatigue, (iii) spring fatigue. After ANSI/API 682.

8.2 NPSH margin and inlet conditions

Cavitation in a centrifugal pump is governed by the NPSH balance at the impeller eye. ANSI/HI 9.6.1 (2024) provides the recommended margin: NPSH_a (available) must exceed NPSH_r (required) by a minimum of 0.6 m or 10%, whichever is greater. Full suppression of erosive cavitation requires NPSH-margin ratios of 1.5–4.0 depending on application class and rotational speed. Two field conditions reduce NPSH_a: (i) entrained gas in the suction line, which reduces the effective static head and seeds bubble nucleation, and (ii) pressure pulsation at the suction, where the instantaneous low pressure — not the time-average — governs cavitation onset. Both conditions are present in essentially every unconditioned commercial water system.

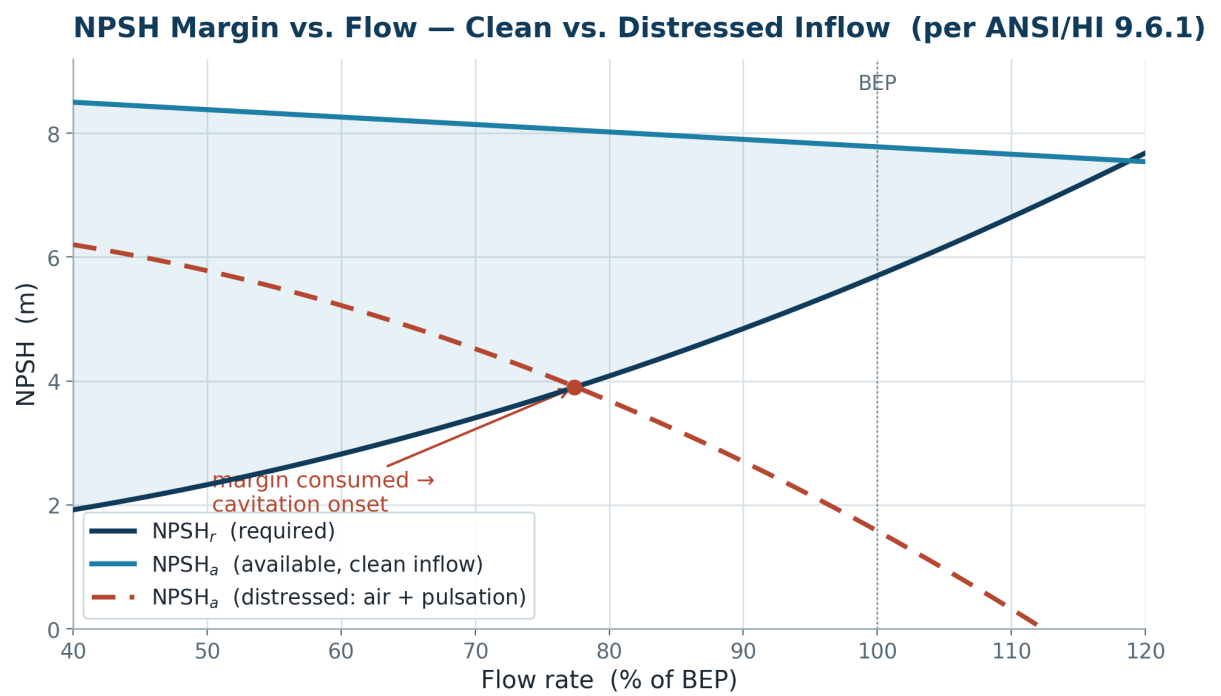

FIGURE 8.3 NPSH margin per ANSI/HI 9.6.1 (2024). Distressed inflow — entrained air plus pulsation — depresses NPSH_a near the BEP, narrowing the margin and entering the cavitation regime. Definitions in side panel.

ENGINEERING INTERPRETATION	The NPSH margin between NPSH_a and NPSH_r is the engineering buffer against cavitation. Distressed inflow — entrained air plus pressure pulsation at the suction — depresses NPSH_a and may consume the buffer near the BEP.
DESIGN IMPLICATION	NPSH-margin calculations performed at nameplate static head do not capture the dynamic depression caused by upstream disturbance. Field instrumentation at the pump suction is the only definitive measurement.

8.3 Asymmetric inflow and bearing radial loading

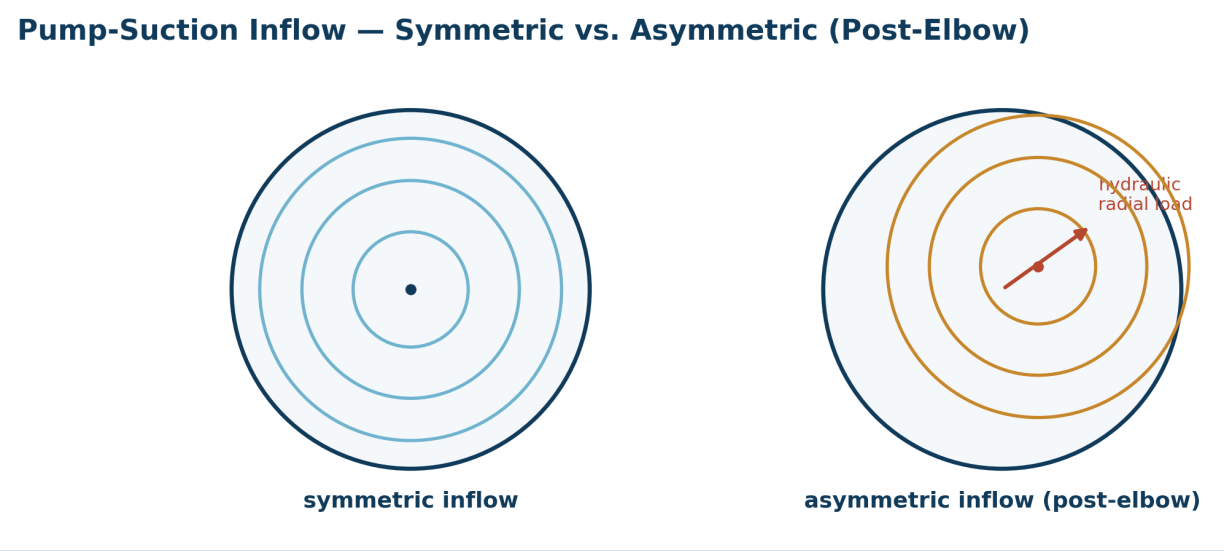

FIGURE 8.4 Pump suction inflow — symmetric (left) versus asymmetric, post-elbow (right). After Karassik et al. (2008); Brennen (1994). The asymmetric case produces non-uniform blade loading and a hydraulic radial load.

WHY THIS MATTERS · SECTION 8

- Mechanical-seal failure accounts for a substantial fraction of pump failures; vibration, pulsation, and misalignment dominate the root-cause categories.
- NPSH_a is depressed by both entrained gas and pressure pulsation at the suction; the instantaneous low value governs cavitation.
- Asymmetric inflow from a single 90° elbow reduces BEP head ~4% and efficiency ~5.2% (Wang et al., 2020); coupled elbows ~8% (Liu et al., 2023).
- The hydraulic radial load from asymmetric inflow is transmitted to seal and bearings at shaft frequency.

A pump impeller is designed for axisymmetric inflow at the eye. Velocity-profile asymmetry produced by a 90° elbow closer than 5–10 D upstream generates non-uniform blade loading and a hydraulic radial load on the impeller, transmitted to the mechanical seal and bearings on every rotation. Wang et al. (2020) measured a 4% head reduction and 5.2% efficiency reduction at the BEP under single-elbow asymmetric inflow; Liu et al. (2023) reported approximately 8% efficiency loss under coupled-elbow inflow distortion. The associated cyclic radial load on the bearings adds to the cumulative duty and contributes to bearing fatigue.

Effects on Valves, Solenoids, and Diaphragm Devices

Solenoid valves, pressure-reducing valves, backflow preventers, diaphragm valves, and check valves represent the highest-population control elements in commercial water systems. They share two structural features: an elastomeric or polymer diaphragm or seat that closes under pressure differential, and an actuation cycle that loads and unloads the seal on every operation. Each is degraded by upstream pressure pulsation and entrained air.

9.1 Solenoid valve diaphragm fatigue

Solenoid-valve diaphragm failure is one of the most common service-call categories in commercial laundry, car wash, irrigation, and process service. The literature attributes the dominant failure mode to overpressure events that produce tears in the diaphragm at the radial stiffening rib (manufacturer service literature: Tameson, Bürkert, Plast-O-Matic). Pressure spikes in commercial water systems have been documented at multiples of normal static pressure during transient events. Plastic solenoid-valve bodies subjected to repeated overpressure exhibit microscopic crack initiation at the body-to-bonnet interface, leading to slow seepage failures after 10^5–10^6 operating cycles. Manufacturers explicitly recommend upstream pressure regulators and surge dampers to mitigate these effects.

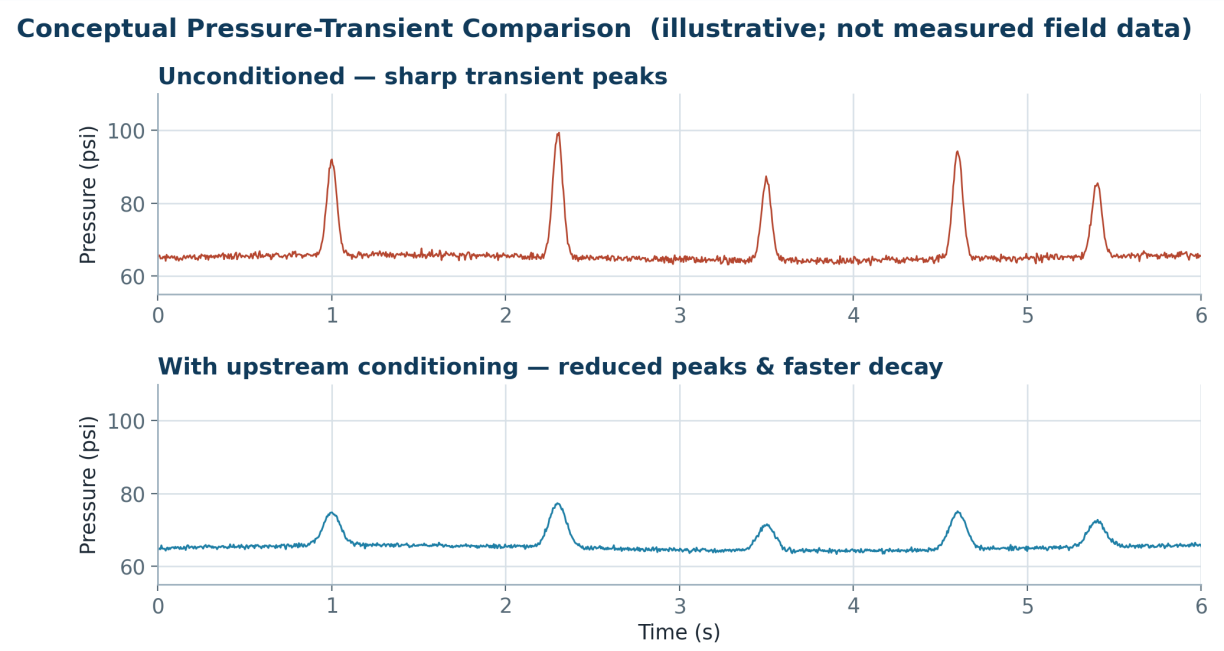

FIGURE 9.1 Conceptual pressure-transient comparison — unconditioned (top) and with upstream conditioning present (bottom). The traces illustrate the principle that reduced initiating pulsation and reduced wave-speed modifiers may lower peak surge and shorten envelope decay. Illustrative only; not measured AquaFlow field data.

9.2 Backflow preventers, PRVs, and check valves

Reduced-pressure backflow preventers (RPBPs) are tested annually under ASSE 1013 and USC FCCCHR protocols; their field failure mode is invariably spring fatigue or check-element seat wear, both pressure-cycle-driven. A typical RPBP installed at a commercial building service entrance experiences on the order of 10^4 pressure cycles per year under normal

service; under unconditioned service with multiple daily pump-cycle and PRV-cycle events, the cycle count can exceed 10^5 per year, accelerating fatigue. Pressure-reducing valves operate continuously at the boundary between two pressure zones and modulate in response to every dynamic pressure event. Manufacturers (Watts, Wilkins, Cla-Val) document accelerated stem-seal and pilot-line wear under unstable upstream pressure. Swing check valves accumulate hinge-pin and seat wear from every closing event; rapid check-valve slam following pump trip is the documented initiator of many distribution-system surge events.

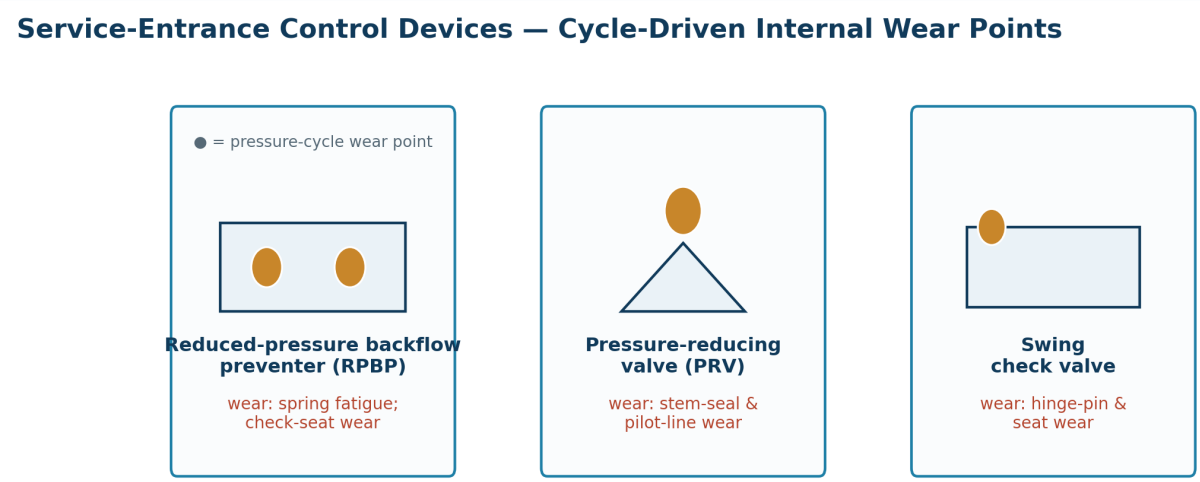

FIGURE 9.2 Service-entrance control devices — internal wear points. Cumulative pressure cycling at the rates typical of unconditioned service accelerates fatigue at the marked locations. After ASSE 1013; AWWA C512; manufacturer service literature.

Effects on Heat Exchangers, Boilers, and Cooling Loops

Heat-transfer equipment combines hydraulic loading with thermal loading. The same surfaces that transfer heat are also the surfaces most vulnerable to entrained-air-driven hot-spot scaling and pressure-pulsation-driven fatigue.

10.1 Entrained-air accumulation at heat-transfer surfaces

Entrained air in a heat-exchanger circuit accumulates preferentially at high points — the tops of vertical tube passes, the tops of cylindrical shell volumes, the tops of water heaters and storage tanks. Once accumulated, the air-filled volume presents no convective heat-transfer surface and produces a local hot spot in adjacent metal. The temperature gradient drives accelerated scale precipitation ($CaCO_3$ solubility decreases with temperature) and pit corrosion at the metal surface. ASHRAE Handbook—HVAC Systems & Equipment (2020) recommends air separators (Spirotherm, Taco, Armstrong) at the high points of hydronic loops for this reason. The same engineering principle applies to commercial domestic-water systems where the air ingress is upstream rather than internal but the consequence at the heat-transfer surface is the same.

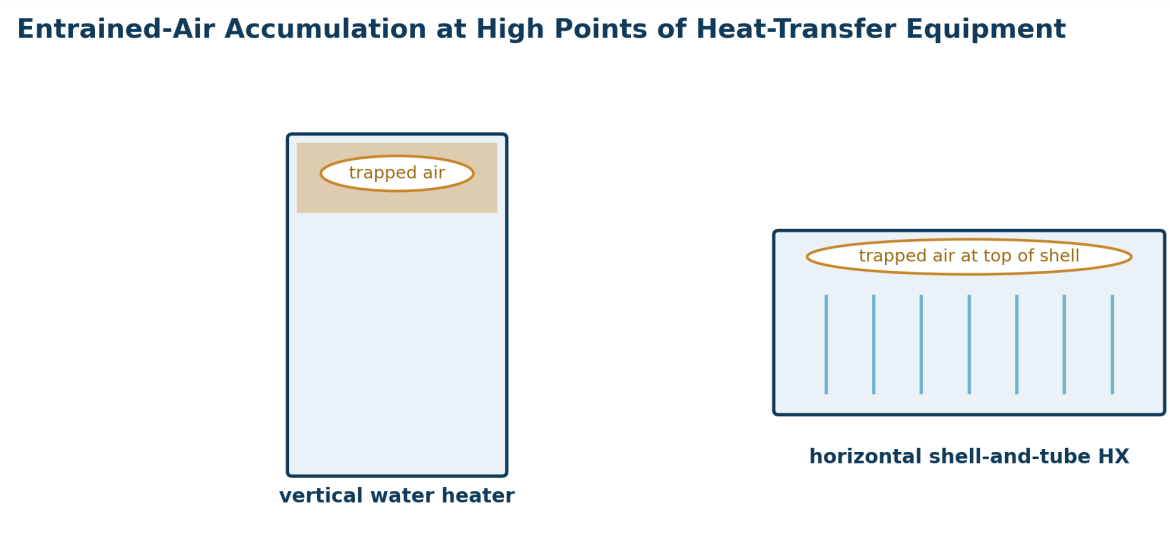

FIGURE 10.1 Entrained-air accumulation at high points of a vertical water heater (left) and a horizontal shell-and-tube heat exchanger (right). After ASHRAE Handbook (2020) Ch. 22.

10.2 Cooling-tower basin vortex and condenser-pump cavitation

A characteristic and well-documented failure mode in commercial cooling-tower service is air ingestion at the basin outlet vortex. When the suction connection is undersized for the flow rate, or when the basin water level is too low, a vortex forms above the suction nozzle and entrains air into the suction pipe (ASHRAE Handbook—HVAC Systems & Equipment 2020, Ch. 40; CTI STD-202; ANSI/HI 9.8). The entrained air is transported to the condenser water pump, where it produces noise, vibration, and accelerated impeller and seal wear. The standard countermeasures are vortex breakers and increased submergence (ANSI/HI 9.8). Reducing upstream entrained-air loading reduces basin air loading independent of basin geometry.

Cooling-Tower Basin Vortex — Air-Ingestion Pathway to the Condenser Pump

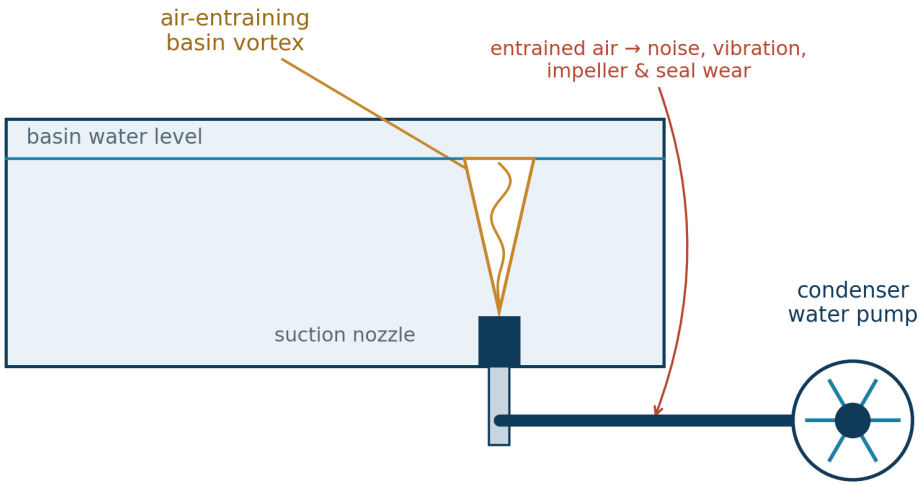

FIGURE 10.2 Cooling-tower basin vortex and air-ingestion pathway to the condenser water pump. After ASHRAE Handbook (2020) Ch. 40; ANSI/HI 9.8.

FIELD OBSERVATION · SECTION 10

- Entrained air accumulates at high points of heat-transfer equipment; the air pocket presents no convective surface and produces a local hot spot.
- $CaCO_3$ solubility decreases with temperature; localized hot spots accelerate scale precipitation at the metal surface.
- ASHRAE Handbook (2020) recommends air separators at hydronic-loop high points; the same engineering principle applies to potable-water service.
- Cooling-tower basin vortex is a documented air-ingestion mechanism; upstream entrained-air management reduces basin air loading independent of basin geometry.

Effects on Pipe Joints, Gaskets, Meters, and Instrumentation

Passive components — pipe joints, gaskets, threaded connections, flow meters, and instrumentation lines — fail through cumulative fatigue, not through single events. Their failure rates are governed by the integrated pressure-cycle and flow-pulsation history, not by any peak value.

11.1 Joint fatigue and corrosion fatigue

Threaded joints in carbon-steel pipe are particularly vulnerable to corrosion fatigue: each pressure cycle exposes a slightly different metal surface to dissolved oxygen and chloride at the thread root, accelerating pit initiation. Bonds (2005, Journal AWWA, “Corrosion and corrosion control of iron pipe: 75 years of research”) summarized the corrosion literature for water-utility piping. Gasketed flanges face the same problem in different geometry: the gasket extrudes and recovers on every pressure cycle, eventually losing the recoverable strain it relies on to maintain the seal. Cumulative pressure cycles in unconditioned commercial service have been measured at 10^5 per year (AWWA WITAF #4660, 2017); the ASME Section VIII Div. 2 S–N curve places this in the fatigue-damage region for typical service stress amplitudes.

10^5 cyc/yr	0.5% α	25–50+ D
pressure cycles in unconditioned commercial service (AWWA WITAF #4660)	void fraction that invalidates an ultrasonic transit-time meter (Wood's eq.)	straight-pipe AWWA M6 / ISO 5167 require for meter accuracy

11.2 Flow meters and instrumentation

Every commercial flow meter — positive-displacement, turbine, ultrasonic, electromagnetic, or Coriolis — is calibrated on the assumption of fully-developed, single-phase, axisymmetric flow. The accuracy specifications stamped on the meter nameplate are laboratory accuracies under controlled inlet conditions. AWWA M6, ISO 4064, OIML R 49, and ISO 5167 all specify upstream and downstream straight-pipe requirements precisely because velocity-profile asymmetry and swirl bias every meter type. Ultrasonic transit-time meters are particularly sensitive to entrained gas: per Wood’s equation, even a void fraction of 0.5% collapses the mixture sound speed and invalidates the timing model underlying the meter. The published meter-class error responses to entrained gas are summarized in API MPMS Chapter 5 and in the meter-vendor application notes.

DESIGN CONSEQUENCE · SECTION 11

- Threaded carbon-steel joints accumulate corrosion-fatigue damage with each pressure cycle at the thread root.
- Gasketed flanges lose recoverable strain over 10^4–10^5 cycles/year and may exhibit seal degradation over service life.
- Every commercial flow-meter type is calibrated against fully-developed, single-phase, axisymmetric flow — rarely the field condition.
- Ultrasonic transit-time meters are particularly sensitive: $\alpha \approx 0.5\%$ collapses mixture sound speed and invalidates the timing model.

PART II

Hydraulic Conditioning as a Discipline.

Industrial precedent, the published performance of flow-conditioning devices, velocity-profile recovery, swirl attenuation, turbulence decay, and the mechanisms by which upstream conditioning influences cavitation inception at downstream rotating equipment. AquaFlow is not introduced in this part; the conditioning concept is examined on its own merits.

Industrial Flow-Conditioner Family — Cross-Sectional Geometry

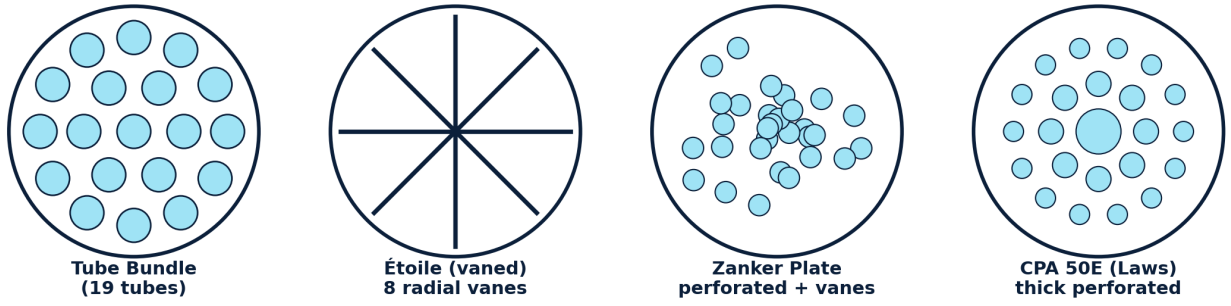

After Laws (1990); Laws & Ouazzane (1995); API MPMS Ch. 22. Performance characterized by ΔP coefficient, velocity-profile recovery distance, and swirl attenuation.

Figure II.1 — Four industrial flow-conditioner classes. The hydraulic-conditioning discipline is mature engineering with seventy years of industrial practice.

The Conditioning Concept — Industrial Precedent and Standards

A flow conditioner is a passive device installed in a pipe to modify the velocity profile and turbulence structure of the flow downstream. The device works by imposing a controlled, graded resistance across the pipe cross-section that re-distributes momentum, removes swirl, and accelerates the recovery of the velocity profile toward its fully-developed shape. The conditioning concept is mature engineering: the earliest tube-bundle and étoile conditioners were developed for differential-pressure (orifice) flow measurement in the 1930s–1950s; the Zanker plate (Zanker, 1958) became a recognized standard; the Laws plate (Laws, 1990) — commercialized as the CPA 50E — is the current state of the art for ultrasonic and turbine custody-transfer service.

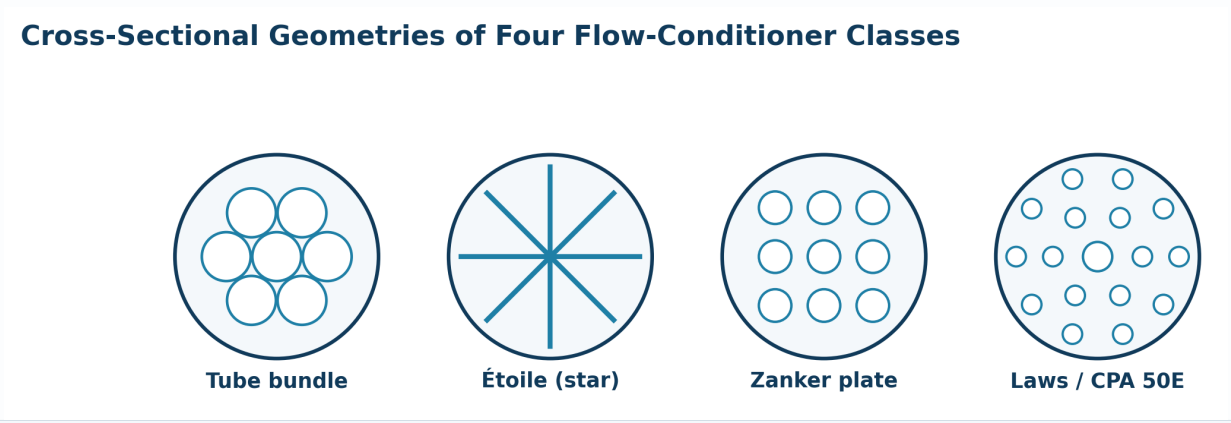

FIGURE 12.1 Cross-sectional geometries of four conditioner classes. After Laws (1990); Laws & Ouazzane (1995); API MPMS Ch. 22.

12.1 Codification in engineering standards

Hydraulic conditioning is codified across multiple engineering standards: ISO 5167-1 specifies upstream conditioning requirements for orifice, nozzle, and Venturi flow meters; ISO 17089 specifies analogous requirements for ultrasonic meters; AGA Report No. 9 provides the parallel for natural-gas service; API MPMS Chapter 5 covers liquid metering. The HVAC literature (ASHRAE Handbook—HVAC Systems & Equipment, 2020) identifies hydronic-loop air separators (Spirotherm, Taco, Armstrong) as a recognized conditioning element specifically for entrained-air management. In oil-and-gas custody transfer, the Lease Automatic Custody Transfer (LACT) skid integrates flow conditioning, air elimination, and strainer protection in a single engineered package — the highest-fidelity application of the conditioning principle in industrial service.

12.2 Performance metrics

A flow conditioner is characterized by three engineering quantities: (i) the pressure-loss coefficient K_c, the dimensionless head loss across the conditioner per unit dynamic pressure; (ii) the velocity-profile recovery distance, the downstream L/D at which the integrated profile error against the fully-developed reference falls below a stated threshold (typically 1% or 5%); and (iii) the swirl-attenuation distance, the downstream L/D at which the swirl intensity S = ω·R/u_axial falls below a stated threshold (typically 2° or 5°). The classical Zanker plate exhibits high K_c (above 5) but achieves excellent profile and swirl

performance; the Laws / CPA 50E achieves comparable performance at K_c ≈ 3.2 (Laws & Ouazzane, 1995, Flow Measurement and Instrumentation 6:1).

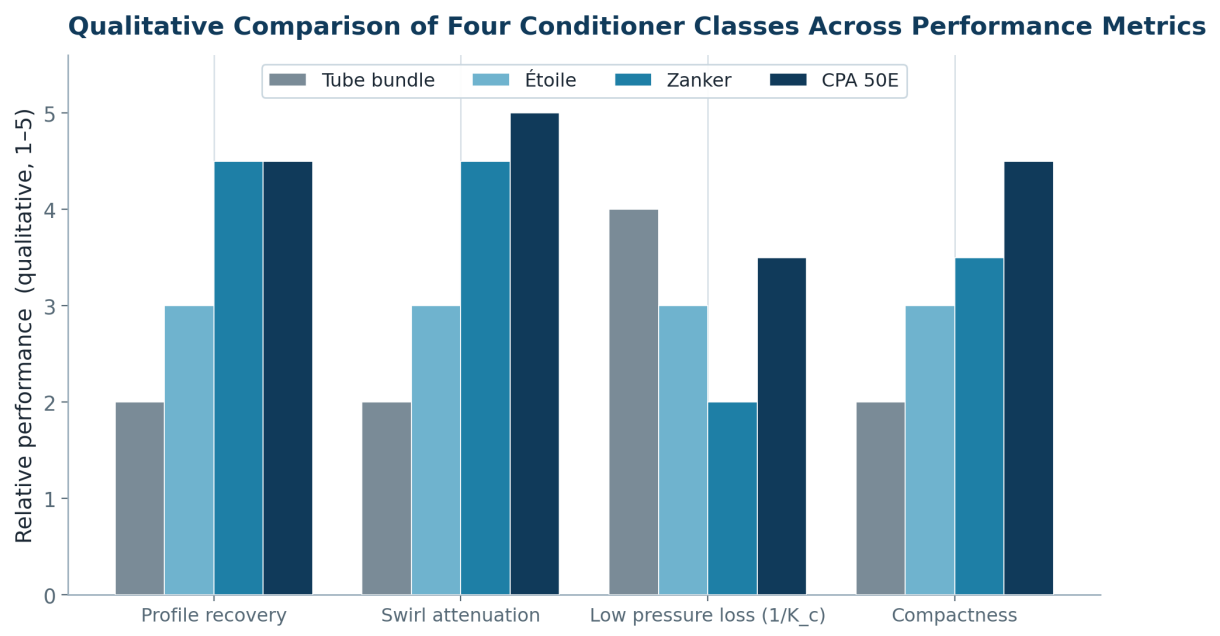

FIGURE 12.2 Qualitative engineering comparison of four conditioner classes across five performance metrics. After Laws (1990); Laws & Ouazzane (1995); Karnik et al. (1994); Studzinski et al. (1996, 2007).

PRACTICAL IMPLICATION · SECTION 12

- Hydraulic conditioning is mature engineering — codified across ISO 5167, ISO 17089, AGA 9, API MPMS Ch. 5, and the ASHRAE Handbook.
- Three engineering quantities characterize any conditioner: pressure-loss coefficient K_c, profile recovery distance, and swirl attenuation distance.
- Zanker plate is the historical performance benchmark; CPA 50E (Laws plate) achieves comparable performance at lower K_c.
- LACT skids represent the highest-fidelity industrial implementation of the conditioning principle, with seven decades of custody-transfer service.

Velocity Profile Recovery and Turbulence Decay

The performance of a flow conditioner is governed by two physical processes: the rate at which the disturbed flow downstream of an upstream fitting recovers toward the fully-developed velocity profile, and the rate at which the elevated turbulence kinetic energy decays toward its equilibrium level. Both processes are well characterized in the experimental literature.

13.1 Velocity-profile recovery measurements

Mattingly & Yeh (1991, ASME Fluids Engineering Conference) measured velocity-profile recovery downstream of a single 90° elbow in turbulent pipe flow using laser Doppler velocimetry; they reported recovery to within 5% of the fully-developed profile at 20–30 D and within 1% at 40–60 D. Studzinski et al. (1996; subsequent CIATEQ work, 2007) measured analogous data downstream of coupled-elbow configurations and reported recovery distances of 40+ D for in-plane coupled elbows and 50+ D for out-of-plane configurations. Murakami et al. (1969) provided the historical baseline measurements that established the canonical recovery-length numbers. Recovery downstream of Zanker and CPA conditioners has been measured at 4–10 D for recovery to within 5% of fully-developed, with full equilibrium (within 1%) by 25 D. Karnik et al. (1994) reported that the turbulent equilibrium state is not fully reached even at 50 D downstream of a Zanker conditioner — meaning the conditioning effect on the energy spectrum persists over longer distances than the mean-profile recovery.

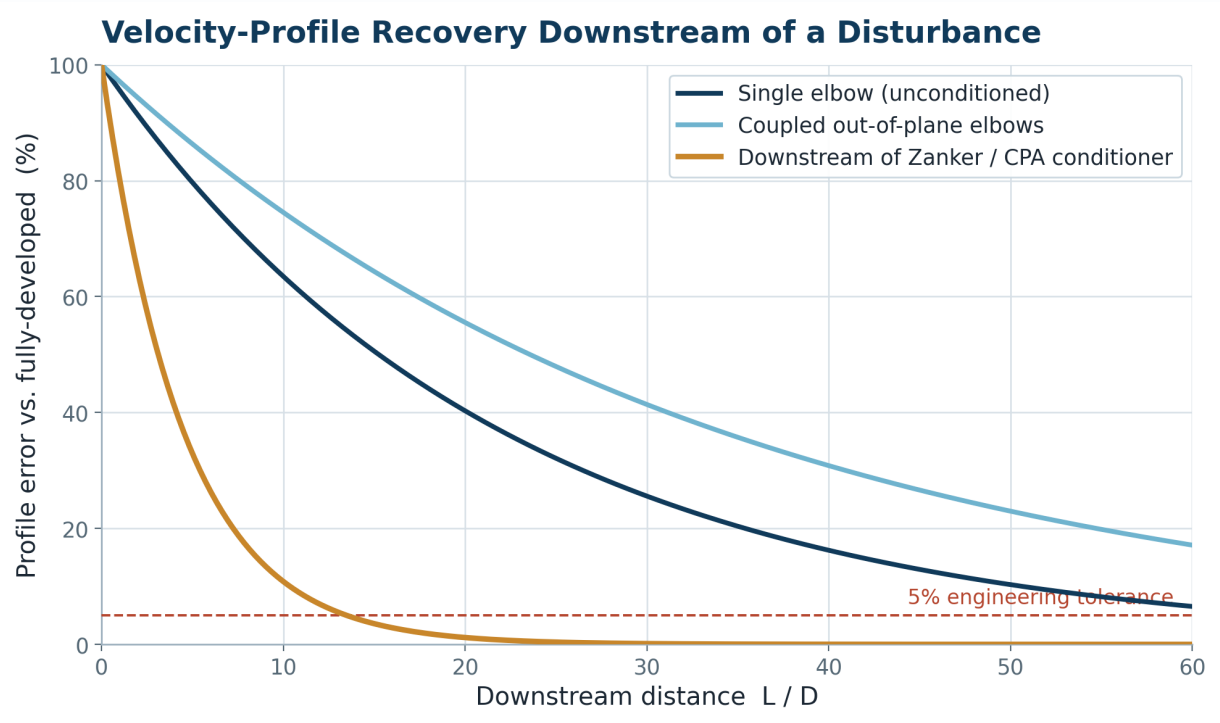

FIGURE 13.1 Velocity-profile recovery downstream of a flow disturbance. After Mattingly & Yeh (1991); Laws & Ouazzane (1995); Studzinski et al. (1996); Karnik et al. (1994).

13.2 Turbulence kinetic energy decay

Downstream of a grid, screen, or conditioner, turbulence kinetic energy k decays as a power law k ∝ (x/M)^(−n), where M is the mesh or hole spacing and the exponent n ≈ 1.2–1.4 for isotropic grid-generated turbulence (Batchelor & Townsend, 1948; Comte-Bellot & Corrsin, 1971). For anisotropic pipe-internal turbulence, the decay is slower and the exponent depends on the relative orientation of the velocity-gradient and shear-stress tensors. The engineering implication for conditioning is that the elevated turbulence intensity introduced by the conditioner itself decays rapidly in the near field (x/M < 10), while the inherited large-scale structures of the upstream disturbance persist for longer. Conditioning benefit is strongest in the near field and diminishes with distance from the conditioner and with each downstream fitting.

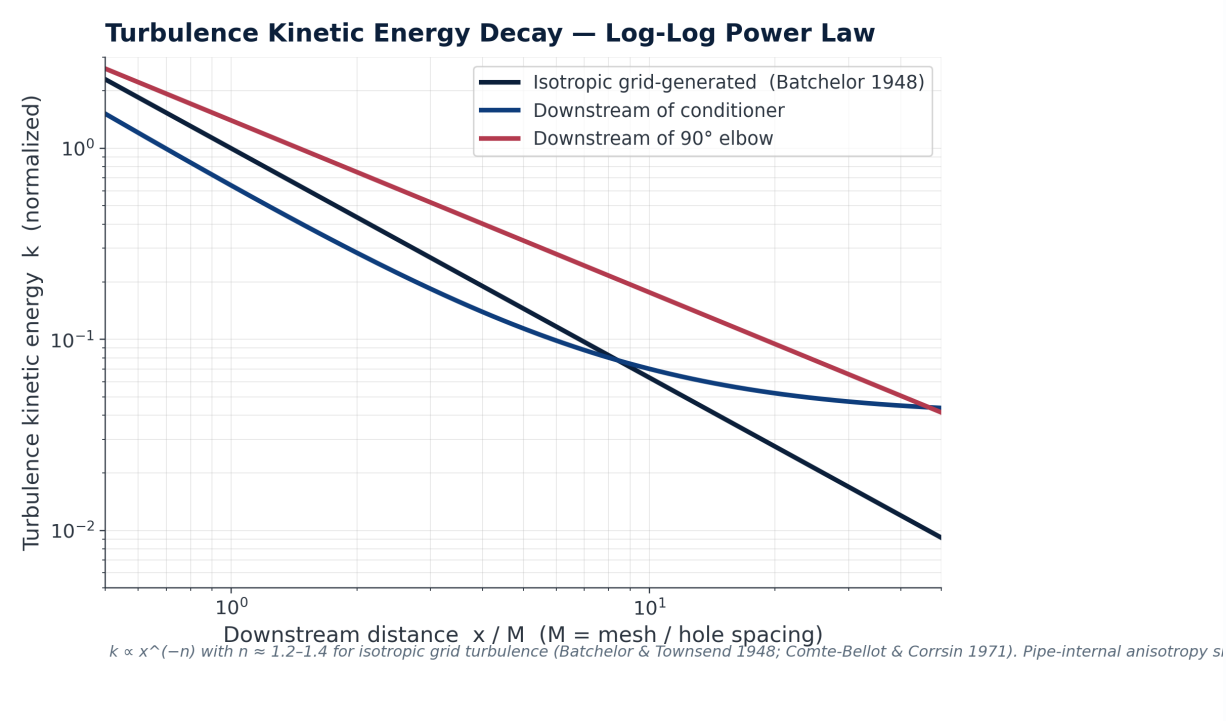

FIGURE 13.2 Turbulence kinetic energy decay on log-log axes. Power-law decay k ∝ x^(−n). After Batchelor & Townsend (1948); Comte-Bellot & Corrsin (1971). Pipe-internal turbulence decays more slowly than isotropic grid turbulence.

ENGINEERING SIGNIFICANCE · SECTION 13

- Single-elbow profile recovery typically requires 25–50 D; coupled out-of-plane elbows require 40+ D.
- Downstream of Zanker / CPA conditioner, recovery to <5% of fully-developed reference occurs within 4–10 D.
- Turbulent kinetic energy decays as k ∝ x^(-n), n ≈ 1.2–1.4 for isotropic grid-generated turbulence.
- Conditioning improves flow organization within a turbulent regime; it does not produce truly laminar flow at commercial Re.

Swirl Attenuation and Asymmetric-Inflow Correction

Swirl — coherent tangential motion superimposed on the bulk axial flow — is the most persistent disturbance produced by upstream fittings. Single elbows generate moderate swirl; coupled elbows in the same plane generate stronger swirl whose direction depends on geometry; out-of-plane coupled elbows generate the strongest swirl, persisting for 40–50+ D downstream in the absence of conditioning. Swirl is quantified by the swirl number S = (axial flux of tangential momentum) / (axial flux of axial momentum × pipe radius), or equivalently by the swirl angle at the centerline. Mean swirl angles greater than 2° degrade flow-meter accuracy beyond acceptable tolerance for custody-transfer service.

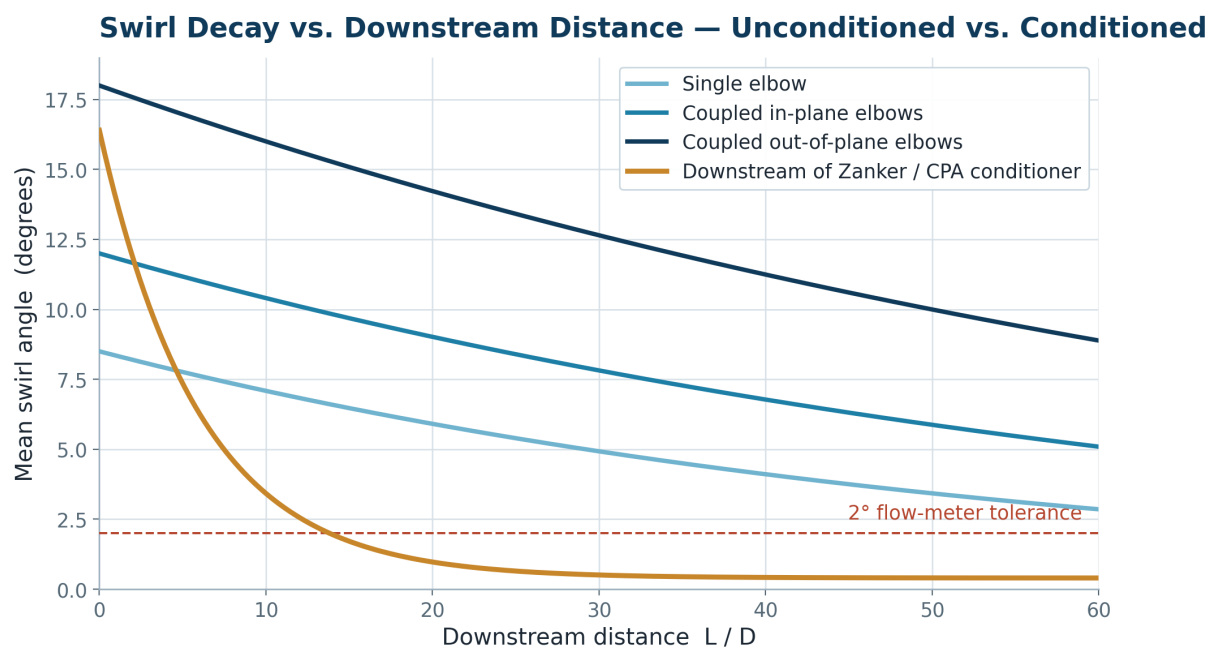

FIGURE 14.1 Swirl decay vs. downstream distance for single elbow, coupled in-plane elbows, coupled out-of-plane elbows, and downstream of a Zanker/CPA conditioner. After Mattingly (1991); Karnik et al. (1994); Laws & Ouazzane (1995); Studzinski et al. (2007).

14.1 Why a graded-resistance plate attenuates swirl effectively

The Zanker plate combines a perforated graded-resistance distribution with a downstream vane structure that removes the tangential velocity component directly. The Laws / CPA 50E plate uses a thick perforated plate with concentric arrays of segmented annular passages and a central circular passage; the geometry imposes a near-rigid mapping of inflow to outflow through the plate, breaking up any organized tangential motion in transit. Both designs reduce incoming swirl by approximately 90–98% in a single plate-length (Laws & Ouazzane, 1995). The residual swirl decays in the far field exponentially with downstream distance, with decay constants 3–5× faster than the unconditioned case (Karnik et al., 1994).

Conceptual Flow Conditioning — Asymmetric Inflow Re-Organized to a Symmetric Profile

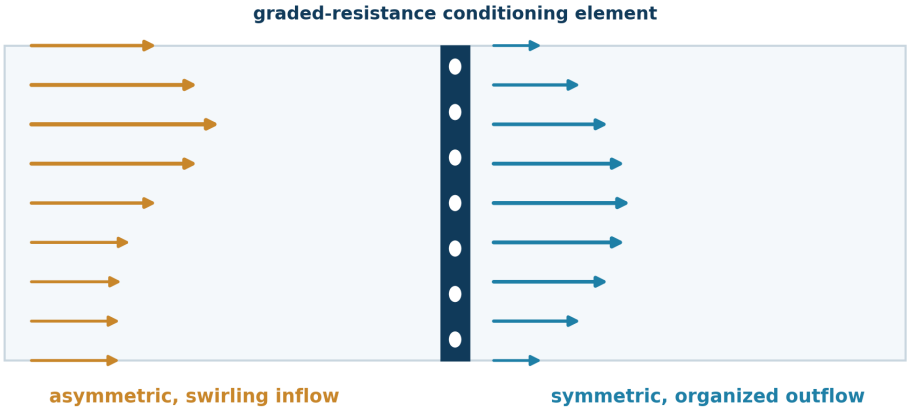

Illustrative CFD-style schematic; quantitative recovery data in Sections 13–14 (Laws & Ouazzane 1995).

FIGURE 14.2 Conceptual CFD-style schematic. Asymmetric turbulent inflow re-organizes through a perforated conditioning element; downstream profile recovers toward axisymmetric. Illustrative; quantitative data in Laws & Ouazzane (1995) and CPA validation reports.

ENGINEERING INTERPRETATION	Graded-resistance perforated plates remap inflow turbulent structure into a near-symmetric outflow distribution. Recovery to within engineering tolerance occurs in 4–10 D downstream — an order of magnitude faster than the unconditioned case.
DESIGN IMPLICATION	The benefit is strongest in the near field. Components installed within ~25 D of the conditioner receive the most organized profile; benefit decays with distance and with each downstream fitting.

ENGINEERING SIGNIFICANCE · SECTION 14

- Coupled out-of-plane elbows generate the strongest swirl; unconditioned recovery requires 40–50+ L/D.
- A Zanker / CPA-class plate reduces incoming swirl by approximately 90–98% in a single plate length.
- Residual far-field swirl decays 3–5× faster than the unconditioned case.
- Mean swirl angles above 2° degrade flow-meter accuracy beyond custody-transfer tolerance.

Cavitation Mitigation by Upstream Conditioning

Upstream hydraulic conditioning may influence cavitation inception at downstream components through three converging mechanisms, each independently documented in the pump-engineering literature. The combined effect is to shift the cavitation envelope and reduce the duty cycle within the envelope.

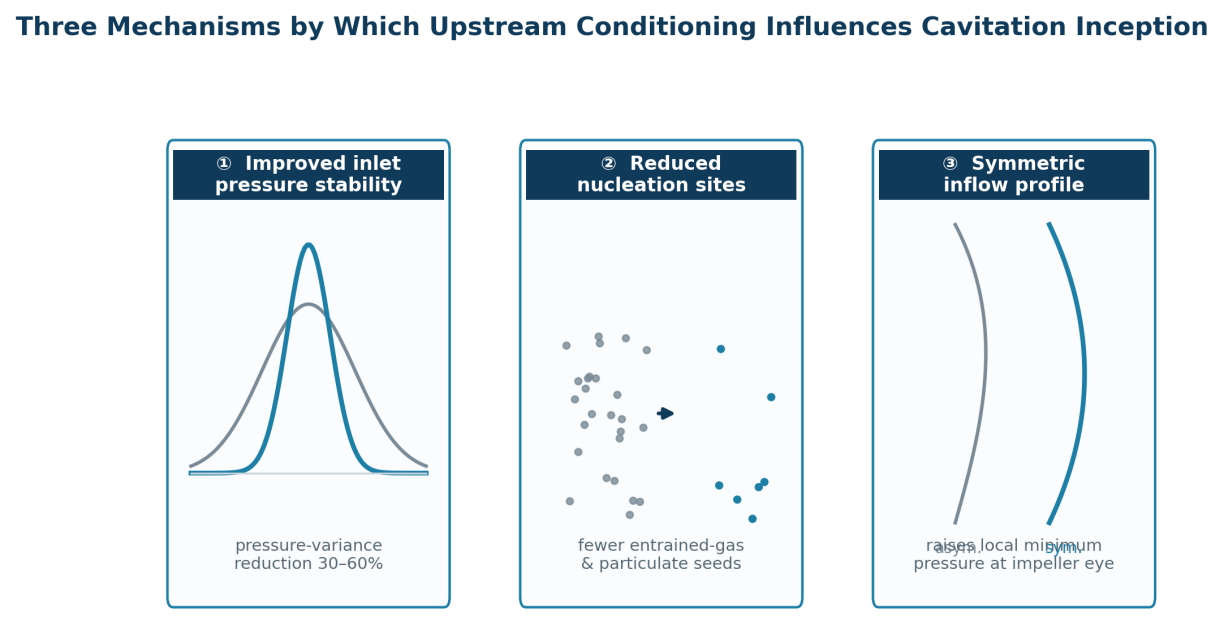

FIGURE 15.1 Three mechanisms by which upstream conditioning may influence cavitation inception. After Brennen (1995); ANSI/HI 9.6.1 (2024); Karassik et al. (2008).

15.1 Mechanism 1 — improved inlet pressure stability

Cavitation onset is governed by the instantaneous local pressure, not the time-average. A conditioner reduces the variance of the pressure signal arriving at the impeller eye. For a fixed mean static head, a narrower instantaneous pressure distribution places fewer samples below the cavitation threshold. The effect is proportional to the variance reduction and is reported in the literature at typical values of 30–60% reduction in pressure standard deviation across the operating envelope (Bloch, 1994; ANSI/HI 9.6.1 2024).

15.2 Mechanism 2 — reduced nucleation sites

Cavitation nucleates preferentially on pre-existing gas inclusions and on submicroscopic particulate. Reducing the entrained-gas content of the inflow reduces the population density of nucleation sites in direct proportion. The effective nucleation threshold rises (Brennen, 1995, Ch. 4); incipient cavitation occurs at a lower σ_local for a given pressure history. The mechanism is independent of mechanism 1 and adds linearly.

15.3 Mechanism 3 — symmetric inflow profile

A symmetric, low-swirl velocity profile at the suction of a centrifugal pump produces a higher minimum static pressure at the impeller eye than an asymmetric profile of the same mean head. The reason is geometric: in the asymmetric case the local velocity is highest on the high-flow side of the inlet, and Bernoulli's relation places the lowest static pressure at that location. Eliminating the asymmetry raises the local minimum by the dynamic-pressure differential — typically 0.5–2.0 m of H_2O on a 4–6 inch pump suction.

CONSERVATIVE FRAMING · SECTION 15

- Upstream conditioning may improve inlet conditions that influence cavitation inception — through three converging mechanisms.
- Pressure-variance reduction narrows the instantaneous distribution; reported variance reductions of 30–60% in HI/Bloch literature.
- Reduced entrained-gas content lowers the nucleation-site population; the effective nucleation threshold rises.
- Improved profile symmetry raises local minimum pressure at the impeller eye; the quantitative effect is application-specific.

PART II — SYNTHESIS

70 yrs precedent	**4–10 D**	**90–98%** swirl
industrial flow-conditioning in custody-transfer service	Zanker / CPA profile recovery vs. 25–50+ D unconditioned	single-plate swirl reduction (Laws & Ouazzane 1995)

Part II has established hydraulic conditioning as a mature, codified engineering discipline — with characterized recovery distances, swirl-attenuation factors, and three independent mechanisms by which it influences downstream cavitation. Part III applies this discipline to one device.

PART III

Application — The AquaFlow Valve.

AquaFlow as one device within the hydraulic-conditioning lineage, designed for installation immediately downstream of the master meter on the customer-owned side of the property. Position in the engineering family; technical specification; industry-specific applications; and engineering conclusion.

Figure III.1 — AquaFlow Valve, service-entrance hydraulic conditioner.

AquaFlow as a Service-Entrance Conditioning Device

AquaFlow Technologies manufactures a passive inline hydraulic-conditioning device — the AquaFlow Valve — designed for installation at the commercial water service entrance, immediately downstream of the master meter, on the customer-owned side of the property. The device combines, in a single sealed valve body, three of the conditioning functions characterized in Part II: pressure stabilization (reduction of dynamic pressure variation), entrained-air management (compression and re-dissolution of micro-bubbles per Henry's Law), and flow conditioning (restoration of a symmetric, low-swirl velocity profile through a perforated internal geometry analogous to the Laws / CPA 50E plate).

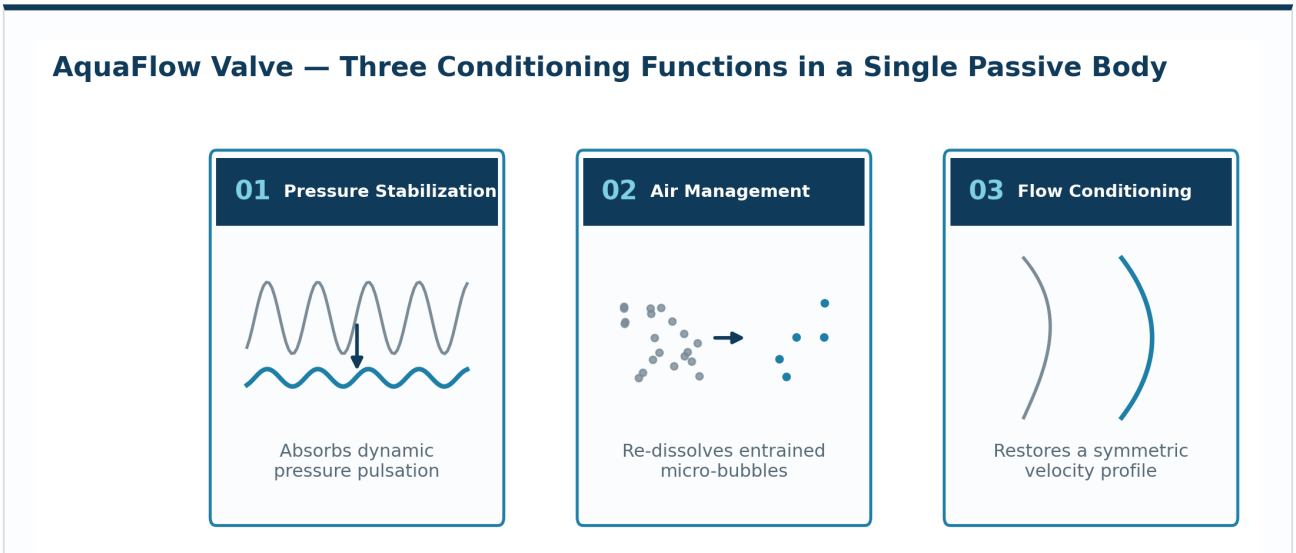

FIGURE 16.1 AquaFlow Valve — three conditioning functions combined in a single passive inline body.

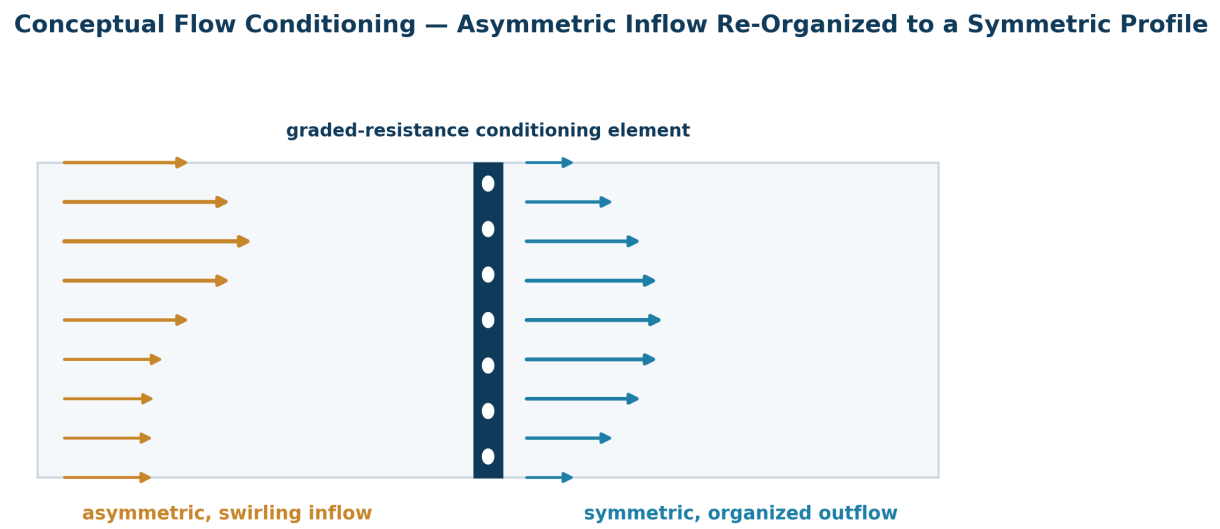

FIGURE 16.2 Conceptual flow conditioning. Asymmetric, swirling inflow is re-organized to a symmetric, low-swirl profile through the perforated graded-resistance element — the mechanism characterized quantitatively in Sections 13–14 (Laws & Ouazzane, 1995).

CONDITIONING CONCEPT

The internal geometry imposes a near-rigid inflow-to-outflow mapping, breaking up organized swirl and re-imposing a symmetric profile within a few pipe diameters downstream — an order of magnitude faster than the unconditioned recovery length.

16.1 Installation position

The AquaFlow Valve is installed on the customer-owned side of the property, immediately downstream of the master meter and upstream of the backflow preventer (both of which are customer-side components). The valve is not installed on the utility-owned side of the meter. The position is consistent with the Cross-Connection Control practices codified in the USC FCCCHR Manual and with AWWA Manual M14 (Recommended Practice for Backflow Prevention and Cross-Connection Control).

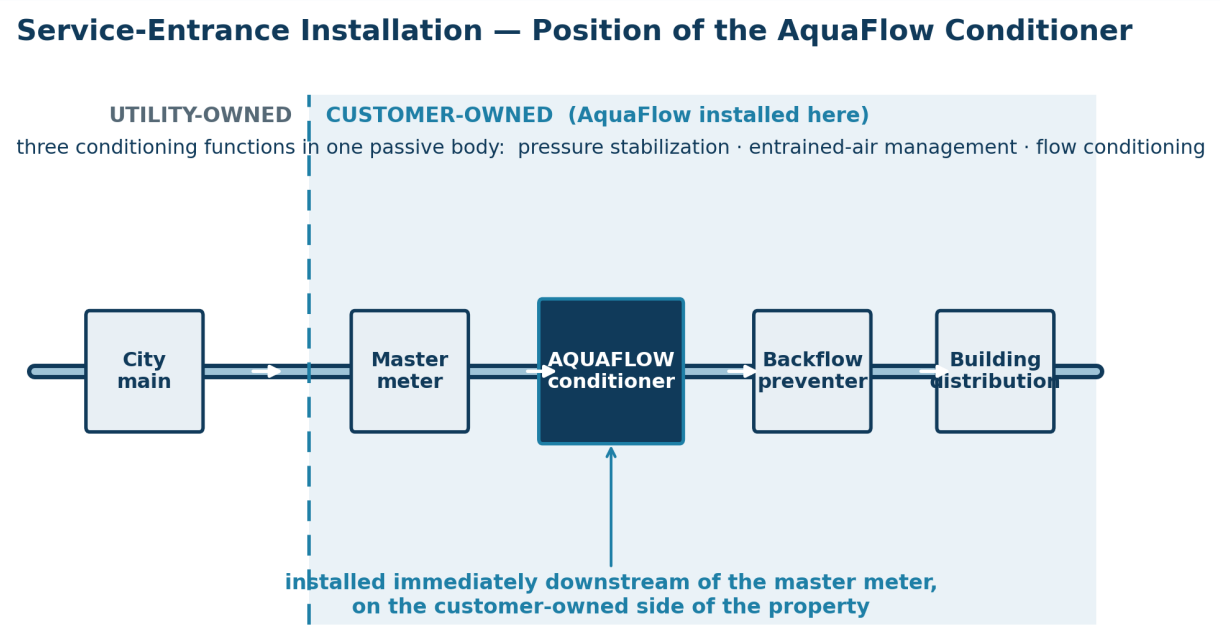

FIGURE 16.3 Service-entrance installation. The AquaFlow conditioner is installed on the customer-owned side of the property, immediately downstream of the master meter and upstream of the backflow preventer — never on the utility-owned side.

INSTALLATION POSITION · SECTION 16

- AquaFlow is installed on the customer-owned side of the property, downstream of the master meter.
- Standard position is upstream of the backflow preventer when that location remains on the customer-owned side.
- Not installed on the utility-owned side of the meter.
- Per USC FCCCHR Cross-Connection Control Manual; AWWA Manual M14; local plumbing code.

Engineering Specification and Position in the Lineage

The AquaFlow Valve occupies a defined position within the hydraulic-conditioning lineage characterized in Part II. The comparison below identifies the function, industry-standard equivalent, and AquaFlow implementation for each conditioning task — it does not claim equivalency with industrial custody-transfer conditioners in custody-transfer service.

CONDITIONING FUNCTION	INDUSTRY-STANDARD EQUIVALENT	AQUAFLOW IMPLEMENTATION
Flow profile conditioning	Zanker plate (1958); Laws / CPA 50E (1990); Vortab VTP; Emerson Daniel	Internal perforated graded-resistance geometry with a downstream profile-restoration element.
Entrained-air management	Spirotherm ASME deaerator; HVAC Spirovent / Taco KV / Armstrong; LACT air eliminator	Engineered pressure-recovery zone may drive micro-bubble compression and re-dissolution per Henry's Law.
Pressure stabilization	Surge dampers; pressure-tank accumulators; commissioned air vessels	Spring-loaded internal core absorbs a portion of upstream dynamic pressure pulsation.
Particulate protection	Combination strainer-eliminator (Smith Meter; Liquid Controls S-Series; Brodie)	Integral strainer element retains particulates that would otherwise reach downstream meter and seat surfaces.
Passive, sealed, zero-maintenance	Liquid Controls A-Series (refined-products terminal service, 40+ years)	Fixed-geometry passive design; no electronics, no scheduled service interval.

17.1 Technical specifications

½–26 in	**20–180 psi**	**316L SS**
size range, threaded or flanged end connections	operating pressure; published loss < 0.8 psi	stainless body; NSF/ANSI 61, IAPMO, KIWA listed

AQUAFLOW VALVE — ENGINEERING SPECIFICATION SUMMARY	
Body material	316L stainless steel (brass option where the application warrants)
Size range	½ in through 26 in
End connections	Threaded (NPT) or flanged (ANSI B16.5 Class 150 / 300)
Operating pressure	20 – 180 psi
Published pressure loss	< 0.8 psi across the size range
Temperature rating	33 – 180 °F (1 – 82 °C)
Internal configuration	Spring-loaded conditioning core; perforated graded-resistance element; downstream profile-restoration disc
Power / electronics	None — fully passive design
Scheduled maintenance	None — sealed, fixed-geometry mechanical design
Certifications	NSF/ANSI 61 (drinking-water health effects); IAPMO UPC listing; KIWA potable-water listing

FIGURE 17.1 Published technical specification. NSF/ANSI 61 conformance addresses drinking-water health-effect requirements for potable-water service.

17.2 Internal construction

The internal stabilization assembly comprises (1) the outer body, (2) the inlet connection, (3) the spring-loaded conditioning core, (4) the flow-reorganizing element, and (5) the downstream profile-restoration disc. The configuration is a fixed-geometry passive design with no electronic components and no scheduled service interval. Body materials are 316L stainless steel (primary) or brass options where the application warrants. Cavitation erosion resistance of 316L is approximately 200% greater than that of mild carbon steel per ASTM G32-16 vibratory cavitation test data (Section 5).

FIGURE 17.2 Internal cutaway showing component layout: (1) outer body, (2) inlet connection, (3) spring-loaded conditioning core, (4) flow-reorganizing element, (5) downstream profile-restoration disc.

TECHNICAL SPECIFICATION SUMMARY · SECTION 17

- Body: 316L stainless steel; sizes 1/2 in through 26 in; threaded or flanged end connections.
- Operating pressure 20–180 psi; published pressure loss < 0.8 psi across the size range.
- Passive, sealed mechanical design; no external power; no scheduled maintenance interval.
- Certifications: NSF/ANSI 61 (drinking-water health effects), IAPMO UPC listing, KIWA potable-water listing.

Industry-Specific Applications

The relative weight of upstream hydraulic-conditioning benefits depends on the facility class and on which hydraulic stress mechanisms dominate the maintenance cost structure. The matrix below maps the principal mechanisms to facility classes; the cards that follow summarize how each mechanism is reported in the published service literature for that class.

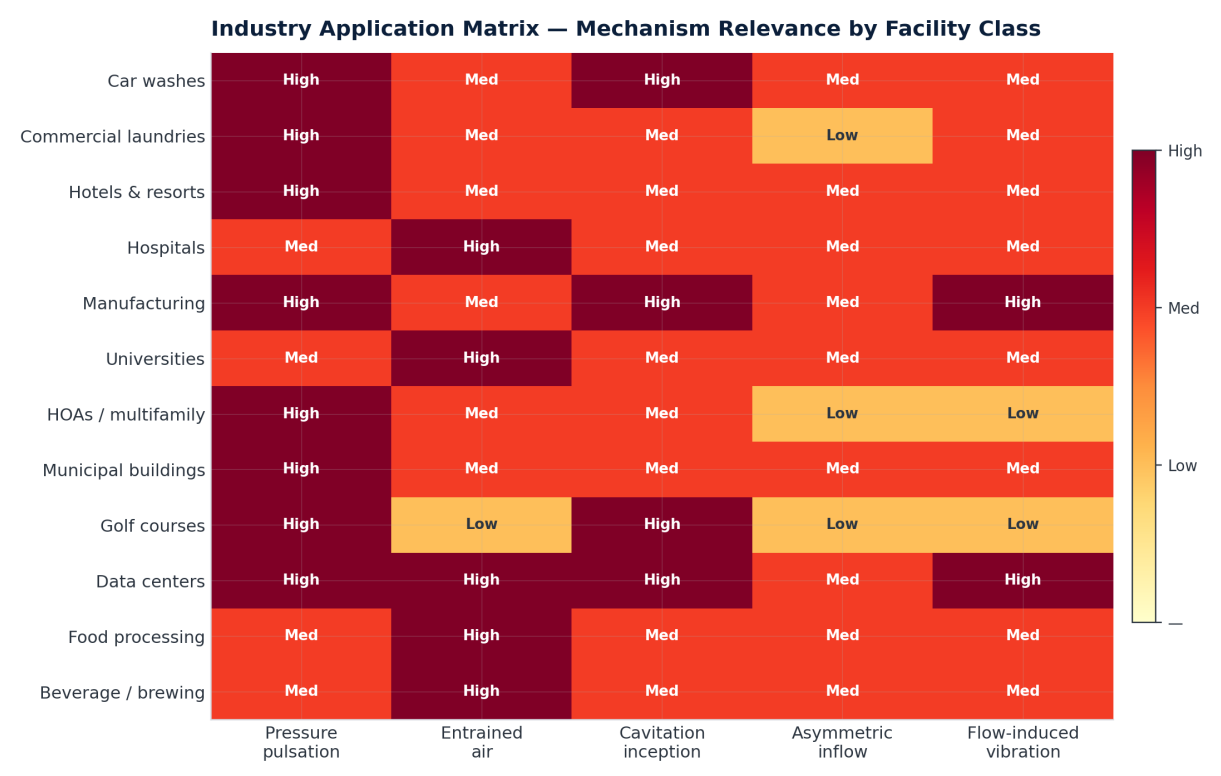

FIGURE 18.1 Industry application matrix — relevance of each hydraulic stress mechanism by facility class. Engineering-judgment scoring; each cell is supported by the mechanisms covered in Part I.

Car Washes

High-pressure plunger pumps, solenoid valves, spray nozzles, and mixing valves. Documented failure modes include plunger packing wear, solenoid coil fatigue, and nozzle erosion. Conditioning may reduce inlet pressure pulsation and entrained-air loading at the high-pressure pump suction (Sections 3, 4, 8).

Commercial Laundry

Solenoid fill valves, mixing valves, washer-extractor pumps. Diaphragm failure from overpressure is the dominant call-out cause per manufacturer literature (Tameson, Bürkert, Plast-O-Matic). Conditioning may reduce per-fill-cycle transient amplitude (Sections 3, 9).

Hotels & Resorts

Booster sets, central mixing valves, recirculation loops, water heaters, guestroom fixtures. Guest-experience reports of water-temperature instability are commonly traced to pressure pulsation at the mixing valve (ASHRAE Handbook).

Hospitals

Central plant cooling and heating loops, sterilizer water feeds, dialysis-grade water systems. Sterilizers impose tight inlet specifications and exhibit process-cycle anomalies when inlet air content varies (USP <645>; CDC sterilization guidance).

Manufacturing Facilities

Process pumps, cooling loops, instrumentation lines. Control loops tune to a quieter inlet pressure signal when upstream pulsation is reduced; ASME PVP literature documents the FIV mechanisms.

Universities

Central plant chilled-water and hot-water loops, lab process water, campus distribution. Engineering staff can measure the change directly via existing SCADA instrumentation; methodology consistent with Stephens et al. (2008).

HOAs & Multifamily

Booster pumps, irrigation valves, recirculation systems. Recirculation loops are particularly prone to entrained-air accumulation at high points (ASHRAE Handbook).

Municipal Buildings

Distribution PRVs, booster stations, meter installations. Conditioning may extend service intervals at district PRV stations whose spring-and-diaphragm assemblies are cycled by every upstream transient.

Golf Courses

Irrigation pumps and central control valves at high seasonal duty cycle. Stabilized supply may reduce pump cycling and irrigation-valve diaphragm wear; deaerated inflow may reduce pump-priming difficulty.

Data Centers

Chilled-water loops, cooling-tower makeup, CDU pumps. Tier-IV reliability targets (99.999%+) make the incremental contribution from upstream conditioning quantitatively meaningful even when the absolute improvement on any one component is modest.

Food Processing

CIP loops, plate heat exchangers, sanitary valves, fillers. Air ingestion in CIP loops produces incomplete cleaning cycles, a documented regulatory concern (FDA 21 CFR 110). Upstream conditioning is a clean intervention with no process impact.

Beverage & Brewing

Bottling fillers, CIP, makeup water, process metering, blending. Entrained-CO_2 management is the principal challenge for the carbonated-beverage process; the conditioning concept applies equally to other gases per Henry’s Law.

Conclusion

The fluid-mechanics mechanisms by which unconditioned flow degrades commercial water systems are well established and extensively published. Turbulent shear, pressure pulsation, entrained air, cavitation inception, water hammer, flow-induced vibration, and velocity-profile asymmetry each contribute to documented failure modes in pumps, valves, heat exchangers, pipework, and instrumentation. Each mechanism is the subject of dedicated standards and a substantial body of peer-reviewed literature, summarized in Part I.

Hydraulic conditioning is a mature engineering discipline. Industrial flow-conditioning devices have been used in custody-transfer service for seven decades, codified across API, ISO, AGA, OIML, and AWWA standards. The mean-profile and turbulence performance of the Zanker plate, the Laws / CPA 50E, and analogous designs is well characterized, with recovery distances and swirl-attenuation factors established in the open literature. Upstream conditioning may reduce, through three independent mechanisms, the cavitation duty cycle at downstream rotating equipment; may reduce, through pressure-variance reduction, the fatigue duty on solenoids, diaphragms, gaskets, and joints; and may reduce, through entrained-air management, the air-driven thermal and mechanical stresses at heat-transfer surfaces and pump suctions.

The AquaFlow Valve is one device within that lineage, engineered for installation immediately downstream of the master meter on the customer-owned side of the property. The device performs three of the conditioning functions in a single passive inline body. Its position in the engineering taxonomy is established by reference to the industrial standards it draws upon; its mechanical specification is published in the manufacturer’s spec sheet; its certifications (NSF/ANSI 61, IAPMO, KIWA) address the regulatory requirements for potable-water service. The engineering position supported by this document is that hydraulic conditioning at the service entrance is a defensible intervention that reduces exposure to known hydraulic stress mechanisms; the magnitude of the benefit at any specific facility is application-specific.

ENGINEERING CONCLUSION · SECTION 19

- Turbulent shear, pressure pulsation, entrained air, cavitation inception, water hammer, flow-induced vibration, and velocity-profile asymmetry all contribute to documented failure modes in commercial water systems.
- Hydraulic conditioning is mature engineering with seven decades of industrial precedent across API, ISO, AGA, OIML, and AWWA standards.
- Upstream conditioning at the service entrance reduces exposure to known hydraulic stress mechanisms — pressure-variance reduction, entrained-air reduction, and profile-symmetry improvement.
- The magnitude of benefit at any specific facility is application-specific and is best evaluated through before-and-after instrumentation and maintenance-record analysis.

WHAT THIS DOCUMENT IS, AND IS NOT · SECTION 19

This document is an engineering reference on the mechanisms by which unconditioned flow degrades commercial water systems and on the published performance of upstream hydraulic-conditioning devices. It is not a sales document. It does not address utility billing, water consumption, water-bill savings, return on investment, or payback. Every quantitative claim is referenced; every limitation is stated. The conclusion supported by the literature is that hydraulic conditioning at the service entrance is a defensible engineering intervention.

Appendix A · Symbols and Nomenclature

REFERENCE

SYMBOL	QUANTITY	TYPICAL UNITS
Re	Reynolds number (ρvD/μ)	dimensionless
De	Dean number Re·(D/2R_c)^(1/2)	dimensionless
St	Strouhal number (fD/U)	dimensionless
f	Darcy friction factor	dimensionless
ε	Pipe absolute roughness	mm
ε/D	Relative roughness	dimensionless
ν, μ	Kinematic / dynamic viscosity	m²/s, Pa·s
ρ	Fluid density	kg/m³
v, U	Mean / bulk velocity	m/s
D, R, R_c	Pipe diameter, radius, centerline curvature radius	m
a	Wave speed in pipe-fluid system	m/s
α	Void fraction	%
k	Henry's Law constant; turbulence kinetic energy	mol/(kg·Pa); m²/s²
σ, σ_i, σ_3	Cavitation number, incipient, 3% head-drop	dimensionless
NPSH_a, NPSH_r, NPSH₃	Available, required, 3% head-drop NPSH	m or ft H_2O
ΔP, Δv	Pressure surge, velocity change	Pa, m/s
L_e, L/D	Hydrodynamic entrance length, downstream distance	pipe diameters (D)
S, ω	Swirl intensity, angular velocity	dimensionless, rad/s
K, K_c	Minor-loss coefficient, conditioner pressure-loss coefficient	dimensionless
BEP	Best Efficiency Point (pump operation)	—
P_v(T)	Liquid vapor pressure at temperature T	Pa

Appendix B · Standards Index

REFERENCE

B.1 WATER INDUSTRY

AWWA M6 — Water Meters: Selection, Installation, Testing, and Maintenance.

AWWA M11 — Steel Pipe: A Guide for Design and Installation.

AWWA M14 — Recommended Practice for Backflow Prevention and Cross-Connection Control.

AWWA M51 — Air Valves: Air Release, Air/Vacuum, and Combination.

AWWA C512 — Air Release, Air/Vacuum, and Combination Air Valves.

AWWA C700–C712 — Cold Water Meters (PD, Turbine, Compound, EM, Ultrasonic).

AWWA WITAF #4660 (2017) — Pressure Transient Monitoring.

NSF/ANSI 61 — Drinking Water System Components, Health Effects.

IAPMO — Uniform Plumbing Code Listing.

USC FCCCHR — Manual of Cross-Connection Control.

ASSE 1013 — RPBP performance standard.

B.2 MECHANICAL AND ROTATING EQUIPMENT

ANSI/HI 9.6.1 (2024) — Rotodynamic Pumps Guideline for NPSH Margin.

ANSI/HI 9.8 — Pump Intake Design.

ASME B73.1 — Horizontal End-Suction Centrifugal Pumps.

ASME Section III subsection NG-3133 — Tube Vibration.

ASME Section VIII Div. 2, Annex 3.F — Fatigue Analysis.

ANSI/API 682 — Shaft Sealing Systems for Centrifugal and Rotary Pumps.

API 610 — Centrifugal Pumps for Petroleum / Natural Gas Service.

API MPMS Chapter 5 — Liquid Metering.

API MPMS Chapter 22 — Multiphase Custody Transfer.

ISO 5167 — Measurement of Fluid Flow by Pressure Differential Devices.

ISO 4064 — Water Meters for Cold Potable Water.

ISO 17089 — Ultrasonic Meters for Liquid Flow.

OIML R 49 — Water Meters for Cold Potable Water.

ASTM G32-16 — Cavitation Erosion Vibratory Test.

B.3 BUILDING SYSTEMS AND PROCESS

ASHRAE Handbook — Systems and Equipment.

ASHRAE Handbook — HVAC Applications.

CTI STD-202 — Cooling Tower Manufacturers Standards.

TEMA RGP-RCB-4 — Tube Vibration Standards.

USP <645> — Water for Injection.

ASTM D5127 — Ultra-Pure Water for Semiconductor Processing.

Crane TP-410 — Flow of Fluids through Valves, Fittings, and Pipe.

NIST Handbook 44 — Weighing and Measuring Devices.

FDA 21 CFR 110 — Current Good Manufacturing Practice.

Appendix C · References

BIBLIOGRAPHY

Antaki, G. A. (2003). Piping and Pipeline Engineering: Design, Construction, Maintenance, Integrity, and Repair. Marcel Dekker.

Batchelor, G. K., and Townsend, A. A. (1948). “Decay of isotropic turbulence in the initial period,” Proc. Roy. Soc. A 193: 539–558.

Bergant, A., Simpson, A. R., and Tijsseling, A. S. (2006). “Water hammer with column separation: A historical review,” J. Fluids and Structures 22(2): 135–171.

Berger, S. A., Talbot, L., and Yao, L. (1983). “Flow in curved pipes,” Annu. Rev. Fluid Mech. 15: 461–512.

Bhatti, M. S., and Shah, R. K. (1987). In Handbook of Single-Phase Convective Heat Transfer, Ch. 4. Wiley.

Bloch, H. P., and Geitner, F. K. (1994). Machinery Failure Analysis and Troubleshooting (3rd ed.). Gulf Publishing.

Bonds, R. W. (2005). “Corrosion and corrosion control of iron pipe: 75 years of research,” Journal AWWA 97(6): 88–98.

Brennen, C. E. (1994). Hydrodynamics of Pumps. Concepts ETI / Oxford University Press.

Brennen, C. E. (1995). Cavitation and Bubble Dynamics. Oxford University Press.

Bull, M. K. (1996). “Wall-pressure fluctuations beneath turbulent boundary layers,” J. Sound Vibration 190(3): 299–315.

Chiu, K.-Y., Cheng, F.-T., and Man, H.-C. (2005). “Cavitation erosion of NiTi coating,” Wear 258(11–12): 1700–1705.

Comte-Bellot, G., and Corrsin, S. (1971). “Simple Eulerian time correlation … in grid-generated, isotropic turbulence,” J. Fluid Mech. 48: 273–337.

Connors, H. J. (1970). “Fluidelastic vibration of tube arrays excited by cross flow,” Flow-Induced Vibration in Heat Exchangers, ASME.

Crighton, D. G. (1985). “The Kutta condition in unsteady flow,” Annu. Rev. Fluid Mech. 17: 411–445.

Dean, W. R. (1928). “The streamline motion of fluid in a curved pipe,” Philos. Mag. (Ser. 7) 5(30): 673–695.

Flitney, R. K., and Nau, B. S. (1990, 1992). Mechanical Seals in Process Plant. Univ. Southampton EPSRC.

Goody, M. (2004). “Empirical spectral model of surface pressure fluctuations,” AIAA J. 42(9): 1788–1794.

Hammitt, F. G. (1980). Cavitation and Multiphase Flow Phenomena. McGraw-Hill.

Heymann, F. J. (1992). In ASM Handbook Vol. 18, Friction, Lubrication, and Wear Technology.

Joukowsky, N. (1898). “Über den hydraulischen Stoss in Wasserleitungsröhren,” Mémoires de l’Académie Impériale des Sciences de St.-Pétersbourg.

Karassik, I. J., Messina, J. P., Cooper, P., and Heald, C. C. (2008). Pump Handbook (4th ed.). McGraw-Hill.

Karnik, U., Studzinski, W., and Geerligs, J. (1994). “A method for assessing installation effects on orifice meters with various flow conditioners,” ASME Fluids Eng. Conf.

Karplus, H. B. (1958). The Velocity of Sound in a Liquid Containing Gas Bubbles. Argonne National Laboratory ANL-4996.

Laws, E. M. (1990). “A further investigation into flow conditioner design,” Flow Meas. Instrum. 1: 165–172.

Laws, E. M., and Ouazzane, A. K. (1995). “A further investigation into flow conditioner design …,” Flow Meas. Instrum. 6: 187–198.

Liu, S., et al. (2023). “Effects of non-uniform elbow inflow on the unsteady flow … of a centrifugal pump,” Phys. Fluids 35: 015152.

Mandhane, J. M., Gregory, G. A., and Aziz, K. (1974). “A flow pattern map for gas-liquid flow in horizontal pipes,” Int. J. Multiphase Flow 1: 537–553.

Mattingly, G. E., and Yeh, T. T. (1991). “Effects of pipe elbows and tube bundles on selected types of flowmeters,” Flow Meas. Instrum. 2: 4–13.

Misiunas, D. (2003). Failure Monitoring and Asset Condition Assessment in Water Supply Systems. Doctoral Thesis, Lund University.

Moody, L. F. (1944). “Friction factors for pipe flow,” Trans. ASME 66: 671–684.

Murakami, M., Shimizu, Y., and Shiragami, H. (1969). “Studies of fluid flow in three-dimensional bends,” JSME Bulletin 12: 1369–1379.

Nikuradse, J. (1932). “Gesetzmässigkeit der turbulenten Strömung in glatten Rohren,” VDI-Forschungsheft 356.

Païdoussis, M. P. (2014). Fluid-Structure Interactions: Slender Structures and Axial Flow, Vol. 1 (2nd ed.). Elsevier.

Pettigrew, M. J., and Taylor, C. E. (2003). “Vibration analysis of shell-and-tube heat exchangers — Part 1,” J. Fluids Struct. 18: 469–483.

Plesset, M. S., and Chapman, R. B. (1971). “Collapse of an initially spherical vapour cavity near a solid boundary,” J. Fluid Mech. 47: 283–290.

Reynolds, O. (1883). “An experimental investigation … direct or sinuous,” Phil. Trans. R. Soc. Lond. 174: 935–982.

Rotta, J. (1956). “Experimenteller Beitrag zur Entstehung turbulenter Strömung im Rohr,” Ing.-Arch. 24: 258–281.

Sander, R. (2015). “Compilation of Henry’s law constants (version 4.0) for water as solvent,” Atmos. Chem. Phys. 15: 4399–4981.

Schlichting, H., and Gersten, K. (2017). Boundary Layer Theory (9th ed.). Springer.

Stephens, M. L., Lambert, M. F., Simpson, A. R., Vitkovsky, J. P. (2008). “Field measurements of pressure transients in a water distribution system,” WDSA Conf., ASCE.

Studzinski, W., Karnik, U., LaNasa, P. (1996). “White paper on orifice meter installation configurations …,” GRI-99/0262, Gas Research Institute.

Taitel, Y., and Dukler, A. E. (1976). “A model for predicting flow regime transitions in horizontal … gas-liquid flow,” AIChE J. 22: 47–55.

Tomita, Y., and Shima, A. (1986). “Mechanisms of impulsive pressure generation and damage pit formation by bubble collapse,” J. Fluid Mech. 169: 535–564.

Tullis, J. P. (1989). Hydraulics of Pipelines: Pumps, Valves, Cavitation, Transients. John Wiley & Sons.

Wang, X., et al. (2020). “Effect of 90° elbows on pump inlet flow conditions,” Applied Water Science 10: 226.

White, F. M. (2015). Fluid Mechanics (8th ed.). McGraw-Hill.

Wood, A. B. (1930). A Textbook of Sound. G. Bell & Sons.

Wygnanski, I. J., and Champagne, F. H. (1973). “On transition in a pipe. Part 1,” J. Fluid Mech. 59: 281–335.

Wylie, E. B., and Streeter, V. L. (1993). Fluid Transients in Systems. Prentice-Hall.

Zanker, K. J. (1958). “The development of a flow straightener for use with orifice-plate flowmeters in disturbed flows,” Modern Developments in Flow Measurement, IEE.

AQUAFLOW

DISCLAIMER

This document is provided for engineering reference. Performance characterizations are conceptual and directional unless explicitly identified as measured field data; actual performance depends on the installation environment, supply characteristics, downstream configuration, and operating conditions. AquaFlow Technologies makes no warranty of specific quantitative outcomes on any component class. Every claim is referenced to published engineering literature, recognized standards, or peer-reviewed research; reviewers are encouraged to verify the literature independently.

AquaFlow Technologies, Inc. — Engineered hydraulic conditioning for municipal, commercial, and industrial water infrastructure.

www.aquaflow.com · support@aquaflow.com · AF-ERE-2026-001 · Rev 2.0 · 2026 · Engineering Reference Edition